Assessing Friction in Bolted Joints and its Implications on Steel Framed Structures

Master of Science (MSc.) Thesis

Hrishika Rastogi

TU Delft

worley

Assessing Friction in Bolted Joints and its Implications on Steel Framed Structures

By

Hrishika Rastogi

For the fulfilment of the requirements of the degree of

Master of Science
in Civil Engineering

at the Delft University of Technology

Student number : 5726026

Project duration : January 2024 - August 2024

Thesis committee :

Dr. Alessandro Cabboi (chair)	Mechanics and Physics of Structures (TU Delft)
Dr. Trayana Tankova	Steel and Composite Structures (TU Delft)
Dr. Ir. Mohammed Ismail	Principal Structural Engineer (Worley)

Cover: Designed by Freepik

An electronic version of this thesis is available at http://repository.tudelft.nl/

TU Delft

worley
DELIVERING SUSTAINABLE CHANGE

Abstract

Bolted steel joints are critical components in steel structures, influencing force transfer, deformation, and energy dissipation mechanisms. In traditional analysis of steel structures, beam-column joints are often simplified as either pinned or rigid. While this simplification eases analysis and reduces computational demands, it fails to accurately capture the semi-rigid joint behaviour, underestimating designs, especially in multi-story steel structures where the cumulative effects of joint flexibility and frictional slip can be relevant. The complexity of accurately modelling semi-rigid joints in finite element analysis (FEA) arises from challenges such as geometric and material nonlinearities, frictional contact interactions, and detailed meshing, all of which increase computational demands, necessitating the use of simplified joint behaviour models. This study identifies and attempts to address a persistent gap in efficiently modelling these semi-rigid joints during structural analysis.

The primary goal of this MSc thesis is to investigate the behaviour of semi-rigid joints and propose a relatively cost-efficient approach to incorporating more realistic joint behaviour into structural analysis. To achieve this, the research explores the frictional behaviour and potential relaxation of bolted joints, focusing on the relative sliding of plates in frictional contact. The study specifically examines how these factors influence load transfer, energy dissipation, and overall structural performance. In multi-story constructions, the cumulative effect of small joint relaxations at each story level can lead to increased lateral sway and amplified second-order effects, raising significant concerns about structural integrity.

The research begins with a detailed examination of an individual beam-column joint assembly consisting of top, bottom and web plates welded to the column flange and bolted to the beam flanges and webs. Through numerical simulations in ANSYS, the study analyzed the joint under both monotonic and cyclic loading conditions, focusing on the force transfer mechanisms and relative deformations between various components of the connection. A parametric study, varying friction, bolt pretension, and loading magnitude, was performed to further explore how these parameters influence the stiffness, energy dissipation, and overall behaviour of the joint assembly. Based on the force-displacement response of different components of a beam-column connection, a Component-Based Spring Method (CBSM) is proposed to simplify the modelling of semi-rigid joints in 2-D multi-story frame structures. This method involves creating equivalent spring elements that simulate the load transfer and deformation behaviours observed in various components of a connection. The study then extended the analysis to the global behaviour of a three-story steel frame structure, comparing the performance of rigid and semi-rigid frames. The simplified CBSM approach was validated by applying it to a three-story steel frame structure and comparing the results with those obtained from detailed solid connection modelling.

The investigation into the local behaviour of the beam-column connection identified key components, such as the Top Plate & Top Beam Flange, Web Plate & Beam Web, and Bottom Plate & Bottom Beam Flange, that govern the force transfer and deformation within the joint assembly. The force-displacement curves of each component provided insights into the pre-yield and post-yield behaviour of the connection. The results revealed that the friction coefficient and bolt preload significantly influence the stiffness and energy dissipation capacity of the joints. Higher friction coefficients and bolt pretension enhanced joint stiffness but reduced energy dissipation, indicating a trade-off that must be balanced in design if dynamic vibration is a concern. The Component-Based Spring Method was validated against detailed solid models, achieving accuracy in frame deflection results of 93% to 96% while reducing computational time by 99.5%. The analysis of the global behaviour of joints within the frame structure revealed that semi-rigid frames exhibit significantly higher lateral deflections, up to 40.63% more when compared to rigid frames, highlighting the risks of oversimplified rigid joint models. These findings highlight the importance of accurately modelling the behaviour of semi-rigid joints to ensure realistic structural performance and the safety of steel frame structures.

Acknowledgement

This thesis represents the culmination of my Master's programme in Civil Engineering at TU Delft, focussing on the behaviour of bolted beam-column joints in frame structures and proposing a cost-efficient approach to integrating realistic joint behaviour into structural analysis. This journey has been both challenging and rewarding, offering a steep learning curve that took me from exploring intricate technical details to appreciating the broader implications of my research.

I wish to extend my heartfelt appreciation to everyone who has contributed to this project. I am deeply grateful to Alessandro Cabboi, the chair of my committee, for his invaluable insights into the intersection of structural mechanics and steel in my research. His continuous involvement and unwavering support have been fundamental to my learning and progress. I am especially thankful to him for facilitating my collaboration with Worley. I am particularly grateful to Mohammed Ismail, my company supervisor and mentor throughout this journey, for the detailed discussions, and guidance that were pivotal in navigating the complexities of this thesis. His mentorship extended beyond the technical aspects of my work, offering inspiration and valuable advice on staying focused, dedicated, and prepared for the future. The constructive feedback from both Alessandro and Mohammed during our progress meetings was instrumental in shaping this study. I am also grateful to Trayana Tankova for her feedback on modelling, calculations, and expertise in steel joints. Her insights significantly deepened my understanding and elevated the quality of my work.

I would like to express my sincere appreciation to Worley for providing the resources and a conducive environment that were essential for the successful completion of this thesis. My time at the company's office in The Hague was marked by the unwavering support of my colleagues, who not only made me feel at home but also engaged actively with my research, offering valuable suggestions that enriched my work. Their guidance and encouragement were instrumental throughout my journey, and I am deeply thankful for the opportunity to collaborate with such a dedicated team.

I am deeply thankful to my friends, who have been my pillars of support, making the rigorous demands of academic life at TU Delft more manageable and enjoyable. To Janki and Mallika, for their unwavering support during difficult times; to Dharmil, for his constant belief in me, encouragement, and genuine care; to Shriyash and Atharva, for sharing the highs and lows of this Master's journey together. I am also grateful to my friends in India, who stayed connected and lifted my spirits from afar. A special thanks to everyone at U-BASE for creating a space where I could connect with others and build lasting memories. To Abishek and Saurabh, your encouragement and our collaborative brainstorming sessions were instrumental in my academic journey.

Finally, I dedicate this thesis to my parents and sister as a token of my sincere appreciation and gratitude. Pursuing a master's degree far from home was not something I initially envisioned, but my parents' unwavering confidence and support pushed me to aim higher and persevere through every challenge. Their constant strength has been my foundation, and I would not have reached this point without them.

Hrishika Rastogi
Delft, August 2024

Contents

List of Figures

List of Tables

1

Introduction

1.1. Background

Steel structures are the backbone of modern construction, providing the necessary strength and flexibility to support projects ranging from towering skyscrapers to expansive industrial complexes. Their popularity stems from the exceptional properties of steel, including its high strength, durability, and adaptability. However, the failure of these structures can have significant socio-economic impacts, making it crucial to understand their response under varied loading conditions. The integrity of steel structures depends largely on the performance of their supporting members, especially the beam-column joints, which play a critical role in the overall stability and resilience of the structure.

Traditionally, beam-to-column joints are classified as either pinned or rigid. The pinned joints are considered to have no rotational stiffness resulting in no moment transfer and displacement, while rigid joints are assumed to possess infinite rotational stiffness, enabling them to transfer moment and displacement. While this classification simplifies design calculations, it does not accurately reflect the real behaviour of these joints. In reality, the behaviour of joints in steel structures is semi-rigid, exhibiting characteristics that fall between the extremes of pinned and rigid joints, as shown in Figure 1.1. This semi-rigid behaviour significantly affects the load transfer and moment characteristics of steel members, including how energy from various structural loads is dissipated. Additionally, bolted joints are preferred for their ease of fabrication and adaptability and are widely used to connect beams and columns. They contribute significantly to damping and non-linearities, accounting for up to 90% of dynamic energy dis-

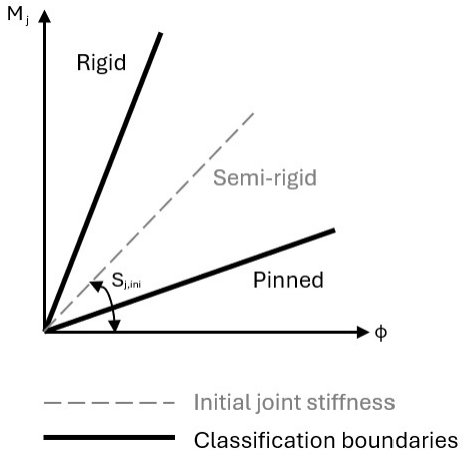

Figure 1.1: Joint stiffness

sipation primarily due to slip in the frictional contact at their interfaces [1]. The behaviour of these joints significantly impacts the performance of steel structures. Understanding this behaviour is essential for developing more accurate and reliable design methods.

Advancements in computational technology and revisions to design codes have made it easier to analyze and design large structures. The joints that connect beams to columns consist of connection elements like plates, angles, welds, and bolts, which are deformable and exhibit nonlinear behaviour. Modelling these joint behaviours requires accounting for material and geometric non-linearities, as well as computationally expensive contact interactions. This often leads structural engineers to simplify joint behaviour, omitting realistic simulations in structural analysis. This gap between theoretical assumptions and practical realities can lead to conservative or unsafe designs. Consequently, understanding the semi-rigid behaviour of joints and incorporating this understanding into design practices is essential for improving the safety and efficiency of steel structures. Therefore, simplified analysis methods that can help engineers account for joint behaviour and achieve realistic structural behaviour without extensive computational resources are highly important.

1.2. Problem Statement

Steel beam-to-column connections are often subjected to bending moment, shear force and axial force. In multi-story buildings with significant lateral loading, the cumulative effect of friction and relaxation at each joint can significantly influence the lateral sway of the structure. The reduction in stiffness and load-bearing capacity of connections can exacerbate second-order effects, such as the P-Delta effect, where vertical loads interact with lateral displacements, leading to increased stress and deformation. The behaviour of a bolted joint is influenced by contact friction and bolt preload, affecting the stiffness and load transfer mechanisms of a connection. Additionally, the practice of using oversized holes in steel structures for in-situ assembly, which facilitates easier alignment and fitting at construction sites, leads to increased slippage in joints due to the additional room for bolt movement.

Understanding the dynamics of friction and relaxation in bolted connections and their contribution to second-order effects in steel structural systems is essential. These dynamics are influenced by material properties, load types, and joint configurations, as well as the cumulative behaviour of these connections across the entire structure. This research delves into the specifics of bolted steel joints subjected to external loads, highlighting their critical role in the overall structural framework. Understanding the individual behaviour of bolted beam-column connections, specifically exploring how different parameters, such as friction, preload, and load magnitude, affect the hysteretic behaviour of these connections, is essential for assessing their dynamic response on the frame structure.

In multi-story structures, where the integrity of each connection is paramount, overlooking the nuanced behaviour of these connections can result in an underestimation of second-order effects, leading to a more demanding global structural design. The design of structures with semi-rigid connections has not been widely adopted due to its perceived complexity and the lack of effective tools for comprehensive analysis. Addressing these research challenges is essential for advancing structural engineering, particularly in the static design and analysis of multi-story steel structures with bolted connections.

1.3. Research Objectives

The overarching goal of this thesis is to enhance the resilience and robustness of steel frame structures and their ability to withstand various loads by considering joint flexibility. This involves a comprehensive analysis of the frictional contact and slip behaviour of beam-column connections with oversized holes under both static and dynamic loading conditions. It is worth emphasizing that the contribution of bearing contact between the bolts and the side of plate holes is not part of the scope of this study. The emphasis is on the relative sliding between steel plates in frictional contact. It is assumed that this sliding amplitude remains within the gap between the bolts and the sides of the oversized holes. The primary objective will be achieved through the development of a numerical model to assess the stiffness

and damping phenomenon observed in bolted joints. This will include examining the slip behaviour in joints, considering parameters such as friction coefficient, bolt preload, and loading amplitude. The validity of the numerical model will be verified through comparison with manual calculations based on Eurocode standards.

Incorporating joint behaviour during the design phase can significantly assist engineers in predicting the realistic behaviour of structures. This research aims to integrate joint behaviour into the design and analysis of frame structures. The study will focus on creating precise Finite Element (FE) models of beam-column connections for accurate predictions while also simplifying these models using multiple nonlinear-spring models to enhance computational efficiency. Additionally, the research will investigate the second-order effects on global frame structures due to semi-rigid joint behaviour, examining load transfer and lateral drift at various stories of a multi-story frame structure under lateral wind loads.

The development of accurate FE models will be a critical component of the research, providing a detailed understanding of the individual joint behaviour under various loading conditions. These models will be used to simulate the performance of beam-column connections and assess their impact on the overall structural response. Moreover, the study will explore the implications of joint flexibility on the design and analysis of steel structures. By incorporating the semi-rigid behaviour of joints into the design process, engineers can develop more accurate and efficient structural solutions that enhance the safety and performance of buildings. This will involve evaluating the impact of joint flexibility on key design parameters, such as load distribution, lateral drift, and second-order effects.

Based on the research objectives, the main research question involves:

”How does the friction behaviour in bolted joints impact the overall structural performance of multi-story frame structures?”

To answer this, the following sub-questions are addressed:

1. What are the effects of varying friction resistance, bolt preloads, and loading conditions on the stiffness and damping characteristics of bolted beam-column connections?
2. How can the Finite Element Method (FEM) be optimized to efficiently simulate the behaviour of semi-rigid joints for the design and analysis of frame structures?
3. How does the flexibility of joints influence the performance of 2D multi-story steel frame structures?

1.4. Methodology

The theoretical foundation of this study is grounded in structural engineering principles, focusing on the behaviour of bolted joints and their impact on multi-story steel constructions. The research unfolds in two distinct phases, as illustrated in Figure 1.2, examining joint behaviour both locally, through its components, and globally through the assessment of a three-story steel frame structure.

The first phase focuses on analyzing individual semi-rigid beam-column connections under both monotonic and cyclic loading conditions. Key parameters such as bolt preload, friction coefficient, and load magnitude are varied to study their effects on the hysteretic behaviour of the connections. This investigation produces force-displacement graphs and hysteresis curves, from which pre-yield stiffness, post-yield stiffness, equivalent stiffness, and energy dissipation characteristics of the connections are derived. The results of this phase provide a detailed understanding of the local behaviour of the connections, which is essential for developing a simplified model for further analysis.

The second phase examines the deflection response of a three-story steel framed structure for both rigid and semi-rigid joint behaviour. A Component-Based Spring Method (CBSM) is employed to simplify the connection behaviour into a set of equivalent spring elements. These elements are based

on the deformation and force-transfer mechanisms identified in Phase 1. By incorporating nonlinear spring stiffness values derived from the earlier analysis, this approach allows for an accurate yet computationally efficient modelling of connection behaviour within a multi-story frame structure. Structural analysis is then performed on the frame, focusing on the effects of simplified connection behaviour on lateral drift and second-order effects, providing a realistic evaluation of the connection's impact on overall structural performance.

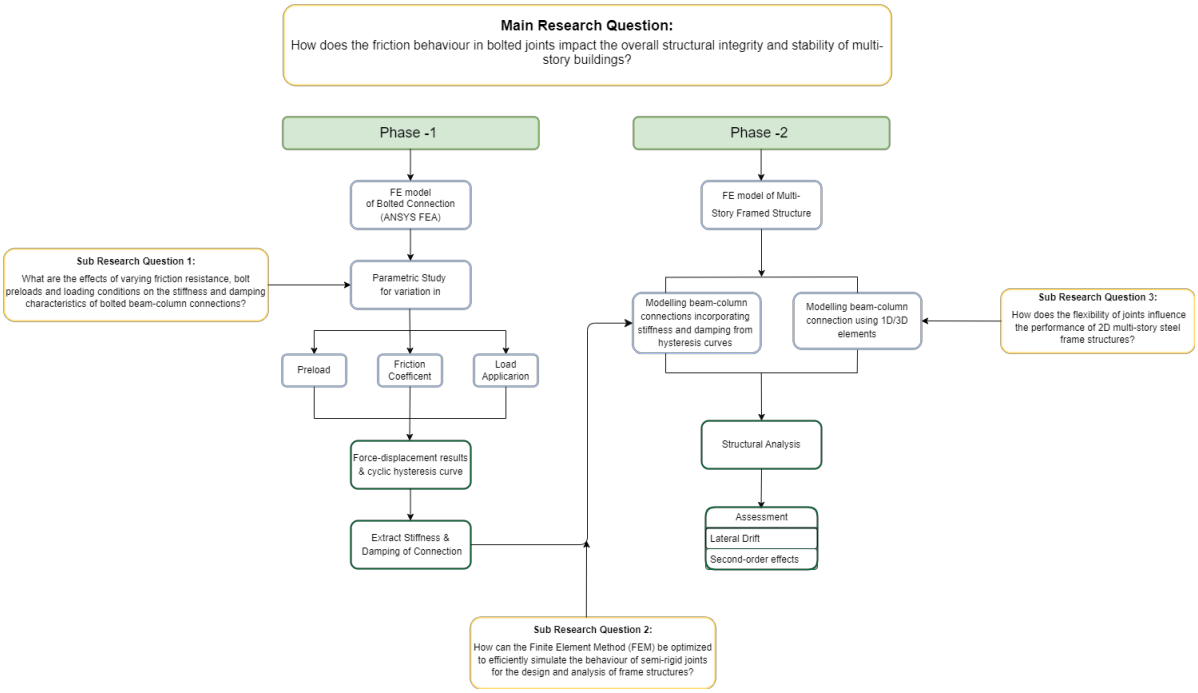

Figure 1.2: Research methodology

Predicting the cyclic behaviour of steel bolted joints presents challenges due to complex geometrical configurations, material nonlinearity, nonlinear friction contact and slip behaviour. While experimental testing offers accuracy, it is often impractical due to time and financial constraints, especially for parametric studies. Therefore, this research employs finite element modelling to examine joint behaviours under various conditions. Validation of the FEM technique is achieved by comparing finite element analysis (FEA) results with manual calculations based on Eurocode standards.

The research utilizes ANSYS R2 2022, a widely recognized and validated FEA software, for detailed simulations of structural components. The capability of ANSYS Workbench to handle highly nonlinear geometry, material and contact algorithms is crucial for Phase 1, as it effectively accounts for friction and relative slippage between components. In Phase 2, a detailed model of a three-story framed structure is developed, with structural analysis performed to understand the influence of joint flexibility on lateral drift and deformation of the structure.

2

Literature Review

This chapter provides an overview of the existing literature on the behaviour of joints in steel structures, with a particular focus on semi-rigid beam-column connections. It aims to equip the reader with a thorough understanding of the behaviours exhibited by bolted steel joints. The review further delves into the mechanics of bolted connections such as friction and relaxation, especially as they occur in oversized bolt holes within a semi-rigid connection. By examining these aspects, the chapter presents a detailed exploration of the critical factors influencing the performance and reliability of steel frame connections.

2.1. Overview of Joints in Steel Frame Structure

Steel structures, when subjected to static and dynamic loads, are characterized by numerous energy dissipation zones that significantly enhance their overall resilience. These critical zones are typically located at the beam ends, within the beam-column joints, and at the lower ends of columns where they connect to the frame supports [2]. In traditional analysis of steel structures, beam-column joints are often simplified as either pinned or rigid for ease of analysis. In an ideal pinned joint, no moment is transferred between the beam and the column, as these connections lack rotational stiffness. Conversely, a perfectly rigid joint implies complete rotational and displacement capability and can transfer all types of loads between the beam and column.

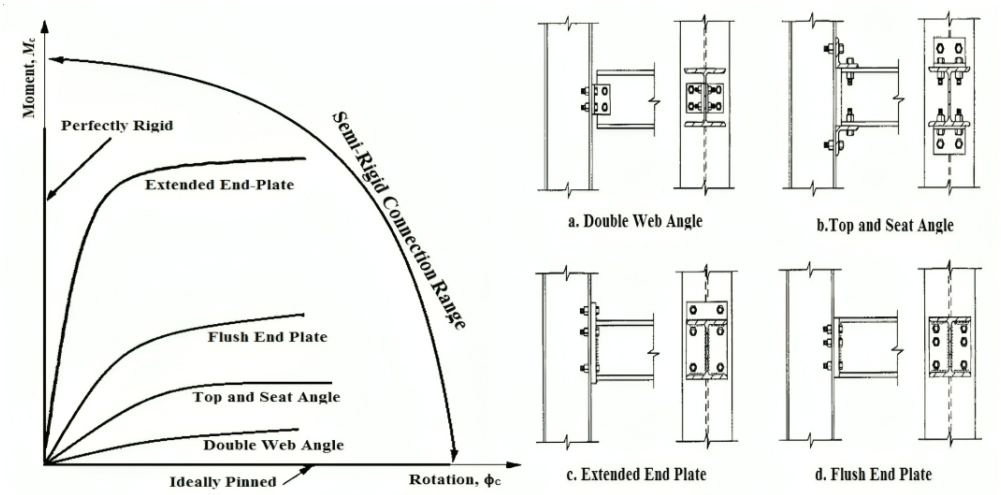

Figure 2.1: Types of beam-column connections and moment-rotation curves [3]

In reality, joints exhibit some degree of rotational stiffness and moment transfer, a characteristic known as semi-rigid behaviour, which lies between the pinned and rigid extremes. Figure 2.1 illustrates examples of practical beam-column connections that are considered semi-rigid, with the joint behaviour depicted using a moment-rotation curve $(M - \phi)$. The flexibility of a joint significantly influences the distribution of internal forces and the displacement of the structure. Joints have a considerable impact on the overall stiffness, resistance, and stability of the structure, as well as on the energy dissipation caused by cyclic loading. Therefore, it is crucial to take into account the actual behaviour of the joints in frame analysis to ensure accurate and reliable structural performance.

2.1.1. Influence of Joint behaviour on Structural Integrity

Extensive research has been conducted to better understand the influence of joint behaviour on the integrity and performance of structures. The deflection of structural members is significantly impacted by the flexibility of the connections involved. Studies have demonstrated that beam-column connections play a crucial role in the static and dynamic performance of structures, with semi-rigid connections providing economic and construction advantages due to their flexibility and reduced material requirements [4]–[6].

Notably, a study involving eight experiments on two-story frames compared the performance of frames with semi-rigid and rigid connections under different load patterns, including monotonic, cyclic, and quasi-dynamic conditions [4]. Additionally, an experimental investigation examined the behaviour of rigid and semi-rigid frames by exploring various beam-to-column connections, such as fully welded, bolted end-plate, and bolted angle types [7]. These studies highlighted that, despite their lower stiffness and load-bearing capacity compared to rigid frames, semi-rigid connections exhibit significant energy dissipation capacities through stable and repeatable force-displacement cycles. Additionally, extensive experimental studies have been conducted on end-plate moment connections [8] and bolted T-stub connections made from welded plates [9], providing crucial insights into the resistivity, stiffness, and deformation capabilities of semi-rigid assemblies. In recent years, more extensive studies have been conducted to numerically capture the dynamic behaviour of frame structures. Rigi et al. [10] explored the seismic performance of steel moment-resisting frames with varying connection rigidities (full, 80%, 70%, and 60%), analyzing frames of different heights using modal analysis, non-linear static analysis, and incremental dynamic analysis (IDA). Their findings indicate that semi-rigid frames, while having lower base shears and higher structural deformations, exhibit enhanced energy absorption capabilities. The results highlighted the critical role of connection rigidity in frame design and retrofitting.

Furthermore, recent studies suggest that the global moment-rotation behaviour of the joint can be deduced from the behaviour of its components. For instance, a model for steel beam-to-column connections with top and seat web angles was developed, taking into account damage accumulation in the stress-strain relationship, bolt behaviour in cyclic shear, and slip between connected elements, though it does not account for hole ovalization or changes in preloading force [11]. The study showed that the interaction of internal forces, particularly axial, shear, and bending moments, has a substantial impact on connection behaviour. Another study proposed a cyclic model based on a lumped approach for the tensile and compressive zones, suggesting that the overall energy dissipation of the connection can be obtained by summing the energies dissipated by the various joint components [12].

From the aforementioned literature, it is evident that joint behaviour is not isolated and is dependent on each component of the joint. The behaviour of each component is influenced by various phenomena, including its elements, contact behaviour, and load transfer. The characterization of each component can be achieved through experimental, numerical, or analytical models, which are further examined in a subsequent section.

2.2. Methods to Investigate Semi-Rigid Behaviour

Building on the foundational understanding of joint behaviour, semi-rigid joints have been extensively studied through various analytical approaches, including mathematical models, 2D/3D Finite Element (FE) models, and component-based methods.

2.2.1. Mathematical Models based on Experimental Studies

Early research primarily involved experimental investigations, which were used to develop mathematical models representing the moment-rotation response of connections. These studies identified key parameters such as initial stiffness, moment capacity, rotation capacity, and moment-rotation relationships of semi-rigid steel connections ([13]–[16]). However, these mathematical models rely on curve fitting to the available test results, which limits their applicability as connection details change. While experimental studies provide realistic insights into joint behaviour, they are both expensive and time-consuming, restricting their practicality for exploring a wide range of parameters. Nonetheless, these initial efforts have laid the groundwork for more advanced methods, which are discussed in the following section.

2.2.2. Numerical Method - Finite Element Method

Over the past two decades, advancements in computer technology and numerical studies have significantly accelerated and diversified the investigation of joint behaviour. Among these advancements, the Finite Element Method (FEM) has emerged as a popular and effective approach for simulating the behaviour of bolted steel joints [17]–[19]. Utilizing beam, shell, and solid elements, FEM facilitates the construction of sophisticated two- and three-dimensional models. These models enable detailed representation of component geometry, bolts, contact interactions, meshing, and boundary constraints, as illustrated in Figure 2.2. Compared to elaborate and costly experimental setups, FEM offers a cost-effective alternative that achieves a high degree of accuracy in predicting experimental results [20]–[23]. This progress in numerical modelling has been crucial in deepening the understanding of the intricate dynamics involved in bolted connections within structural engineering.

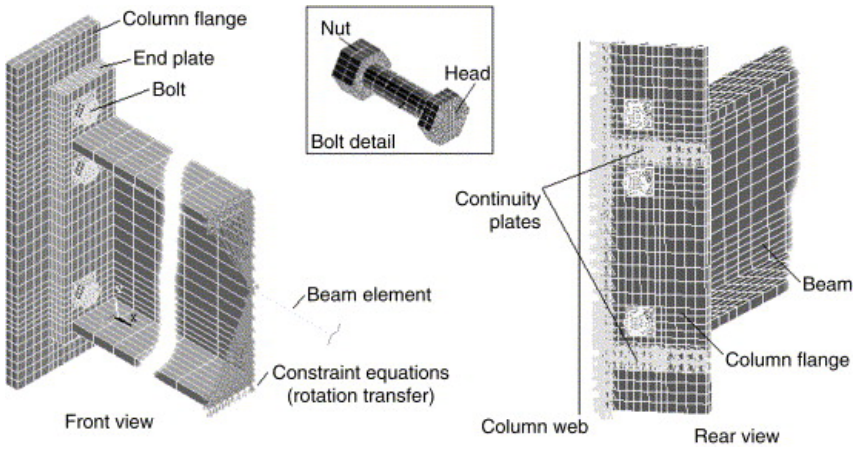

Figure 2.2: Example of 3D FE model of beam-column connection [23]

Semi-rigid beam-to-column joints exhibit significant nonlinear behaviour from the early loading stages, primarily due to their reduced stiffness and bending capacity. This nonlinear behaviour results in a hysteretic response, which is essential for assessing energy dissipation in structures. Da Silva et al. [24] introduced a modelling strategy to represent the dynamic behaviour of semi-rigid connections, incorporating geometrical nonlinearities and non-linear hysteretic connection stiffness in low-rise framed structures. Similarly, Shen and Astaneh-Asl [25] developed a hysteretic model for bolted-angle connections, specifically for the dynamic analysis of semi-rigid steel frames. Their model combined experimen-

tal and analytical results to provide a comprehensive understanding of connection behaviour. These hysteresis models offer valuable insights into deformation behaviour and joint dynamics under cyclic loading. Further research that accounts for additional nonlinear parameters, such as friction and bolt preloading, can enhance our understanding of bolted joint dynamics and cyclic deformation behaviour, leading to more accurate and reliable designs for semi-rigid connections in steel structures.

A well-calibrated finite element (FE) model can minimize the number of experiments needed to understand specific behaviours in a parametric sense. However, the application of semi-rigid design has not gained widespread attention among structural engineers due to its perceived complexity. FE models that incorporate semi-rigid connections require significant computational effort and time, making them impractical for the analysis of large structures. Consequently, analytical models have been developed to design and analyze complex joint behaviour without the intensive computations required by detailed numerical models. These analytical approaches offer a more practical alternative, facilitating the effective assessment and implementation of semi-rigid connections in structural design.

2.2.3. Analytical Method - Component Based Method

While finite element models offer detailed insights into joint behaviour, they often require significant computational resources, making them impractical for analyzing entire structures with complete joint modelling. To address this limitation, analytical methods like the Component-Based Method (CBM) presents a more efficient alternative by simplifying the analysis of complex joint behaviour without compromising accuracy.

Experimental and numerical analyses have shown that the behaviour of joints is not isolated; it is significantly influenced by the individual components, the overall frame, and the loading conditions. The CBM divides a connection into a system of springs, each representing a component of the connection that transfers forces. This method views a connection as a collection of basic components, each with its strength and stiffness, which collectively determine the overall stiffness of the connection. The CBM as outlined in EN 1993-1-8 (2005), involves the following key steps:

1. Identification of Active Components: Determine which components are actively contributing to the joint's behaviour.
2. Evaluation of Stiffness and Resistance Characteristics of Each Component: Analyze the force-displacement relationships and resistance characteristics for each active component.
3. Assembly of All Components: Combine the analyzed components according to the joint's geometrical configuration.
4. Evaluation of the Stiffness and Resistance Characteristics of the Whole Connection: Assess the overall joint properties by considering how the individual components interact when assembled.

This method characterizes the behaviour of different components of a joint using equivalent linear springs. Traditionally, connections have been modelled using moment-rotation springs attached to the ends of beams on both sides of the joint. This approach approximates the internal forces within the joint but does not account for the nonlinear behaviour and local phenomena occurring within the joint.

Over the years, numerous studies have investigated the component-based approach for characterizing structural joints and their overall behaviour in frame structures [26]–[29]. Figure 2.3 illustrates a general framework of CBM for simplifying the analysis of beam-column joint behaviour in steel frame structures. This framework decomposes the joint behaviour into a series of rigid bars and springs, reflecting the force transfer and deformation mechanisms of different components. Each component is modelled with an equivalent nonlinear spring corresponding to its force-displacement relationship. The springs are aligned according to the deformability of the connection component and connected to beam elements to accurately represent the stiffness and strength characteristics of the joint.

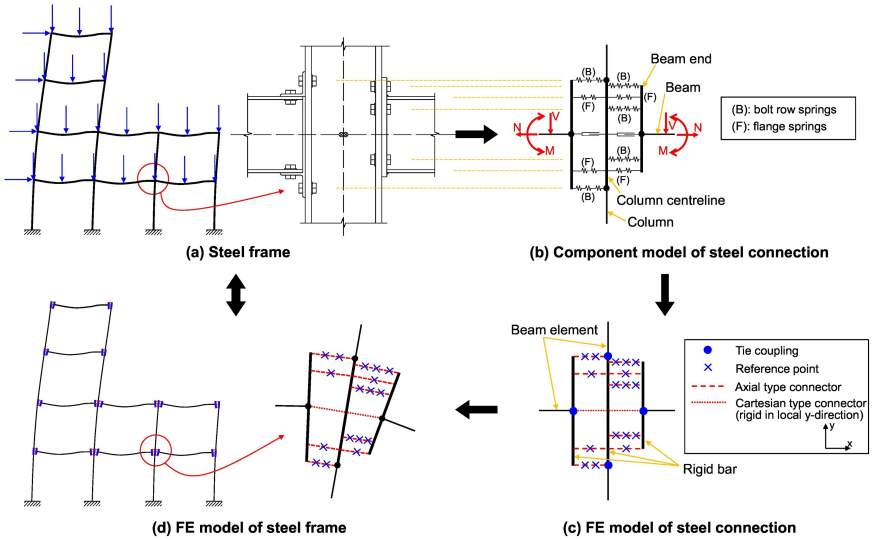

Figure 2.3: Methodology of Component-Based Method in the analysis of steel frame structures [27]

In this research, the Component-Based Method will be applied in finite element models to represent the behaviour of semi-rigid beam-column connections for the analysis of frame structures. This approach will aim to bridge the gap between simple mathematical models and detailed finite element models by incorporating nonlinear geometrical and material properties, including the interaction of local phenomena and internal forces leading to axial and shear deformation of the connection. The stiffness relationships of various components will be formulated separately and then assembled to represent the local joint behaviour. Based on the force-displacement behaviour of the local connection, nonlinear springs will be formulated. These spring elements will be used in advanced computer programs for global analysis, simulating the behaviour of connections at the ends of beams. This research will aim to strike a balance between complexity and accuracy, providing structural engineers with a practical tool to accurately understand connection behaviour and global sway behaviour of a structure under lateral loading.

2.3. Mechanics of Bolted Connections

Semi-rigid joints, widely used in steel structures, often rely on bolted connections due to their versatility and ease of assembly. Bolts provide the necessary flexibility and strength, allowing for the dissipation of energy and accommodating various loading conditions. bolted connections are often pivotal in energy dissipation, stiffness reduction, wear, and even chaotic behaviours in structural systems. However, they introduce nonlinear interactions and a variety of potential failure mechanisms, making the design and analysis of these joints more difficult. The behaviour of bolted connections is multifaceted, influenced by several phenomena like friction, preload, and relaxation, each contributing to their overall performance. Given these factors, this study will also investigate the characteristics and factors influencing the behaviours of bolted connections.

2.3.1. Friction and Contact Mechanics

Understanding the contact mechanics is essential for comprehending the nonlinear behaviour of bolted joints. Bolted joints experience both tensile and compressive loading conditions, leading to multiple force transfer mechanisms. The applied load is primarily transferred through friction between the contact surfaces. Frictional behaviour governs the hysteresis response observed in these joints, which is crucial for evaluating the stiffness and energy dissipation characteristics of the system [30], [31].

Figure 2.4 illustrates the hysteresis behaviour of a single bolted connection under both tensile and compressive loading conditions. The interaction between the plates and bolts results in a stick-slip

mechanism affecting load transfer. Initially, in the ”before slip” phase, the joint behaviour is governed by static friction, with the applied load being transferred through friction between the contact surfaces. When the applied load exceeds the frictional resistance, frictional slip occurs at the interfaces [32], [33]. During the ”slippage” phase, the applied force remains constant while relative motion occurs between the plates. This slip first manifests as micro slip, where a partial slip in the contact area significantly reduces stiffness and increases system damping. As the load increases, the slip progresses to macro slip, characterized by complete slipping across the entire interface. This transition leads to stick-slip behaviour, where the joint surfaces intermittently stick and slip, creating distinct hysteresis patterns in force-displacement or stress-strain curves, forming closed hysteresis loops.

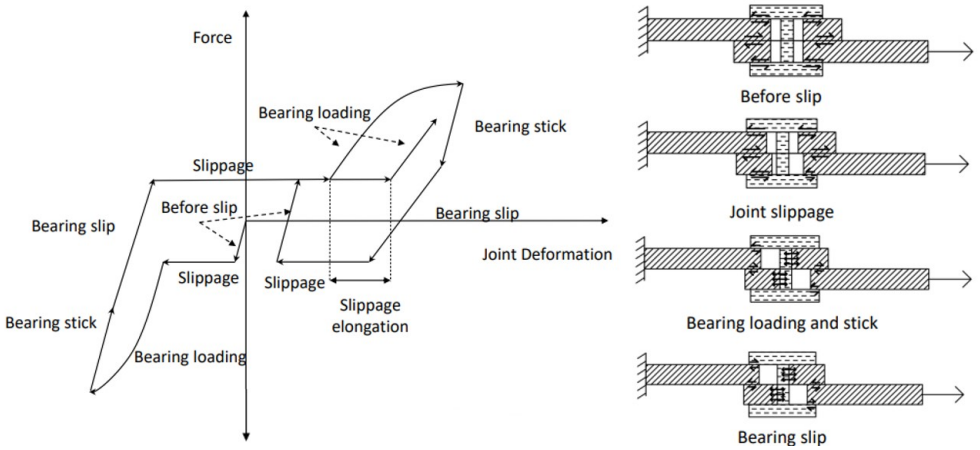

Figure 2.4: Typical force-displacement hysteresis curve of a single bolted connection [33]

The average stiffness of the joint can be calculated using the force-displacement ratio from the hysteresis loop, while joint damping can be determined from the area within the loop [34]. Bolted connections can achieve high ductility and excellent energy dissipation during cyclic loading if the more brittle components are appropriately reinforced with overstrength measures [25]. This makes bolted connections particularly effective in applications where energy dissipation and resilience are critical.

The relationship between the coefficient of friction and surface roughness in bolted connections is complex and integral to understanding contact mechanisms. The coefficient of friction is directly influenced by microscopic interactions at the contact surfaces, where asperities play a significant role in slip resistance and damping. Studies indicate that surface roughness greatly affects contact conditions, such as normal and tangential contact stiffness. Increased roughness reduces the contact area, resulting in less uniform contact pressure and a decrease in active friction elements at the interface, thereby reducing the overall stiffness of the joint [35]–[37]. Even minor deviations in curvature or surface geometry can introduce significant uncertainty in predicting the nonlinear dynamics of these systems [38]. These findings underscore the complexity involved in modelling and predicting the behaviour of joint assemblies. Understanding the friction and contact mechanics between elements, such as bolts and plates, is critical for accurately assessing the nonlinear characteristics of bolted joints.

2.3.2. Preload and Bolt Relaxation

Preload or clamping force in bolted connections provides essential frictional resistance, influencing force transfer and contact mechanics. The level of preloading significantly impacts the slip-resistant behaviour of the connection, particularly in seismic applications [32], [38], [39]. Generally, increasing preload reduces macro-slip, thereby enhancing the connection’s stability. However, this can also lead to heightened force transmission, potentially causing damage to the connection assembly. Conversely, low preload levels may result in greater relative motion, affecting the structural integrity and dynamic response of the assembly [40].

Relaxation in bolted joints, often associated with a loss of preload over time, is a significant concern,

particularly under dynamic conditions like impacts and vibrations [41], [42]. This gradual loss of preload can be influenced by relative motion between connected parts, which can contribute to bolt loosening at the contact interface [43], [44]. Understanding these effects is vital to prevent failures and ensure structural safety. Studies have shown that self-loosening can be initiated by transverse vibration, which leads to a reduction in friction and clamping force. This reduction results from the accumulation of localized slip at the fastener contact surfaces [45], [46]. Additionally, maintaining proper contact pressure at the interface of bolted joints is crucial for joint integrity. Variations in bolt torque and external loads, including cyclic shear and transverse loads, can influence this contact pressure, potentially leading to fretting fatigue at the contact surfaces. This, in turn, reduces friction and increases the risk of bolt loosening [47].

In recent years, the use of oversized or slotted bolt holes has gained popularity due to their facilitation of easier prefabrication and on-site bolt assembly. These connections allow for more frictional sliding compared to standard bolts, which typically show less slippage. Connections with these oversized holes are known for their improved ductility, enhanced load-bearing capacity and substantial energy dissipation with minimal damage [39], [48]–[50]. This makes them particularly advantageous under cyclic loading conditions, where maintaining joint integrity is critical [51], [52].

The comprehensive understanding of bolted connection mechanics—from friction and contact interactions to preload and relaxation dynamics—provides valuable insights for designing robust and resilient structural systems. Continued research and development in this field will enable engineers to optimize bolted connections, ensuring both safety and performance in a wide range of applications.

2.4. Research Gap

In the context of steel structures, developing simple yet effective analytical models using well-established parameters is highly desirable for structural analysis. The literature review has revealed that factors such as bolt preload, friction coefficient, and loading conditions significantly influence the contact mechanics of bolted connections. However, translating these factors into large-scale structural models remains a challenge due to high computational demands.

Accurately modelling the impact of connections on the global behaviour of framed structures is critical. This involves defining a load-displacement relationship that effectively captures the interaction between the force transfer and resultant deformation within the various components of the connection. The current challenge lies in incorporating key parameters such as equivalent stiffness and damping, which are essential in characterizing the properties of connections at a local level and accurately scaling these up to assess the global response of frame structure

Despite advancements in numerical methods like the Finite Element Method (FEM) and the Component-Based Method (CBM), there remains a gap in effectively integrating these approaches for practical, large-scale applications. The computational intensity of FEM models, combined with the complexities of accurately representing nonlinear and hysteretic behaviours, necessitates a more streamlined approach.

This study aims to address these gaps by evaluating key friction-influencing parameters in bolted connections through a parametric study. By altering factors such as preload, friction coefficient, and load amplitude, the research seeks to derive stiffness and damping characteristics from the hysteresis curves of individual joints. These parameters will then be incorporated into the connections of a global frame structure. The approach is expected to provide deeper insights into the behaviour of connections and their influence on the structural integrity of frames. By analyzing the efficiency of this method, the study aims to offer a more refined tool for structural analysis and design, particularly in scenarios where the behaviour of connections critically influences the overall structural response. This could potentially bridge the gap between detailed numerical models and practical, large-scale structural analysis, enhancing both accuracy and efficiency in structural engineering practices.

3

Examination of Beam-Column Connection Behaviour

The theoretical foundation of this study is rooted in structural engineering principles, focusing on the behaviour of bolted joints and their impact on multi-story steel frame structures. This chapter presents both the analytical approach of the Component-Based Method (CBM) and the development and analysis of Finite Element (FE) models to study the structural behaviour of individual bolted connections. Section 3.1 details the component-based method, used to divide the connection into individual components based on the governing force transfer and displacement response. Section 3.2 details the finite element modelling of a beam-column bolted connection subjected to monotonic and cyclic loading conditions. The finite element analysis yields force-displacement graphs and hysteresis curves, from which the pre-yield stiffness, post-yield stiffness, equivalent stiffness, and damping characteristics are derived, as discussed in Section 3.3. The validity of the developed FE model is confirmed through comparisons of computational solutions with manual calculations, as elaborated in Section 3.4. This approach ensures that the numerical model accurately represents the physical behaviour of bolted connections, enabling reliable results and insights.

3.1. Component Based Method on Beam-Column Connection

Common bolted semi-rigid joints include beam-column connections with top and seat angles, double web angles and end plates, among others. This study considers a beam-column connection consisting of top-seat and web plates (TSWP) welded to the column flange and bolted to beam elements, as illustrated in Figure 3.1. The plates are considered welded to the column flange to simplify the connection geometry, eliminating complex bolt interactions at the contact interface. This simplification reduces potential convergence issues associated with increased bolts and streamlines the overall nonlinear analysis process.

The component-based method is used to divide the connection into a system of springs, each representing a component that transfers force. When the connection is loaded, forces are transmitted from the beam to the top-seat and web plates through the bolts, which then transfer the forces to the columns. The TSWP beam-column connection is designed to accommodate the combined effects of axial force, shear force and moment between the beam and column members. The bolted connection between the top-seat plates and the beam flanges results in an axial load transfer mechanism. In contrast, the bolted connection between the web plate and beam web provides a shear load transfer mechanism.

Based on the axial and shear force transfer mechanisms, the chosen beam-column connection can be divided into three main components, as depicted in Figure 3.1:

1. Component 1: Top plate and beam top flange,
2. Component 2: Web plate and beam web, and
3. Component 3: Bottom plate and beam bottom flange.

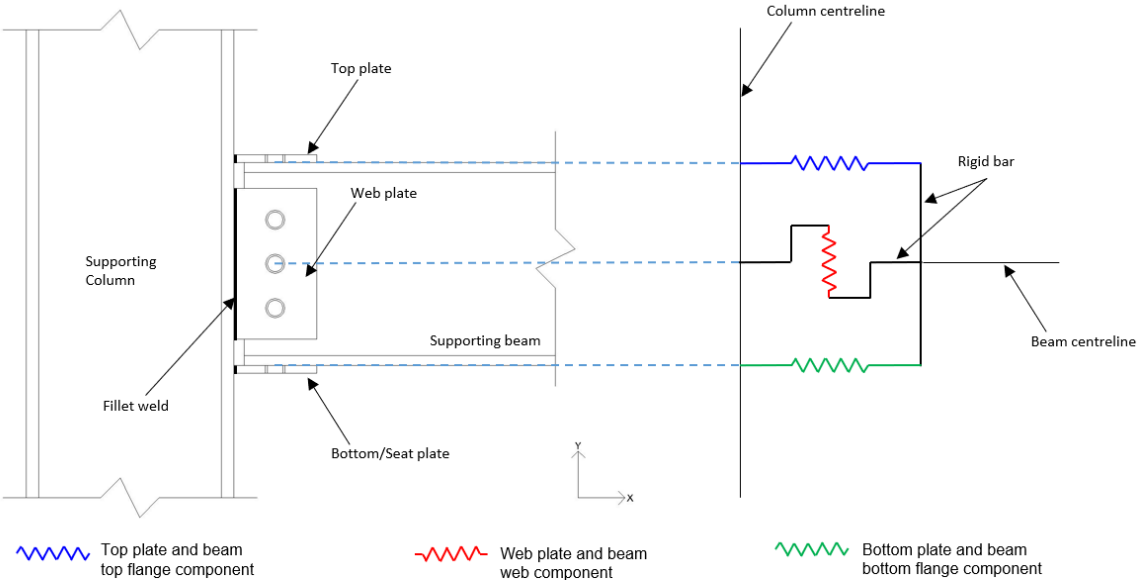

Figure 3.1: Diagram of top-seat and web plate beam-column connection with simplified spring component model

Each component contains multiple bolts, which can be grouped into a single spring interaction. This allows the decomposition of the joint behaviour into individual component behaviour based on the force-displacement characteristic of each component. The stiffness and damping properties of each element can be extracted to estimate the response of the steel connection under both static and dynamic loading conditions. The process of extracting results from the force-displacement response is presented in subsequent sections.

3.1.1. Stiffness and Energy Dissipation

The stiffness due to friction between the sliding plates and beam elements is determined using the slope of the force-displacement curve. This involves analysing the internal force in the direction of slip (x direction for axial load transfer in top and bottom plate components and y direction for shear load transfer in web plate component) and the relative displacement between the friction surfaces of the plates in contact. The nonlinear behaviour obtained in the force-displacement relationships of each component is analysed using a bi-linear envelope, characterised by pre-yield stiffness K_{p1}, post-yield stiffness K_{p2}, and effective stiffness K_e, as illustrated in Fig 3.2.

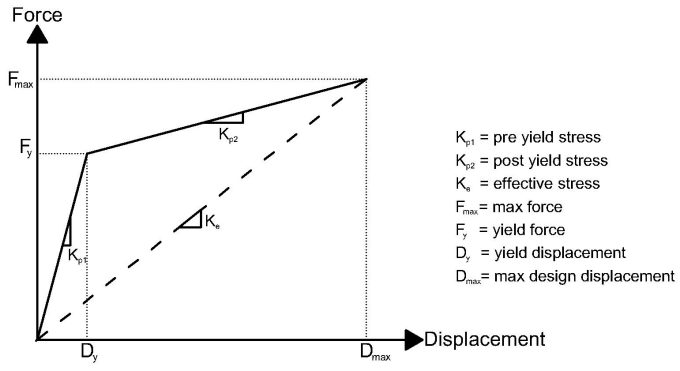

Figure 3.2: Stiffness in force-displacement curve

Pre-yield stiffness K_{p1} refers to the initial stiffness of a structural component before any yielding occurs. It is represented by the slope of the initial linear portion of the force-displacement curve, which corresponds to the elastic behaviour of the material or structure. Post-yield stiffness K_{p2} refers to the stiffness after the connection has yielded and entered the plastic deformation phase. Effective stiffness K_e is a combined measure that reflects the overall stiffness of the structural component throughout the entire loading process, including both the elastic and plastic phases.

For cyclic loading, the force-displacement curves for each plate are identified and captured for both the loading and unloading paths to create a hysteresis loop, as shown in Figure 3.3. This figure represents a typical cyclic behavior observed in the numerical simulations of the study. Here the effective stiffness of each component can be determined by fitting a straight line between the maximum and minimum force obtained in the hysteresis loops. This approach provides a representative stiffness for a connection experiencing cyclic alternate loading, as commonly observed in structures subjected to vibrations.

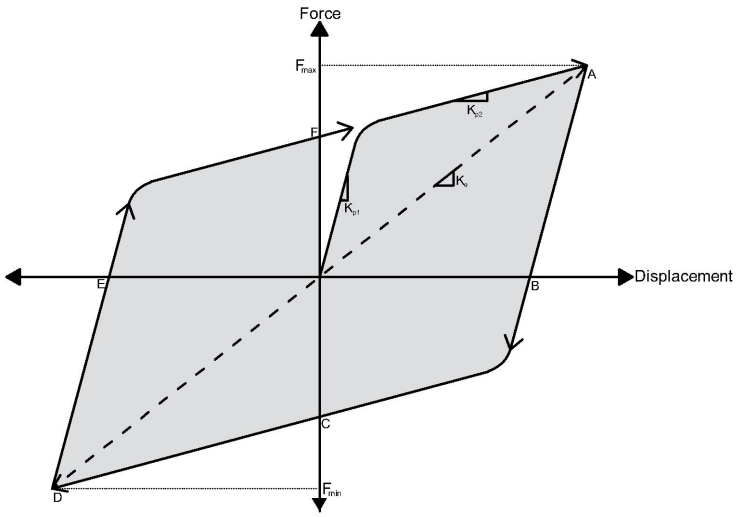

Figure 3.3: Cyclic force-displacement hysteresis curve

Under cyclic loading, the energy dissipation per cycle E_d is determined by the area enclosed in the force-displacement hysteresis loop. This area represents the energy lost due to internal friction and other damping mechanisms within the material and connection components. The energy dissipation can be approximated using the integral of the force over the displacement of a single cycle of the hysteresis loop. In practice, this integral can be approximated by summing the areas of trapezoids formed by discrete data points along the hysteresis loop.

3.2. Numerical Modelling of Connection

This section presents the finite element model developed for simulating the behaviour of an individual beam-column connection. The finite element simulation software ANSYS R2 2022 is utilised for this purpose. The connection geometry is created in ANSYS SpaceClaim, and both static and transient analyses are performed in ANSYS Workbench Mechanical. The complex geometrical configuration, including beams, plates, and bolts, is carefully considered to obtain a reliable FE model. Key aspects such as material nonlinearity, element types, mesh sizes, contact properties, and boundary constraints are meticulously defined.

Consistency in measurement units is important during numerical analysis. For this project, the International System of Units (SI) is adopted, with newtons (N), millimetres (mm), tons (T), and seconds (s) chosen as the standard units of measurement.

3.2.1. Model Geometry Parameters

The beam-column connection geometry, as shown in Figure 3.4, consists of a HEA400 beam with a length of 5560mm connected to a HEB400 column with a length of 800mm using structural elements such as bolts, plates, and welds. The connection includes a top and seat plate bolted to the beam flanges and welded to the column flanges and web plates bolted to the beam web and welded to the column flange. Two M30 bolts secure the top and seat plates to the beam flanges, while three M30 bolts secure the web plate to the beam web. The connection features oversized bolt holes with a 4 mm clearance, resulting in a bolt hole diameter of 38 mm for the M30 bolts.

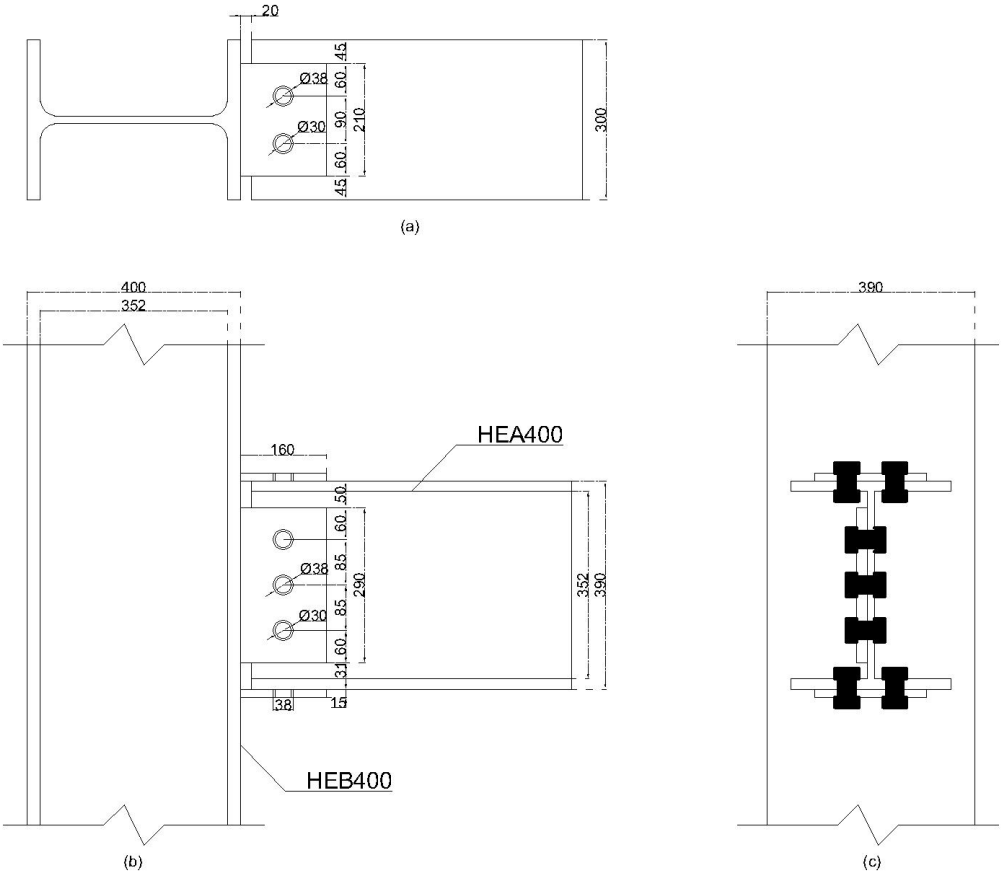

Figure 3.4: Details of beam-column connection with (a) Top view, (b) Front view, and (c) Side view

As illustrated in Figure 3.5, the model consists of two columns spaced 6 meters apart (centre to centre), with a beam connected at each end using the top seat and web plates. The plates, beams, and columns are modelled as 3D solid geometries using first-order solid hexahedral elements (SOLID185), which provide 8 nodes with 3 translational degrees of freedom per node. To simplify the finite element model and reduce computational demands, the bolts are represented as 1D line elements.

Modelling the bolt geometry as solid elements would require a fine mesh to accurately capture the stress distribution. Additionally, solid modelling of bolts necessitates simulating complex contact interactions, significantly increasing computational time and cost due to the higher number of meshed elements. By representing the bolts as 1D line elements, the modelling process is streamlined, reducing computational demands while still capturing the essential mechanical behaviour of the connections. Furthermore, the fillet radius in the beam and column geometry is omitted from the model. These simplifications help maintain the model's accuracy while significantly reducing its complexity.

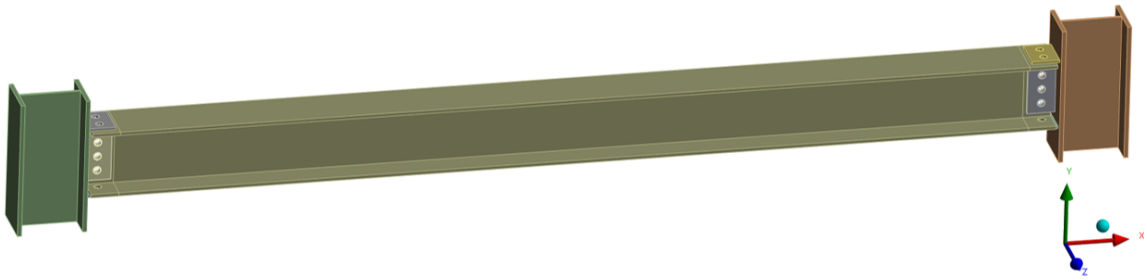

Figure 3.5: FE model of connection

3.2.2. Material Properties

The stress and strain properties of steel are typically obtained from material testing, known as "Engineering" stress-strain curves, calculated based on the initial cross-section of the test specimen. However, to simulate material behaviour in FEM, it's essential to define material properties using true stress and true plastic strain relationships. True stress (σ_{true}) and true plastic strain ($\varepsilon_{\text{pl. true}}$) values are derived from the engineering stress and logarithmic strain relationship using the equations: $\sigma_{\text{true}} = \sigma_{\text{eng}}(1+\varepsilon_{\text{eng}})$ and $\varepsilon_{\text{true}} = \ln(1+\varepsilon_{\text{eng}})$. In the absence of experimental material data, the material model can be obtained from Eurocode guidelines (EN 1993-1-1:2005 and EN 1993-1-8:2005).

The joint assembly consists of columns, beams, plates, and bolts, with their respective dimension and material properties listed in Table 3.1. S275 structural steel, with a yield strength of 275 MPa and an ultimate strength of 430 MPa is utilized for the columns, beams, and plates. The bolts are modelled using grade 8.8 steel, which has a yield strength of 640 MPa and an ultimate strength of 800 MPa. Both materials share a density of $7850\,\text{kg/m}^3$ and Young's modulus of $210000\,\text{MPa}$. Poisson's ratio of $\nu = 0.3$ is adopted, and damage mechanisms such as fracture are not incorporated.

Table 3.1: Dimensions and material properties of connection assembly

Specimen	Dimensions (mm)	Material Steel Grade
Beam	HEA400	S275
Column	HEB400	S275
Top/Bottom Plate	210*160*15	S275
Web Plate	290*160*20	S275
Bolts	M30	8.8 grade

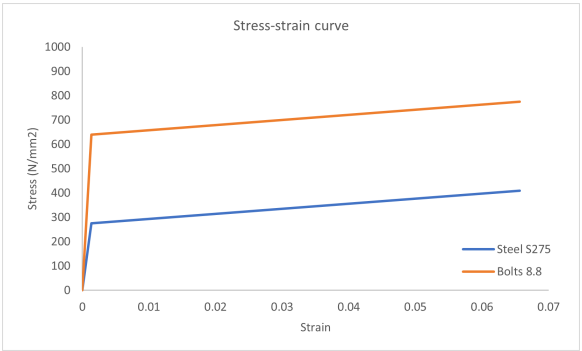

Figure 3.6: Bilinear stress-strain material model in ANSYS

Ansys represents this material behaviour using a bilinear isotropic hardening model, consistent with the Eurocode 1993-1-5 Appendix C6 guidelines for finite element analysis. This model involves two key stages as illustrated in Figure 3.6. Initially, the material behaves elastically, and the yield stress

is applied with a slope corresponding to Young's Modulus (E). Once the yield stress is exceeded, the model transitions to a plastic phase characterised by a reduced slope, known as the Tangent Modulus. According to EN 1995-1-5, the hardening slope is recommended as $E_{\text{sh}} = E/100$ for all types and grades of steel sections.

3.2.3. Meshing and Contact Properties

The Finite Element Method (FEM) discretises a system's domain into a large number of finite-sized elements. Generally, smaller element sizes yield more accurate approximations of the solution up to a certain threshold. Beyond this threshold, further refinement may not significantly enhance accuracy but will substantially increase computational effort. Various mesh sizes were tested to identify an optimal mesh that delivers precise results within a reasonable computational time frame to balance accuracy and computational efficiency.

A finer mesh is employed in regions with contact interfaces and areas of high-stress concentration to capture detailed behaviours. Conversely, a coarser mesh is applied in less critical regions. Figure 3.7 presents an overview of the different meshes used in the FE model. A coarse mesh with a maximum element size of 0.1m is applied along the length of the beam and columns. In contrast, a finer mesh with an element size of 10mm is used on the contact surfaces of the columns, beams, and plates, with further refinement to 6mm around the bolt holes using partitions created around the areas of concern. The line elements of the bolts had a mesh size of 6mm.

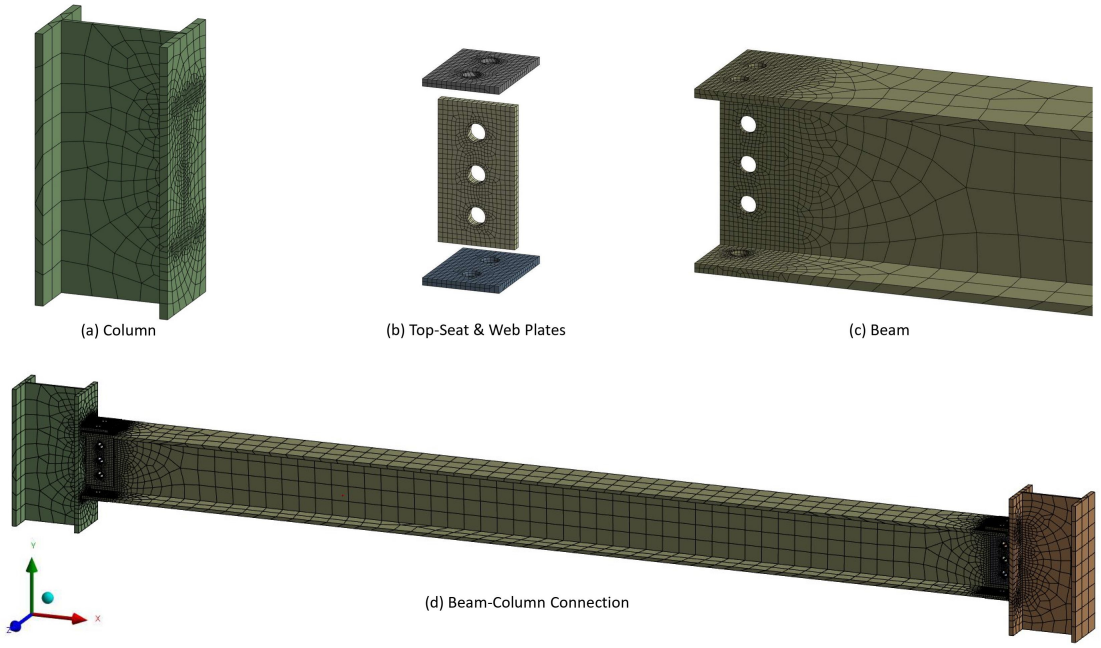

Figure 3.7: Mesh details for various components of FE model

Contact elements are adopted to simulate the force transfer that occurs when two elements come into contact. Surface-to-surface contact elements (TARGE170 and CONTA173) are used to represent geometric discontinuities and simulate interactions between the various components. A general surface-to-surface contact is defined using a 'Penalty' friction formulation with a friction coefficient of 0.2 for the contact interfaces between the plates and beam surfaces. Additionally, the contact elements CONTA174 and TARGE170 are used to simulate contact and potential sliding between 3D target surfaces and their corresponding deformable counterparts. These elements provide each node with three degrees of freedom, allowing for translations in the x, y, and z directions, and are capable of modelling Coulomb friction and shear stresses. Contact is considered to occur when the surface of a CONTA174 element approaches a TARGE170 target segment on a specified target surface.

As previously discussed, the complex structure of bolts, including the head and nut, is simplified and modelled as a line body. This line body is meshed using beam elements, significantly reducing the model size and complexity. The contact areas of the bolt head and nut are effectively tied to the bolt hole of the plate and beam element using Multi-Point Constraints (MPC). These MPCs establish a bonded contact between the ends of the line body and the cylindrical edges of the bolt holes. The constraints connect master nodes to slave nodes via rigid links within a pinball radius that encompasses the cylindrical edges. Additionally, bonded MPC contacts are defined between the contact interface of the column flange and the top-seat and web plates, ensuring a rigid connection between these components. The finite element model accurately captures the intricate behaviours and interactions within the beam-column connection while maintaining computational efficiency by employing these meshing and contact strategies.

3.2.4. Boundary Condition and Load Application

The boundary conditions of the finite element (FE) model have been defined to reflect the simplified geometry used for analysis. The length of the column has been reduced to 800mm to streamline the model without compromising the accuracy of the results. Both ends of the column are constrained with fixed supports, ensuring that all degrees of freedom are restricted, thereby preventing any translational or rotational movement. This setup simulates a rigid connection at the column ends.

As illustrated in Figure 3.8, the analysis is applied in two sequential steps. In the first step of the analysis, a bolt pretension force of 400kN is applied to the length of each bolt line element. This is done gradually in multiple substeps to avoid sudden changes in the model that could affect the convergence and load transfer mechanisms. In Ansys, the 'bolt pretension' feature in the analysis settings is used to apply equal and opposite clamping forces at the beam element, creating a grip between the connected surfaces. Preloading the bolts generates compressive stress in the components they join, establishing a stress baseline before any operational loads are applied. This initial stress impacts both the static and dynamic behaviours of the assembly. According to EC3 standards, the total preload force (F_p) is calculated as $0.7 f_{ub} A_s / \gamma$, where f_{ub} represents the bolt's ultimate strength, A_s is the bolt's tensile stress area, and γ is a safety factor.

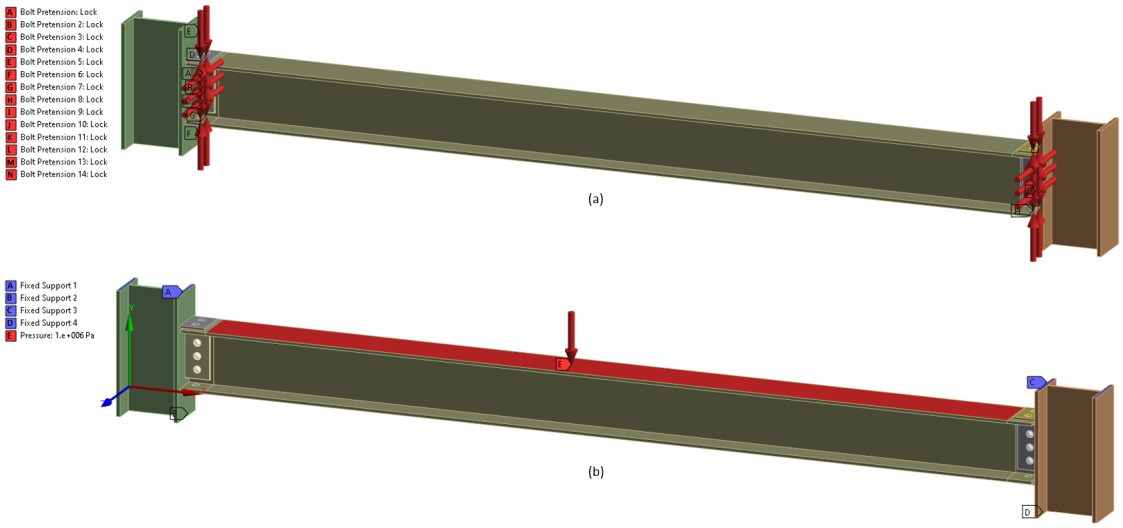

Figure 3.8: FE model of the connection showing (a) Bolt pretension load and (b) Fixed supports and beam load

The second load step involved the application of pressure on the top beam flange. The uniform pressure load prevents local yielding that would have occurred due to a concentrated load at a single point. The pressure facilitates rotational movement at the beam connections, allowing for the measurement of shear and axial displacements at the contact interface. Two different loading protocols are implemented to capture the static and dynamic responses of the beam-column connection, as depicted in Figure 3.9:

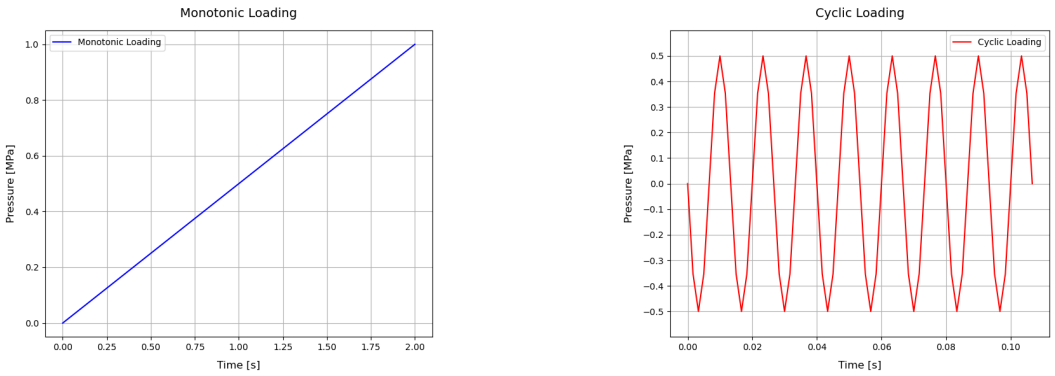

(a) **(b)**

Figure 3.9: (a) Monotonic and (b) Cyclic pressure loading conditions

1. **Monotonic Loading until Failure:** A linearly increasing pressure of 1 MPa is applied to the top flange to simulate the static response of the beam connection until failure. This loading protocol aims to assess the structural behaviour under steadily increasing pressure conditions.

2. **Fully Reversed Cyclic Loading:** This protocol subjects the connection to fully reversed cyclic loading in the range of -0.5 to +0.5 MPa. The applied pressure range represents service loads aimed at evaluating the connection's performance under cyclic loading conditions similar to operational scenarios. The cyclic load is applied incrementally at a frequency of 75 Hz, which was determined through a detailed modal analysis as the resonant frequency of the structure.

   Modal analysis was conducted to identify the natural frequencies and corresponding mode shapes of the structure. The third mode was found to be particularly representative of the beam-column connection's behaviour under vertical loading conditions. By selecting the resonant frequency associated with this mode, the cyclic loading effectively replicates the dynamic conditions most likely to induce significant effects in real-world applications. The choice of 75 Hz is, therefore, crucial for accurately simulating the dynamic response of the connection, including potential resonance phenomena that could amplify displacements and stresses.

   Upon determining this frequency, a transient analysis was performed, applying sinusoidal forces described by $F(t) = F_0 \cdot \sin(\omega t + \phi)$, where ω represents the force excitation frequency in radians per second, t is time in seconds, and ϕ is the phase angle.

3.3. Finite Element Analysis Results

To thoroughly assess the behaviour of the beam-column connection, the finite element model (FEM) results are examined at three critical contact interfaces: between the top plate and the top flange of the beam, between the web plate and web of the beam, and between the bottom plate and bottom flange of the beam. The force-displacement response for each of these components is extracted from the analysed model, providing detailed insights into the performance of the connection under various loading conditions.

3.3.1. Connection under monotonic loading condition

First, the static behaviour of the beam-column connection under monotonic loading conditions is analysed. A linearly increasing pressure of up to 1 MPa was applied to the top beam flange, resulting in the deformation of plates and beam elements of connection as illustrated in Figure 3.10.

As the load is applied to the top flange of the beam, an axial load transfer mechanism is observed between the beam flanges and the top and bottom plates of the connection. Simultaneously, a shear load transfer mechanism between the beam web and the web plates is evident. The force reactions are measured at the contact interface of each plate and the column flange to quantify the force transfer

mechanism. Based on the axial and shear force transfer mechanism, each individual connection can be divided into three main components:

1. Component 1: Top plate and beam top flange,
2. Component 2: Web plate and beam web, and
3. Component 3: Bottom plate and beam bottom flange.

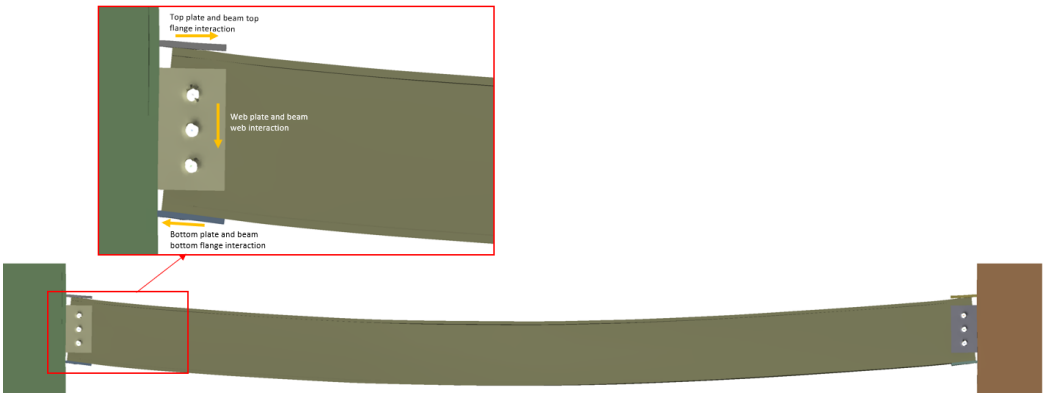

Figure 3.10: Deformed model of connection under monotonic loading conditions

The relative displacements between the beam and joint elements at the contact interfaces are extracted at specific contact points. Figure 3.11 illustrates the FE model of an individual joint assembly, highlighting the key locations where results are extracted. The leftmost section of the figure shows the joint assembly, which includes the beam and associated joint elements. To facilitate detailed analysis, the joint is decomposed to display the surfaces of the beam flanges and web, along with the top-seat and web plates. The figure also indicates the precise points where displacement results are collected. Force-displacement curves are generated by plotting the reaction forces from each plate against their corresponding relative displacements. These curves effectively capture the sliding behaviour between each component's frictional plates and beam elements. Figure 3.12 compares these force-displacement curves under monotonic loading conditions.

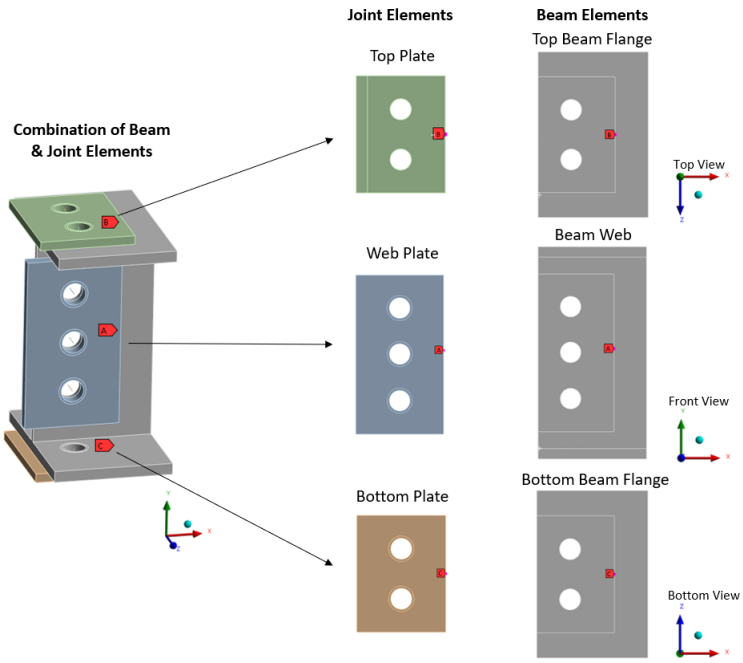

Figure 3.11: Contact points for displacement result extraction at beam and joint interfaces

The force-displacement curves in Figure 3.12 present the complex interaction between the various components of the beam-column connection under static loading. The top and bottom plates, which handle axial loads, exhibit a similar initial elastic response characterised by a steep slope, indicating strong resistance to initial deformation. As the loading progresses, both components transition into a plastic phase, with the top plate displaying more pronounced yielding behaviour. The web plate, which manages shear loads, shows a rapid increase in force initially, followed by a plateau. This plateau suggests a reduction in stiffness, likely due to slipping at the contact interface. To further characterise the stiffness, the responses observed in these curves are simplified into a bi-linear curve as discussed earlier in Section 3.1.1. This allows for the extraction of key stiffness parameters: pre-yield stiffness K_{p1}, post-yield stiffness K_{p2}, and the effective stiffness K_e. The stiffness results of the individual connection under static loads are summarised in Table 3.2.

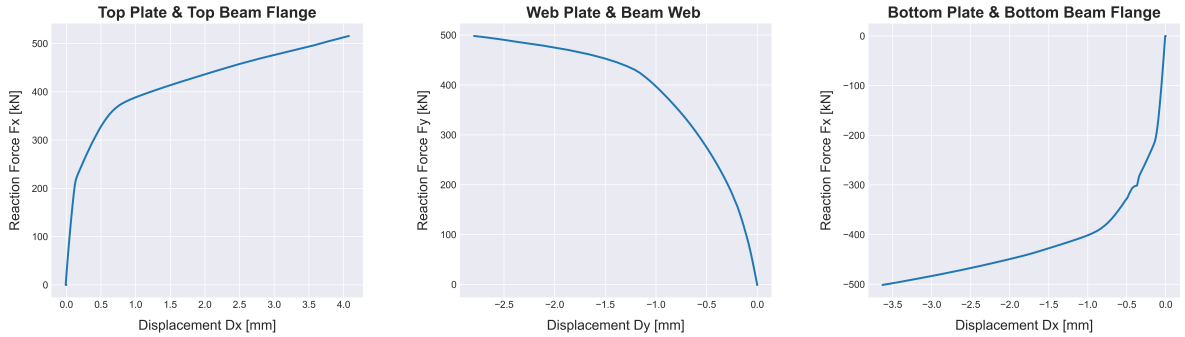

Figure 3.12: Force-displacement curves for monotonic loading condition

Table 3.2: Stiffness results for beam-column connection components under static loading (kN/m)

Component	Top plate & top beam flange	Web plate & beam web	Bottom plate & bottom beam flange
Pre-Yield Stiffness (K_{p1})	1692242.33	860005.54	1697517.47
Post-Yield Stiffness (K_{p2})	39570.56	40303.51	35362.72
Effective Stiffness (K_e)	126434.31	-183152.54	138175.58

3.3.2. Connection under cyclic loading condition

The behaviour of the beam-column connection subjected to fully reversed cyclic loading in the range of -0.5 to +0.5 MPa is analysed over eight cycles to observe the transition from initial fluctuations to a steady-state response. Identifying the steady-state phase is pivotal for understanding the long-term performance of the joint assembly under repeated loading conditions. The transient phase, typically observed during the early cycles, is characterised by temporary adjustments and frictional slips, which do not accurately reflect the behaviour of the connection under sustained loading. Therefore, focusing on the steady-state phase provides a more reliable basis for evaluating the stiffness, energy dissipation, and overall performance of the joint assembly.

Figure 3.13 presents the force-displacement hysteresis curves alongside the time history graphs of reaction force and displacement observed at three key components: the top plate & top beam flange, the web plate & beam web, and the bottom plate & bottom beam flange. The force-displacement hysteresis loops, as shown in Figure 3.13a demonstrates the connection's response to cyclic loading and highlight the sliding behaviour between the frictional plates of each connection component. During the initial cycles, the force-displacement relationship exhibits significant fluctuations due to frictional adjustments and sliding at the contact interfaces. However, as the loading cycles progress, the force-displacement relationship begins to stabilise, indicating a transition towards stead-state behaviour.

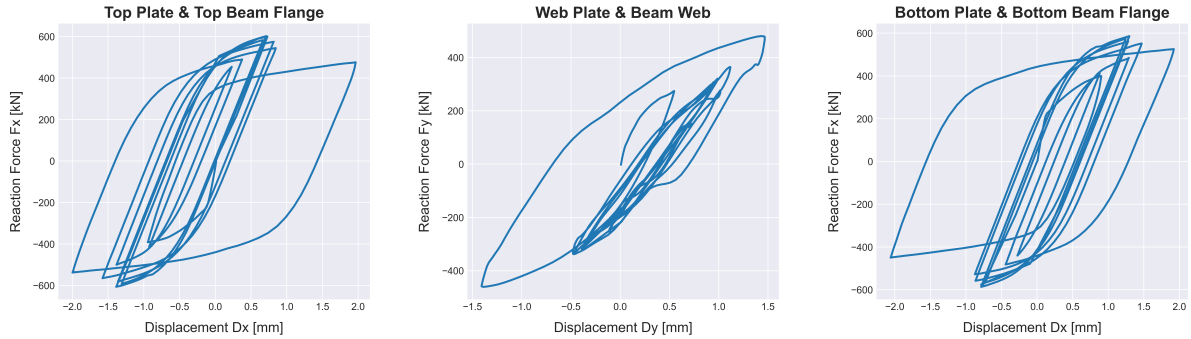

(a) Force-displacement hysteresis curves showing transient to steady-state behaviour

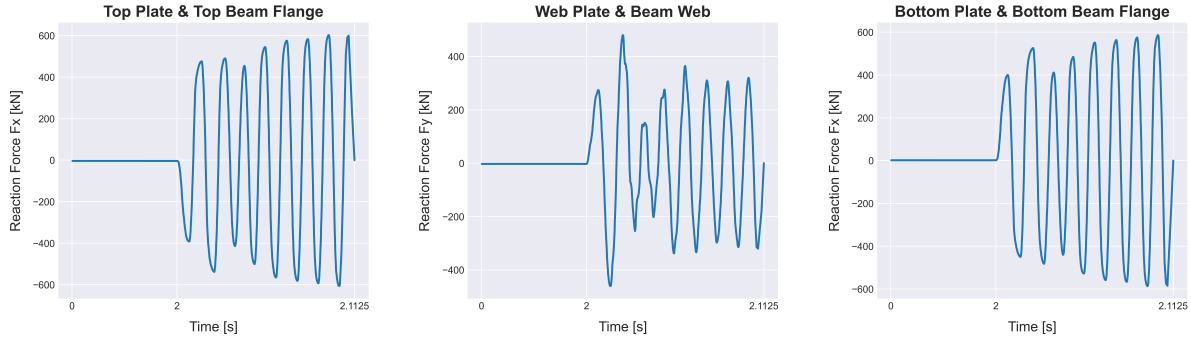

(b) Force vs time history for 8 cycles of cyclic loading

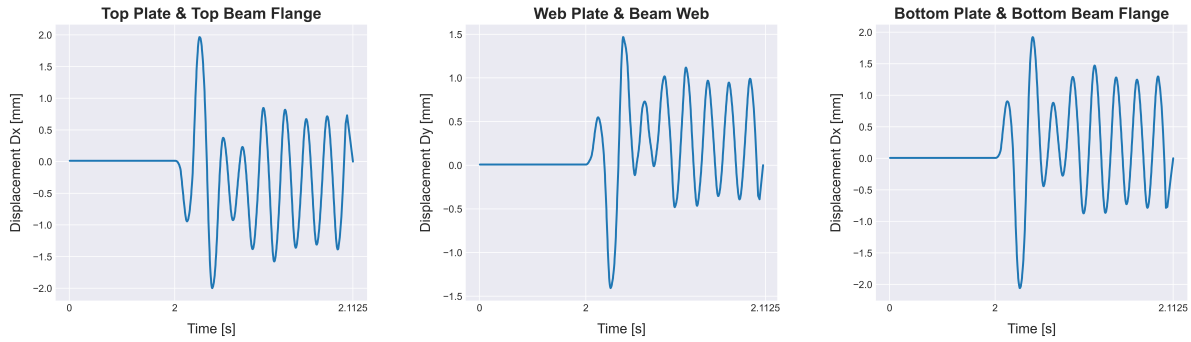

(c) Displacement vs time history for 8 cycles of cyclic loading

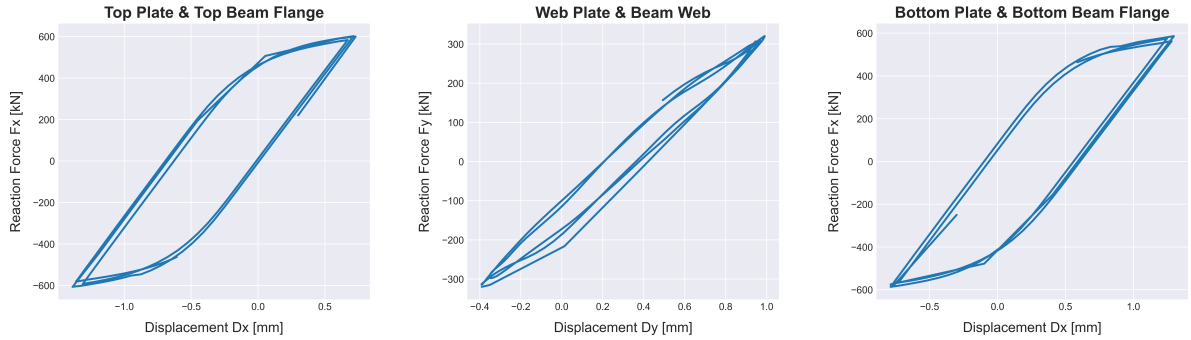

(d) Force-displacement hysteresis curves for cycles 6-8 showing steady-state behaviour

Figure 3.13: Force-displacement and time history graphs under cyclic loading

The emergence of steady-state behaviour is further supported by the time history graphs of force versus time and displacement versus time, as depicted in Figures 3.13b and 3.13c. These graphs reveal considerable variations in the amplitude of both force and displacement during the initial cycles, reflecting the system's adjustment to the applied cyclic loads. However, as the cycles progress, these fluctuations diminish, and the time history graphs begin to exhibit consistent patterns with uniform amplitude, indicating that the connection has reached a stable response. From cycle 6 onwards, the time history patterns remain stable, with consistent amplitudes across cycles, further confirming the steady-state behaviour.

Figure 3.13d focuses on the force-displacement hysteresis behaviour of each connection component during cycles 6-8, highlighting the stabilised response of the connection. The steady-state behaviour observed in these cycles confirms that the connection has adjusted to the cyclic loading. The force-displacement hysteresis loops and time history graphs both show a consistent and repeatable response, indicating that the connection is durable and reliable under repeated loading conditions.

Table 3.3 presents the stiffness and energy dissipation results specifically extracted from cycle 8, which best represents the steady-state behaviour of the connection. The table summarises the pre-yield stiffness K_{p1}, post-yield stiffness K_{p2}, effective stiffness K_e, and energy dissipation for each of the three components: the top plate & top beam flange, the web plate & beam web, and the bottom plate & bottom beam flange.

Table 3.3: Stiffness and energy dissipation results for beam-column connection components under cyclic loading

Component	Top plate & top beam flange	Web plate & beam web	Bottom plate & bottom beam flange
Pre-Yield Stiffness K_{p1} (kN/m)	786799.6	520342.2	719762.4
Post-Yield Stiffness K_{p2} (kN/m)	158109.5	441137.9	144129.0
Effective Stiffness K_e (kN/m)	590336.6	310005.8	571500.3
Energy Dissipation (KJ)	0.778	0.130	0.760

The results show that the top and bottom plates & beam flanges exhibit higher stiffness compared to the web plate & beam web. This difference is largely due to the role of these components in resisting axial loads, resulting in greater stiffness to prevent excessive deformation. The web plate & beam web, on the other hand, is primarily responsible for managing shear forces. The post-yield stiffness is lower than the pre-yield stiffness values, as expected, due to the onset of plastic deformation within the connection. Once the material yields, it loses some of its elastic properties, leading to increased deformations under the same applied loads. This reduction in post-yield stiffness is indicative of the material's transition from elastic to plastic behaviour, where it no longer returns to its original shape upon unloading. The effective stiffness, calculated by fitting a straight line to the extreme ends of hysteresis loops, represents the overall stiffness of the components in their stabilised state under cyclic loading. The effective stiffness remains relatively high in the top and bottom plates & beam flanges even after yielding.

Additionally, the energy dissipation capacity of each component, which is critical for understanding the connection's damping characteristics, was assessed by calculating the area enclosed by each cycle in the force-displacement hysteresis loop. the top and bottom plates & beam flanges demonstrate a greater capacity to absorb and dissipate energy compared to the web plate & beam web. This higher energy dissipation is a result of the larger areas enclosed by their hysteresis loops, which indicate that these components undergo more significant inelastic deformation. The ability to dissipate energy is essential for reducing the amplitude of vibrations and mitigating the effects of dynamic loads, ultimately enhancing the connection's durability and resilience under cyclic loading.

3.3.3. Conclusion

The static and cyclic analysis of the semi-rigid beam-column connection reveals significant insights into the behaviour of the connection under varying loading conditions. The static analysis demonstrates that the top and bottom plates & beam flanges exhibit higher stiffness compared to the web plate & beam web, primarily due to their role in resisting axial loads. The force-displacement curves effectively capture the transition from elastic to plastic behaviour, highlighting the distinct stiffness characteristics at different stages of loading.

Under cyclic loading, the force-displacement hysteresis loops and time history graphs reveal the connection's transition from a transient state to a stable, steady-state behaviour. This transition is key to understanding the variation in stiffness and energy dissipation capabilities of the connection during loading and unloading conditions. The higher stiffness and energy dissipation observed in the top and bottom plates & beam flanges, compared to the web plate & beam web, indicate their greater capacity to resist deformation, further highlighting their significant role in enhancing the durability and resilience of the joint assembly. These findings emphasise the importance of considering the dynamic behaviour of connections in structural design.

The results presented in this chapter are pivotal in integrating simplified joint behaviour into large-scale structural models under both static and dynamic loading conditions. By capturing the essential characteristics of semi-rigid connections, these findings facilitate the application of the Component-Based Spring Method (CBSM) to simplify structural design methodologies. This approach enables engineers to model complex joint behaviours more efficiently without compromising accuracy. CBSM application, discussed in subsequent chapters, leverages these insights to enhance the design and analysis of multi-story steel frame structures, ensuring both computational efficiency and realistic performance predictions.

3.4. Validation Study

This section presents the validation of the non-linear modelling technique used in ANSYS for finite element analysis. The validation process involves comparing the results obtained from the FE model with manual calculations based on Eurocode guidelines. A simpler connection is chosen for validation to minimise complexities and ensure the applicability of Eurocode guidelines. The selected connection is a fin plate beam-column connection, consisting of a single web plate welded to the column flange and bolted to the beam web, as illustrated in Figure 3.14. This simple joint primarily transmits shear forces from the beam web to the supporting member.

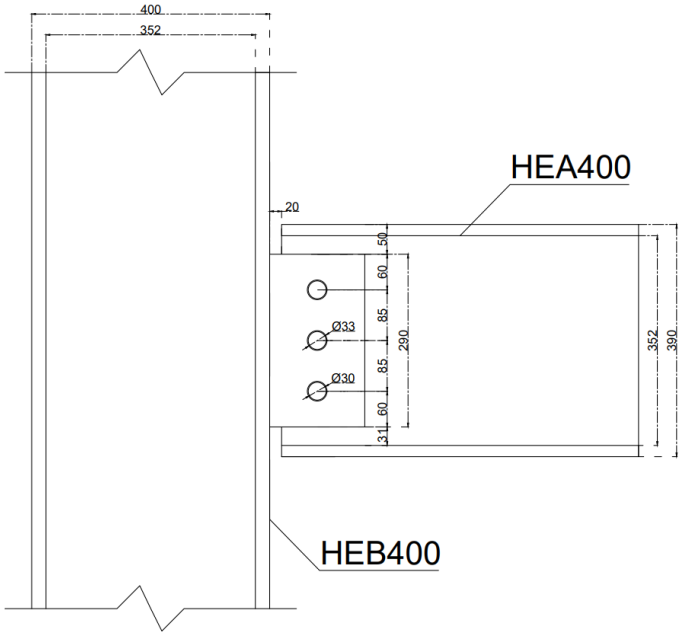

Figure 3.14: Details of fin-plate connection

3.4.1. Finite Element Method

The chosen fin plate for the validation study has a depth of 290 mm, a width of 160 mm, and a thickness of 20 mm, made from steel grade S275. The connection uses three M30 bolts of grade 8.8 to attach the fin plate to the beam web, with a hole clearance of 33 mm. Geometric and material nonlinearity effects are incorporated into the model. In the absence of experimental material data, the material model for monotonic loading in FEA can be formulated based on Eurocode guidelines. As outlined in EN 1993-1-1:2005 and illustrated in Figure 3.15, the elastic-plastic stress-strain characteristics can be represented using a trilinear stress-strain curve.

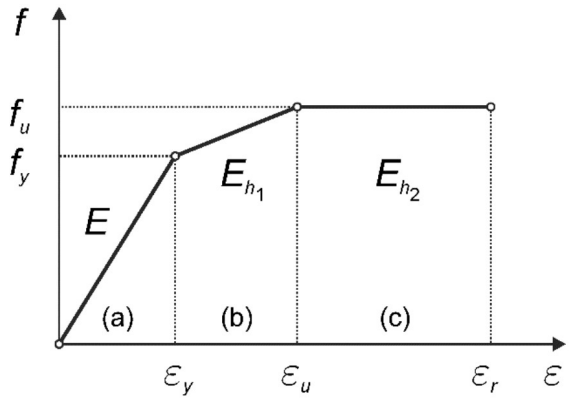

Figure 3.15: Material stress-strain curve as described in EN 1993-1-1:2005

The curve is divided into three distinct regions:

1. Region (a): elastic modulus E, as defined in EN 1993-1-1:2005, Section 3.2.6.
2. Region (b): $E_{h1} = (f_u - f_y)/(\epsilon_u - \epsilon_y)$, with $\epsilon_u = 15\epsilon_y$, where ϵ_u is the ultimate strain, ϵ_y is the yield strain, with $\epsilon_y = f_y/E$, as specified in EN 1993-1-1:2005, Section 3.2.2.
3. Region (c): $E_h = 0$, with $\epsilon_r = 10\epsilon_u$.

As a result, the material behaviour in Ansys is represented using a trilinear-isotropic hardening approach, as illustrated in Figure 3.16. This method involves three key stages: initially, it considers the yield stress, applying a slope corresponding to the Young's Modulus of material(E). Once the yield stress is exceeded, the model transitions into a second phase characterised by a reduced slope known as the Tangent Modulus. This phase continues until reaching a predefined strain level, at which point the model progresses to the third stage where the material exhibits a constant ultimate strength, corresponding to a slope of zero.

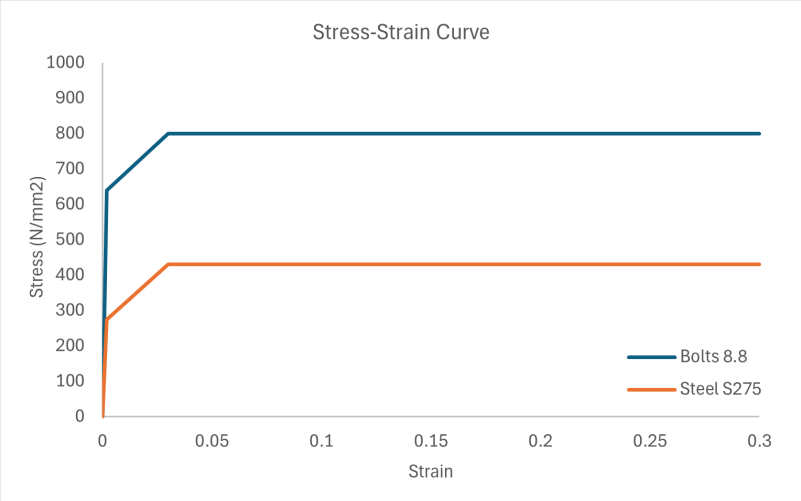

Figure 3.16: Trilinear stress-strain model of material in ANSYS

Meshing is strategically coarser along the beam length but more refined near the connection areas to effectively capture the non-linear effects of bolt interactions. The contact interactions between the fin plates and the beam web are modelled using the penalty method to simulate friction, with a friction coefficient of 0.2. The bolts are represented as 1-D line elements, configured with bonded contacts to the bolt head and nut through Multi-Point Constraints (MPC). Fixed supports are applied to the ends of the fin plate to simulate rigid plate-column connections at both beam ends. To ensure a controlled load application, a uniform pressure load of 1 MPa is distributed along the top flange of the beam using multiple steps and substeps. Static structural analysis is performed to obtain connection response under given loading conditions.

3.4.2. Analytical Method

The fin plate connection is manually evaluated according to Eurocode 3 using the component method. Several checks are performed for each component of the connection, with complete details provided in Appendix A. Local deformations due to bearing near the bolts of the beam web and fin plate, as well as bolt shear deformations, are taken into account. Deformations of the column and welds are neglected.

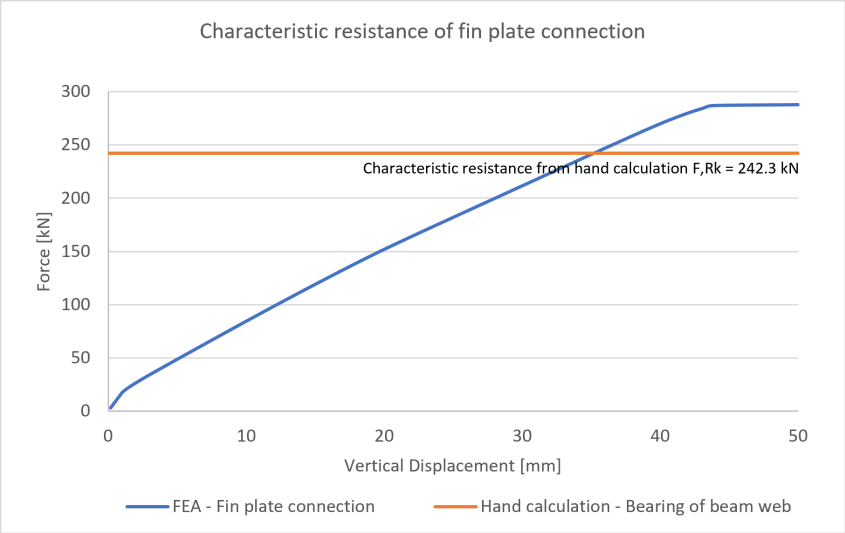

Figure 3.17: FEA result - characteristic resistance of fin plate connection

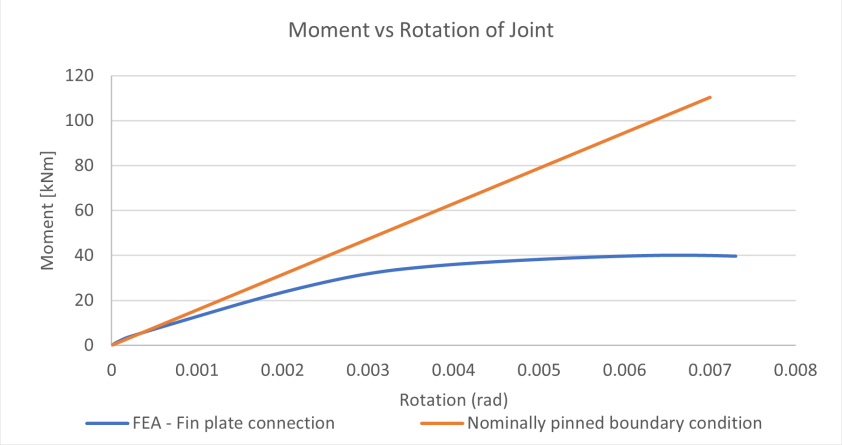

Figure 3.18: FEA result - rotational stiffness of fin plate connection

3.4.3. Result Discussion and Conclusion

The failure mechanism of the fin plate connection, determined through manual calculations, initiates with bearing failure in the web, followed by block shear tearing in the web, as detailed in calculations in Appendix A. Although the fin plate and beam web were modelled with the same S275 material properties, the fin plate is 9mm thicker, which increased its resistance and caused the failure mode to begin with bearing failure in the beam web. The characteristic resistance of the fin plate connection is F, RK = 242kN. The shear resistance of the beam web from FEA shows good agreement with hand calculations, as shown in Figure 3.17. The force reaction before failure of the fin connection from FEA is 223 kN, whereas the characteristic resistance from hand calculations is 242 kN, yielding less than an 8% difference between the FEA results and hand calculations. It is suggested that modelling the bolts in 3D could improve the accuracy of the results by enhancing load distribution around the bolts.

In Figure 3.18, the moment-rotation curve for the beam extends up to 0.0073 radians. This limitation arises because the FE model fails to converge beyond this point due to failure in the beam web. For the applied load, the rotation of the fin plate, calculated manually, is 0.0076 radians. This result from the FEA closely aligns with the hand calculations, confirming the accuracy of the simulated fin plate rotation. Furthermore, the FEA results suggest that the fin plate connection qualifies as a nominally pinned connection, as the rotational stiffness of the joint falls below the threshold set by Eurocode 3. The characteristic moment capacity of the joint, determined through FEA, is M_{Rk} = 36 kNm.

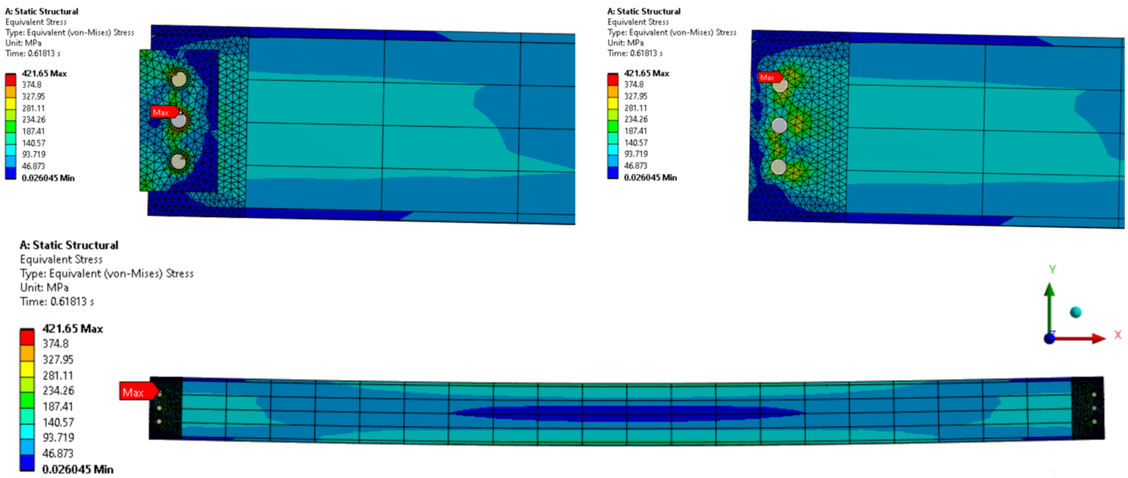

Figure 3.19: Deformed shape and von Mises stresses (in MPa) at failure mode

In Figure 3.19, the failure of the fin plate connection can be attributed to a combination of several failure modes. From the FEA results, it is evident that the initial failure mode is due to the bearing failure of the beam web. The stress around the hole reaches 421 MPa, indicating bearing failure in the beam web. This type of failure is influenced by the ultimate strength of the fin plate, defined as 430 MPa. Additionally, the characteristic resistance of the component can be determined by observing a 3.15% strain in the element, a limit based on the ultimate strain definition in the material properties, where $\epsilon_u = 15\epsilon_y$, as specified in Section 3.4.1. At an incremental resultant load of 221 kN, the plastic strain at the bearing of the web had reached 3.15% strain.

The validation of the modelling techniques used in the FEA is confirmed by comparing the connection resistance, failure modes, and rotation results from the FEA with those obtained from hand calculations. The close agreement between the FEA results and manual calculations demonstrates the reliability and accuracy of the FEA modelling approach. This consistency confirms that the finite element model effectively represents the physical behaviour of bolted connections, ensuring its applicability for predicting the performance of more complex assemblies.

4

Parametric Study

In this chapter, a detailed parametric study is conducted on the beam-to-column bolted connection to assess the influence of various design parameters on the behaviour of the connection. The study focuses on how alterations in key parameters affect the structural response, particularly in terms of stiffness and energy dissipation. The following parameters are systematically varied to understand their impact on joint performance::

1. Influence of Friction Resistance between the plate and beam elements,
2. Influence of Bolt Pretension load
3. Influence of Cyclic Load Application

The finite element model presented in Section 3.2, consisting of top-seat and web plates welded to the column flange and bolted to beam elements, is used for the parametric study. In the base case finite element model, a coefficient of friction (μ) of 0.2 is assumed at the contact interface between the plates and beam elements. Additionally, a bolt pretension load of 400 kN is applied to each bolt within the connection. Following pretensioning, a cyclic load ranging from -0.5 MPa to +0.5 MPa is uniformly applied to the top flange of the beam and a transient dynamic analysis is performed.

This base case setup serves as the reference for assessing the effects of varying friction resistance, bolt pretension load, and cyclic load application on the stiffness and energy dissipation characteristics of the connection. As discussed in Section 3.3.2, the behaviour of the beam-column connection under cyclic loading stabilizes after the sixth cycle. Therefore, the stiffness and damping results for the parametric study are extracted from cycle 8, which reliably represents the steady-state behaviour of the connection. The following sections examine the influence of these parameters, with a focus on analyzing the resulting stiffness and damping behaviour.

4.1. Influence of Friction Contact Interface

This section investigates the influence of friction on the behaviour of the beam-column connection by varying the frictional resistance between the contact interface of the plate and beam elements. The coefficient of friction (μ) is varied between 0.1, which simulates a condition with significant relative slip, to 0.7, representing a nearly ‘stick’ condition. The variations aim to explore the potential effects that frictional contact may have on the cyclic response of the structure.

Tables 4.1 to 4.3 presents the results for the key components: the top plate & top beam flange, the web plate & beam web, and the bottom plate & bottom beam flange. The table presents the pre-yield

stiffness K_{p1}, post-yield stiffness K_{p2}, effective stiffness K_e, and energy dissipation across different friction coefficients. These results provide insights into how changes in friction affect the structural response, particularly in terms of stiffness and damping characteristics.

Table 4.1: Friction parametric study results for component: top plate & beam top flange

Friction Coefficient	Pre-Yield Stiffness (kN/m)	Post-Yield Stiffness (kN/m)	Effective Stiffness (kN/m)	Energy Dissipation (kJ)
0.1	796753.9	155401.3	580508.3	0.662
0.2	817734.1	158109.5	590336.6	0.652
0.3	850586.0	160987.9	598852.3	0.637
0.5	872803.3	226464.9	623925.1	0.409
0.7	876620.1	229753.7	627267.4	0.416

Table 4.2: Friction parametric study results for component: web plate & beam web

Friction Coefficient	Pre-Yield Stiffness (kN/m)	Post-Yield Stiffness (kN/m)	Effective Stiffness (kN/m)	Energy Dissipation (kJ)
0.1	511002.7	327443.5	306213.0	0.079
0.2	520342.2	441137.9	310005.8	0.076
0.3	643611.8	457607.2	470471.4	0.069
0.5	669237.6	469240.6	484355.1	0.038
0.7	845695.7	470594.5	507968.4	0.037

Table 4.3: Friction parametric study results for component: bottom plate & beam bottom flange

Friction Coefficient	Pre-Yield Stiffness (kN/m)	Post-Yield Stiffness (kN/m)	Effective Stiffness (kN/m)	Energy Dissipation (kJ)
0.1	778670.7	143637.9	571291.1	0.661
0.2	788291.4	144129.0	571500.3	0.650
0.3	822629.0	144768.8	571718.2	0.636
0.5	861257.8	201212.1	620202.2	0.393
0.7	862455.8	216600.6	626203.2	0.392

Figures 4.1 illustrate the results presented in the above tables. For the top and bottom plates & beam flanges, the results demonstrate a clear increase in stiffness (pre-yield, post-yield, and effective stiffness) as the friction coefficient increases from 0.1 to 0.7. This trend indicates that higher friction at the contact interface reduces slip, leading to greater resistance to deformation and enhancing the load-bearing capacity of the connection. However, a reduction in energy dissipation is observed with an increase in friction resistance. As friction increases, the ability of these components to absorb and dissipate energy during cyclic loading diminishes, with the lowest energy dissipation observed at the highest friction coefficients. This trade-off highlights the balance between achieving greater rigidity and maintaining sufficient damping capacity.

In the web plate & beam web component, similar trends are observed with respect to stiffness, where higher friction coefficients result in increased pre-yield and post-yield stiffness and effective stiffness. However, the energy dissipation in the web plate & beam web remains relatively low across all friction levels, with only slight variations. This indicates that while the web plate becomes stiffer with higher friction, its contribution to overall energy dissipation remains limited, particularly at higher friction levels where slip is minimized.

Overall, the parametric study shows that increasing the friction coefficient generally enhances the stiffness of the beam-column connection across all components, but this improvement in stiffness is accompanied by a reduction in energy dissipation capacity. These trends highlight the need to carefully balance friction levels in designing beam-column connections to optimize structural integrity and energy absorption, particularly under cyclic loading conditions.

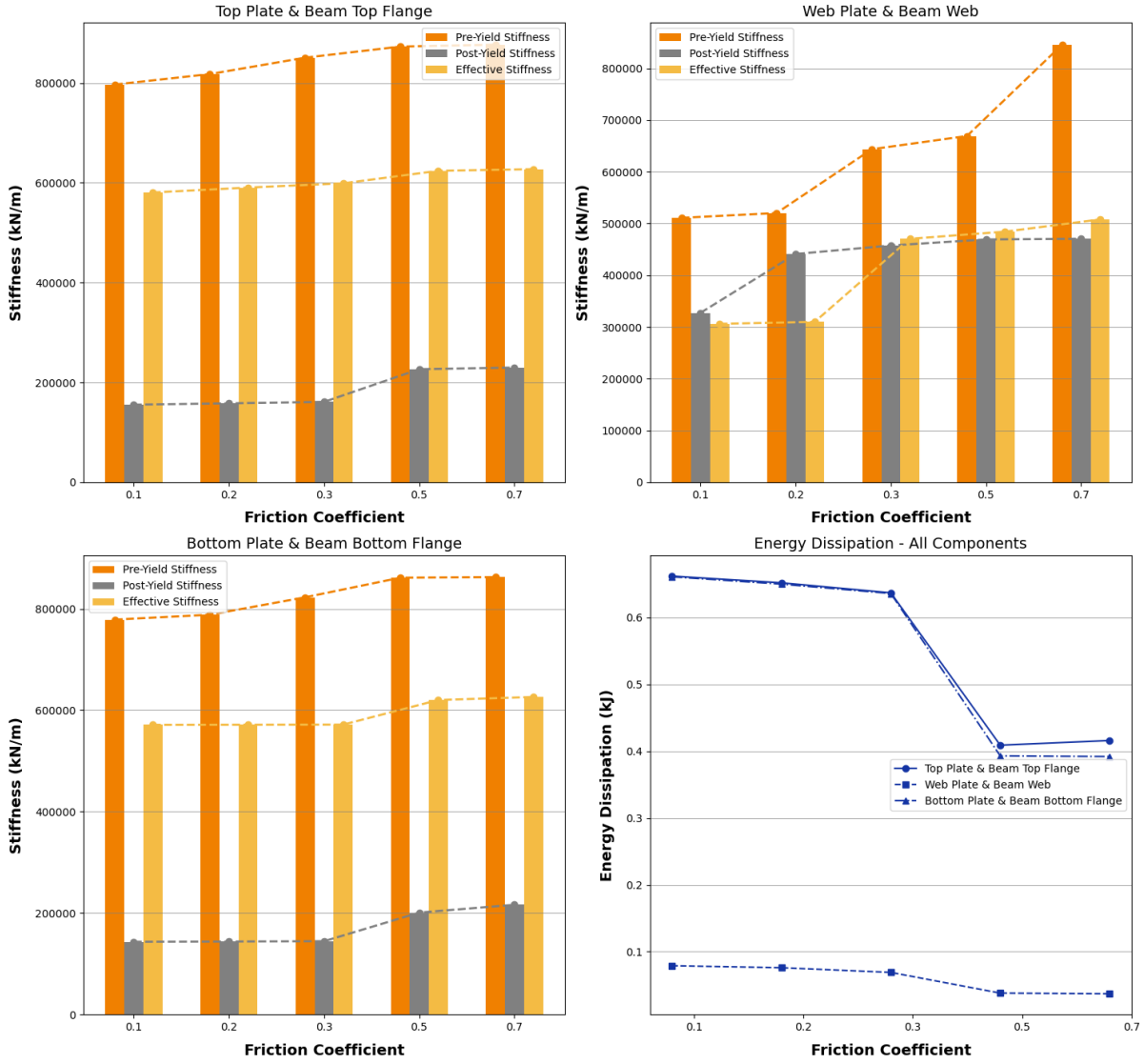

Figure 4.1: Friction parametric results for joint assembly

4.2. Influence of Bolt Pretension

Bolts in steel structures are tightened using pretension force to establish a contact interface between surfaces, thereby enhancing the structure's resistance to deformation under service loads. However, the loss of preload can occur over the service life of bolted connections, particularly those subjected to slip-resistant or fatigue loading. This preload loss can lead to bolt loosening, reducing the connection's load-bearing capacity and posing a risk to the structure's serviceability. Additionally, overloading during service life or the initial tightening process can damage and adversely affect the performance of the connection.

Various degrees of bolt pretension were examined to investigate the impact of bolt pretension on the performance of the connection. As described in Section 3.2.4, according to EN 1993-1-8, the total

bolt preload force (Fp) is calculated as 0.7$f_{ub}A_s$/γ = 400kN, where f_{ub} represents the bolt's ultimate strength, A_s is the bolt's tensile stress area, and γ is a safety factor. This study compared five different bolt pretension magnitudes: 100 kN, 200 kN, 300 kN, 400 kN, and 500 kN, considering scenarios of both pretension loss and overloading. Tables 4.4 to 4.6 presents the pre-yield stiffness K_{p1}, post-yield stiffness K_{p2}, effective stiffness K_e, and energy dissipation results for each of the three components: the top plate & top beam flange, the web plate & beam web, and the bottom plate & bottom beam flange. These results illustrate the relationship between bolt pretension levels and the structural response of the connection.

Table 4.4: Bolt pretension parametric study results for component: top plate & beam top flange

Bolt Pretension [kN]	Pre-Yield Stiffness (kN/m)	Post-Yield Stiffness (kN/m)	Effective Stiffness (kN/m)	Energy Dissipation (kJ)
100	806845.9	144973.9	587747.9	0.719
200	805509.9	144957.0	586504.9	0.719
300	779270.3	150669.3	584611.2	0.674
400	817734.1	158109.5	590336.6	0.652
500	836210.3	164680.7	598993.9	0.645

Table 4.5: Bolt pretension parametric study results for component: web plate & beam web

Bolt Pretension [kN]	Pre-Yield Stiffness (kN/m)	Post-Yield Stiffness (kN/m)	Effective Stiffness (kN/m)	Energy Dissipation (kJ)
100	407595.7	352266.8	455261.1	0.096
200	404001.9	355826.6	454513.5	0.095
300	546219.2	407810.2	303835.8	0.081
400	520342.2	441137.9	310005.8	0.076
500	534098.8	455720.3	316381.4	0.071

Table 4.6: Bolt pretension parametric study results for component: bottom plate & beam bottom flange

Bolt Pretension [kN]	Pre-Yield Stiffness (kN/m)	Post-Yield Stiffness (kN/m)	Effective Stiffness (kN/m)	Energy Dissipation (kJ)
100	335238.1	106060.6	573287.4	0.711
200	334194.9	106473.1	571889.5	0.710
300	707434.9	136918.7	568739.1	0.663
400	788291.4	144129.0	571500.3	0.650
500	845124.7	150766.2	575870.3	0.641

The results displayed in the tables above is depicted in Figure 4.2. For the top and bottom plates & beam flanges, the results indicate that increasing bolt pretension enhances the stiffness of the connection. Both the pre-yield and post-yield stiffness and the effective stiffness increase noticeably with higher pretension levels. This behaviour can be attributed to the increased clamping force exerted by the bolts, which strengthens the contact interface, reduces slip, and improves load transfer between the connected elements. As a result, the resistance of connection to deformation is significantly improved.

However, the increase in stiffness is accompanied by a slight reduction in energy dissipation capacity. As bolt pretension increases, energy dissipation decreases, indicating that while the connection becomes more rigid, its ability to absorb and dissipate energy during cyclic loading is slightly compromised. This trend reflects the balance between increased stiffness and reduced deformation capacity, which can impact the ability of the connection to dissipate dynamic loads.

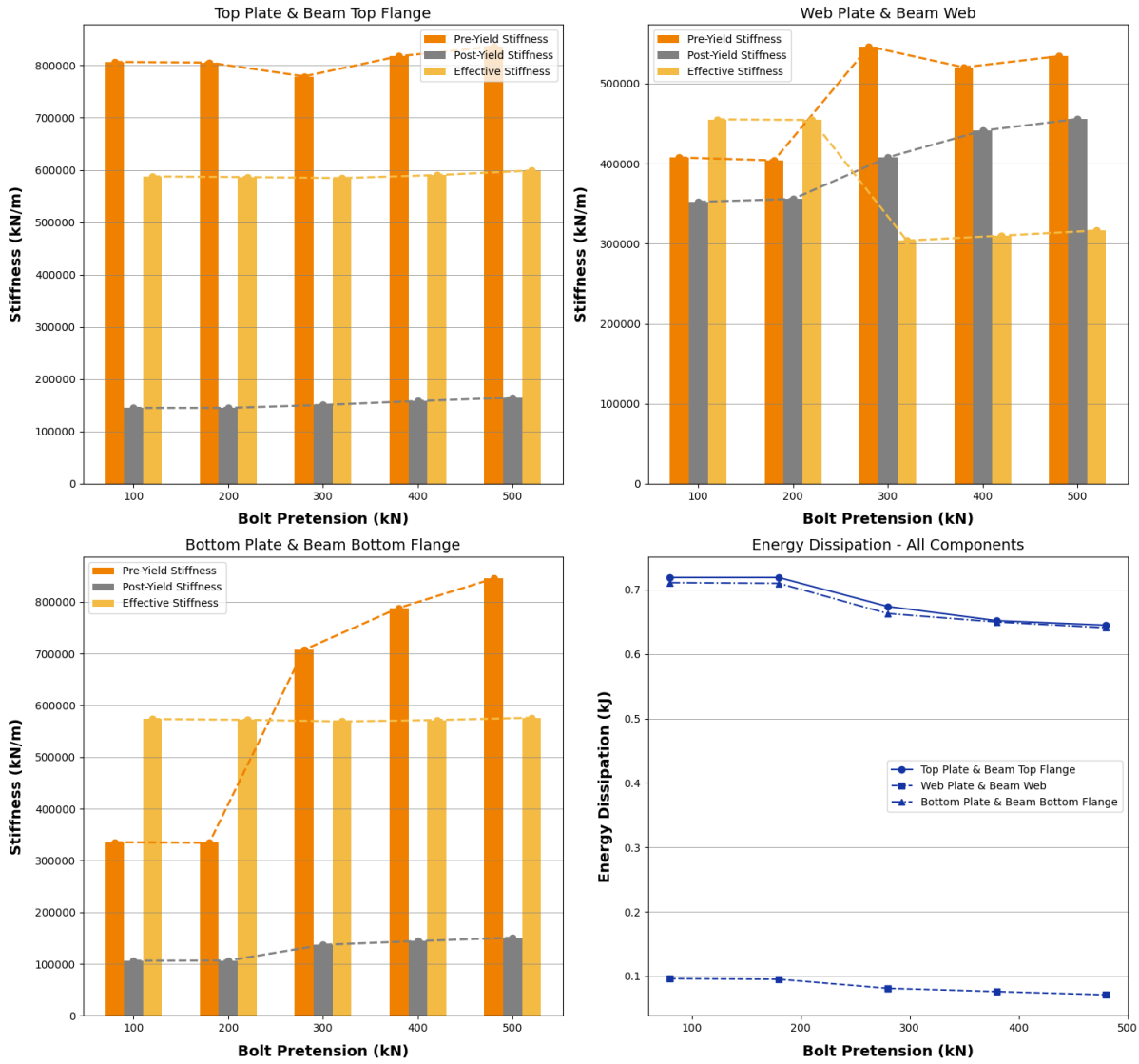

Figure 4.2: Bolt pretension parametric results for joint assembly

In contrast, the web plate & beam web component exhibit a more complex response to increasing bolt pretension. While the post-yield stiffness improves, reflecting an enhanced load-bearing capacity in the plastic range, the effective stiffness and energy dissipation decrease at higher pretension levels. This decrease suggests that higher pretension levels may limit the ability of web plates to undergo inelastic deformation and dissipate energy effectively.

The parametric study results highlight the importance of carefully balancing bolt pretension to achieve the desired structural performance, particularly in terms of stiffness and damping, while considering the specific loading conditions and functional requirements of the connection.

4.3. Influence of Cyclic Load Application

The third parametric study focuses on understanding the effect of varying vertical cyclic loads on the behaviour of beam-column connections in steel frame structures. During the load application, forces are transferred from the beam to the column through the connecting plates and bolts. By varying the magnitudes of cyclic loading, this study aims to evaluate the corresponding changes in the connections' stiffness and energy dissipation characteristics. These insights are essential for optimizing design

parameters and ensuring the structural resilience of multi-story steel frames under diverse loading conditions.

Cyclic loads can induce fatigue, leading to the gradual degradation of structural components over time. Therefore, understanding how different magnitudes of load affect the connection's ability to resist deformation (stiffness) and dissipate energy (damping) is critical for developing safer and more reliable structural designs. This study evaluates the pre-yield stiffness K_{p1}, post-yield stiffness K_{p2}, effective stiffness K_e, and energy dissipation across various load applications, ranging from 0.3 MPa to 0.9 MPa.

The results of the cyclic load application study are presented in Table. The tables summarize the stiffness and energy dissipation changes for the top plate & beam top flange, the web plate & beam web, and the bottom plate & beam bottom flange components as the applied load increases. The observed trends provide insights into how the connection's mechanical properties evolve with increasing cyclic loads.

Table 4.7: Cyclic load parametric study results for component: top plate & beam top flange

Load Application [MPa]	Pre-Yield Stiffness (kN/m)	Post-Yield Stiffness (kN/m)	Effective Stiffness (kN/m)	Energy Dissipation (kJ)
0.3	847936.8	217175.7	690840.4	0.250
0.4	829497.7	184672.9	651657.2	0.378
0.5	817734.1	158109.5	590336.6	0.652
0.7	816589.1	76697.4	506475.2	1.364
0.9	816634.8	93734.9	469231.0	1.855

Table 4.8: Cyclic load parametric study results for component: web plate & beam web

Load Application [MPa]	Pre-Yield Stiffness (kN/m)	Post-Yield Stiffness (kN/m)	Effective Stiffness (kN/m)	Energy Dissipation (kJ)
0.3	567202.6	496009.6	431128.8	0.023
0.4	470829.2	444353.1	409734.3	0.033
0.5	520342.2	441137.9	310005.8	0.076
0.7	469076.5	248656.7	313578.8	0.222
0.9	500059.7	271198.0	302040.5	0.392

Table 4.9: Cyclic load parametric study results for component: bottom plate & beam bottom flange

Load Application [MPa]	Pre-Yield Stiffness (kN/m)	Post-Yield Stiffness (kN/m)	Effective Stiffness (kN/m)	Energy Dissipation (kJ)
0.3	830241.2	194269.4	684490.2	0.255
0.4	806877.6	163847.5	639230.9	0.384
0.5	788291.4	144129.0	571500.3	0.650
0.7	788903.7	64540.1	495550.0	1.325
0.9	779355.4	69321.9	451525.2	1.891

Figures 4.3 depict the results presented in the above tables. The cyclic load parametric study reveals several trends across the three connection components. For the top and bottom plates & beam flanges, increasing the cyclic load magnitude from 0.3 MPa to 0.9 MPa reduces pre-yield, post-yield, and effective stiffness. This reduction indicates a reduced capacity of these components to resist deformation as the applied load intensifies. However, this decrease in stiffness is accompanied by a significant increase in energy dissipation. This trend is particularly pronounced in the top and bottom plates, where

energy dissipation more than doubles as the load increases, underscoring their critical role in mitigating dynamic forces.

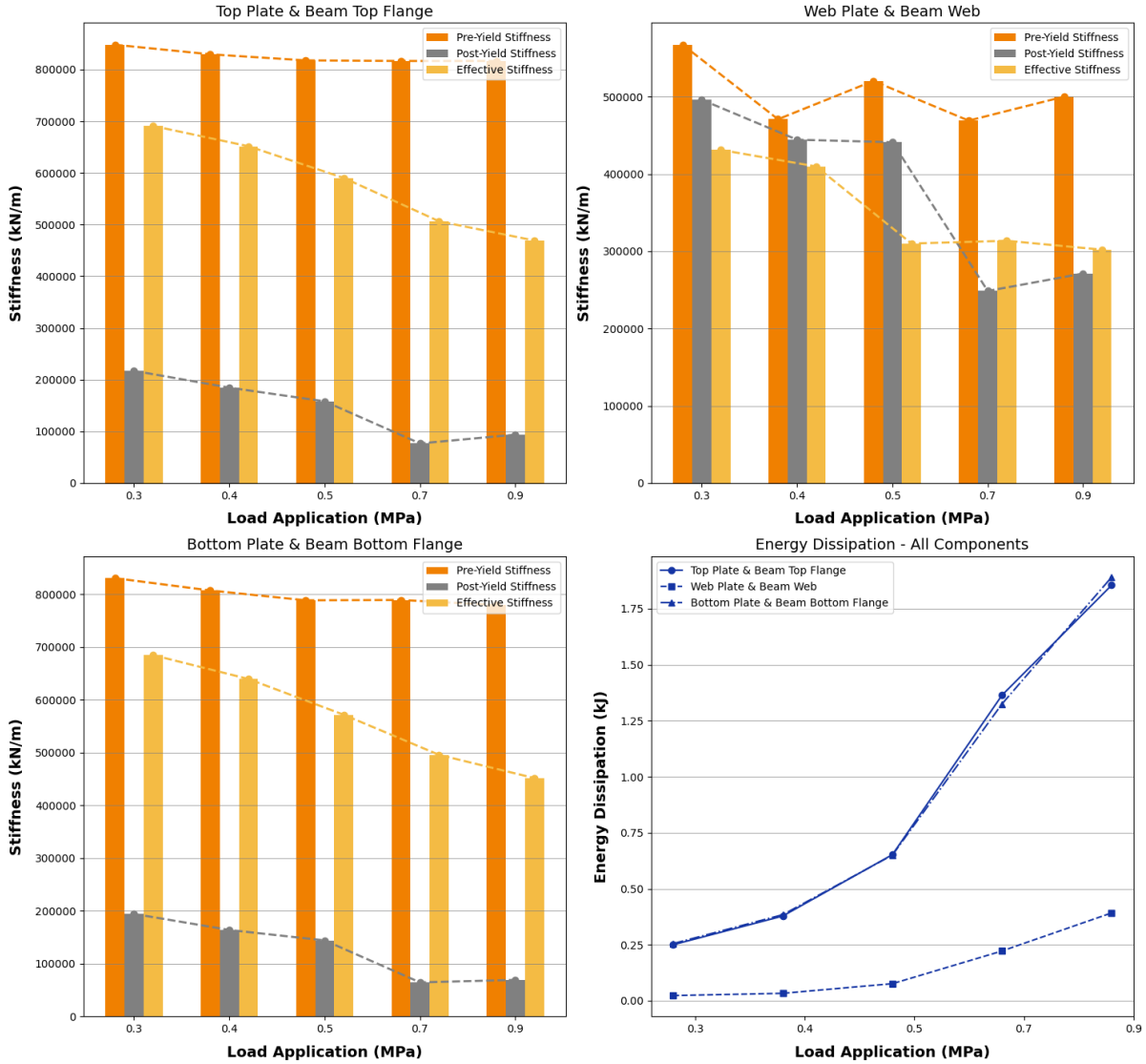

Figure 4.3: Cyclic load application parametric results for joint assembly

In contrast, the web plate & beam web component exhibit a more gradual reduction in stiffness with increasing load. Although the effective stiffness decreases similarly to the other components, the energy dissipation in the web plate shows a notable increase only at the higher load levels (0.7 MPa and 0.9 MPa).

Overall, the results of the parametric study highlight that as the cyclic load magnitude increases, the beam-column connection's stiffness decreases across all components, indicating a reduced ability to resist deformation. Simultaneously, the increase in energy dissipation suggests that the connection components, especially the top and bottom plates, play a vital role in absorbing and mitigating the effects of higher cyclic loads, contributing to the connection's resilience under dynamic service conditions.

4.4. Conclusion

The parametric study explored the impact of friction, bolt pretension, and load magnitude on the performance of beam-column connections, revealing important trends in stiffness and energy dissipation across the connection's components.

The results demonstrate that increasing the friction coefficient generally enhances the stiffness of the connection, particularly in the top and bottom plates & beam flanges. However, this increased stiffness is accompanied by a reduction in energy dissipation, underscoring the necessity of balancing rigidity with sufficient damping capacity. Similarly, higher levels of bolt pretension were found to improve the connection's stiffness, thereby enhancing its resistance to deformation. Yet, this improvement in stiffness is accompanied by a slight decrease in energy dissipation, indicating a potential trade-off between rigidity and the connection's ability to absorb and dissipate energy.

Additionally, the analysis of cyclic load application reveals that as the load magnitude increases, the stiffness of the connection decreases across all components. Despite this decrease in stiffness, there is a significant increase in energy dissipation, particularly in the top and bottom plates, which is crucial for the connection's resilience under dynamic loading conditions. The study highlights the critical need to carefully balance friction, bolt pretension, and cyclic load application when designing beam-column connections.

5

Static Frame Analysis

In industry, beam-column joints in frame structures are often modelled as either rigid or pinned joints. While this approach simplifies the modelling process and reduces computational demands, it does not accurately capture the semi-rigid behaviour of joints that occurs in real structures. The complexity involved in modelling semi-rigid joints due to factors like geometric and material nonlinearities, contact interactions, and others often necessitates simplification in practical modelling, which may not fully capture the behaviour of the structure. This chapter presents a numerical analysis to investigate the influence of beam-column joints on the performance of steel frames while also providing a simplified method to incorporate semi-rigid joint behaviour in frame analysis using the Finite Element Method (FEM) in ANSYS.

In Chapter 3, the Component-Based Method (CBM) was used to evaluate the behaviour of various components within semi-rigid connections under both monotonic and cyclic loading conditions. Building on this, Section 5.1 of the current chapter introduces the methodology of simplifying connection behaviour into a set of equivalent spring elements using the Component-Based Spring Method (CBSM). Subsequently, Section 5.2 examines the response of a three-story steel frame structure under different connection behaviours—rigid and semi-rigid to provide insights into the structural response of semi-rigid frames compared to traditional rigid frame structures.

5.1. Component-Based Spring Method

To accurately evaluate the internal stresses and displacements within a steel structure, it is essential to account for the flexibility of the beam-column joints. This requires considering the governing interactions between various components of a connection, as well as relevant sources of joint deformation. The Component-Based Spring Method (CBSM) is used to simulate joint behaviour in frame structures, in which equivalent spring elements are used to replicate the load transfer and the deformation behaviour of a joint assembly.

The beam-column connection under study consists of top-seat and web plates welded to the column flange and bolted to the beam elements. When a frame structure is subjected to loading, forces within the connection are transferred from the beam to the top-seat and web plates via bolts and subsequently to the columns. This connection can be divided into three primary components, each characterised by distinct force-displacement relationships based on the force-transfer mechanisms and the deformation they introduce into the joint:

- Component 1: Axial spring interaction between the top plate and top beam flange (S1),

- Component 2: Shear spring interaction between the web plate and beam web (S2), and
- Component 3: Axial spring interaction between the bottom plate and bottom beam flange (S3).

The force-displacement response of each component is modelled using nonlinear springs. These springs capture both the tensile and compressive behaviours governed by the relative movements of the beam, column, and plates under loading conditions. Specifically, spring S1 represents the tensile interaction between the top plate and top beam flange, spring S2 models the shear interaction between the web plate and beam web, and spring S3 captures the compressive interaction between the bottom plate and bottom beam flange. This configuration accurately represents the joint's reaction to applied forces.

To implement CBSM, a single-story frame structure with a beam-column connection is analysed in ANSYS Workbench. As illustrated in Figure 5.1, the ends of a beam are connected to columns using a set of plates and bolts. A uniform load of 1000kN is applied to the top flange of the beam. The forces between each plate of the connection and the column flange are extracted and analyzed in relation to the slip mechanism between the plates and beam elements as illustrated in Figure 5.1. These results are used to create simplified spring stiffness models that represent the force transfer mechanisms between the beam and column under loading.

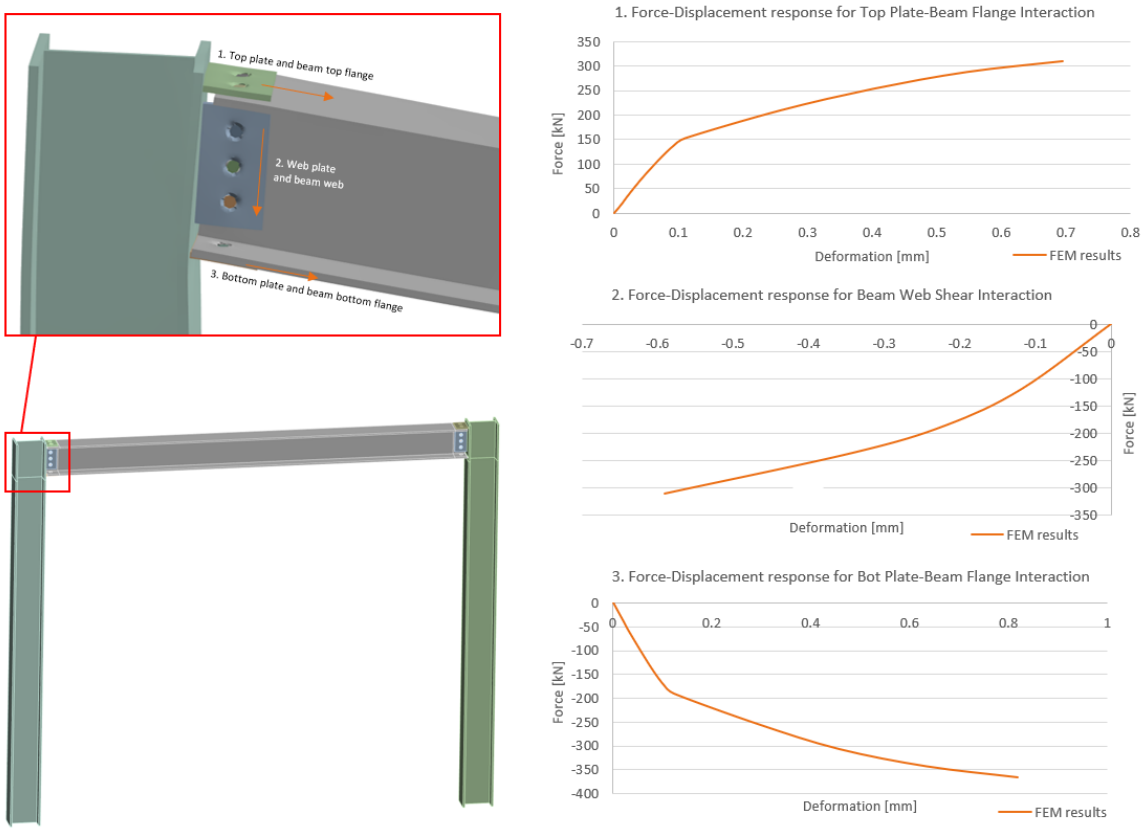

Figure 5.1: Representation of connection components of a single frame structure with respective force-displacement curve

To analyze a frame structure with equivalent connection spring elements, each beam-to-column joint can be modelled using a combination of rigid bars and extensional springs, as previously shown in Figure 3.1. In the simplified FE model, illustrated in Figure 5.2, 1D line elements are used to represent the beam and column structural components. At each beam end, a vertical rigid bar is introduced to represent the height of the beam. This rigid bar is firmly connected to the beam at the intersecting node, ensuring a rigid connection. The extensional springs are strategically positioned between the beam and column based on the contact interface between the plate and beam elements. These

springs account for the axial behaviour between the beam flanges and plates and the shear behaviour between the beam web and web plate. The springs contain nonlinear force-displacement response of the component modelling both pre-yield and post-yield behaviour. The incorporation of slip contact interactions between these components ensures that the model accurately replicates the force transfer and deformation mechanisms of the actual connection under various loading conditions.

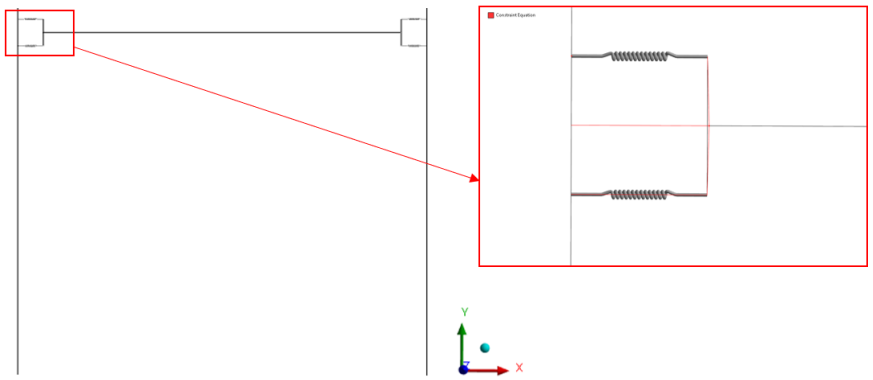

Figure 5.2: Modelling of springs in simplified frame model using CBSM

Various contact elements such as springs, connectors, trusses, or link elements with appropriate stiffness values can be used to model these springs. The choice of the modelling method depends on the capabilities of FEM software and the judgment of the modeller. In this study, the COMBIN39 element in ANSYS is utilized to model springs with nonlinear force-displacement characteristics. The COMBIN39 element is particularly suited for this application because it allows for a user-defined force-deflection curve that can extend beyond the defined range. If the displacement exceeds the values specified in the curve, the element maintains the last defined slope, which can be set to zero if needed. This characteristic is crucial when modelling situations where the connection is expected to undergo large deformations without a significant increase in force, such as yielding or slipping behaviour. This allows the structure to reach its ultimate resistance and experience high deformations in columns, beams, and connections without local connection failure.

ANSYS Parametric Design Language (APDL) commands are used to properly simulate the nonlinear force-displacement response of spring components in a frame construction. These commands accurately define and regulate the behaviour pf each component by simulating both pre-yield and post-yield force-displacement reactions at the connection. This method ensures that the springs correctly replicate the physical interactions in the beam-column connection. Detailed APDL code for modelling these springs is provided in Appendix B.

This modelling approach allows for a detailed representation of the connection behaviour, capturing the essential characteristics of contact interactions and force-transfer mechanism within the joint.

5.2. Steel Frame Analysis

This section investigates the behaviour of beam-column joints within a steel frame structure. The study focuses on a single bay of a three-story frame, comparing the structural response of semi-rigid and rigid joint configurations. Various modelling techniques, including solid elements, 1D line elements, and spring elements, are employed to evaluate both the accuracy and computational efficiency of these approaches. Particular emphasis is given on assessing how the Component-Based Spring Method (CBSM) incorporates connection behaviour within frame structures relative to the detailed modelling of connections using solid elements.

5.2.1. Model Description

Figure 5.3 illustrates the layout of the three-storey single-bay structure, including its frame configuration, member profiles, and loading conditions. HEA400 sections are used for the beams, while HEB400 sections are used for the columns. The structure is made from structural steel grade S275, which has a yield strength of 275 N/mm² and an ultimate strength of 430 N/mm². The material properties of the steel include a modulus of elasticity of 210,000 MPa and a Poisson's ratio of 0.3. These parameters ensure that the material behaviour under loading is accurately represented in the structural analysis.

The loading on the frame is calculated according to Eurocode guidelines. The details of the loads acting on the steel frame structure is provided in Appendix C. In the FE model, a factored uniformly distributed line load of 43.2 kN/m is applied on the first and second floors and 21.6 kN/m on the third floor. Additionally, a factored uniformly distributed wind load of 18 kN/m is applied laterally over the entire length of one of the columns.

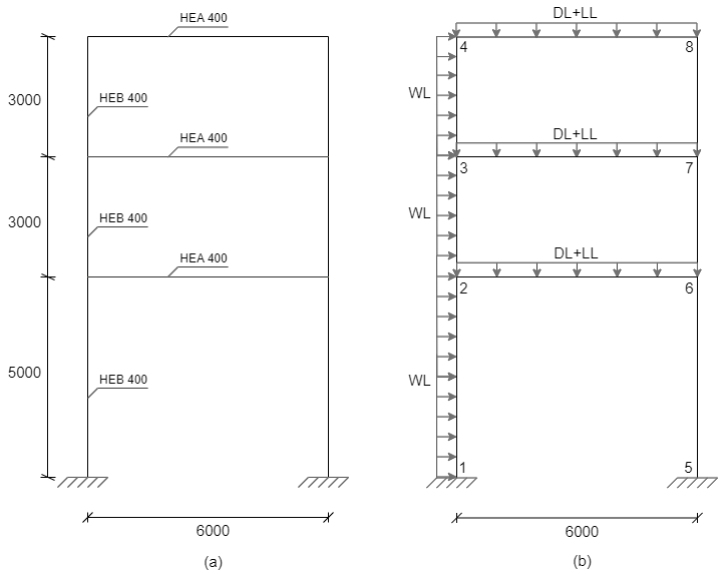

Figure 5.3: (a)Elevation and (b)Load application of frame structure

Rigid and semi-rigid beam-column connections are modelled to incorporate connection behaviour within the frame structure. Different frame and connection modelling techniques are employed to capture the varying complexities of the structure. These techniques include modelling the beam and column using 1D line body and 3D solid elements, addressing the complete range of structural behaviours and connection intricacies. The analysis is conducted on four different FE models, categorized into solid and line frame models. The nomenclature for each case is as follows:

1. **Solid-Rigid -** Frame structure with rigid beam-column joint behaviour modelled using 3D solid elements. The beam ends are rigidly bonded to the column flanges, ensuring that both loads and rotations are fully transferred between the beam and column, thereby simulating a rigid connection where no relative rotation occurs at the joint. (Figure 5.4a)
2. **Line-Rigid -** Frame structure with rigid beam-column joint behaviour modelled using 1D line elements. The nodes at the ends of the beams are bonded directly to the column line elements, creating a rigid connection that prevents any relative movement or rotation between the beam and column at the interface. (Figure 5.4b)
3. **Solid-SemiRigid -** Frame structure with semi-rigid beam-column joint behaviour modelled using 3D solid elements. The joint consists of top-seat and web plates welded to the column flange and bolted to the beam elements. The plates are represented using 3D solid elements, while the bolts are modelled using 1D line elements. (Figure 5.5a)

4. **Line-SemiRigid -** Frame structure with semi-rigid beam-column joint behaviour modelled using CBSM. This method simplifies the semi-rigid connection by using equivalent nonlinear springs positioned between the beam and column according to governing interactions in the connection. These springs are characterized by specific force-displacement relationships that replicate the semi-rigid connection behaviour, accounting for both tensile and compressive interactions. (Figure 5.5b)

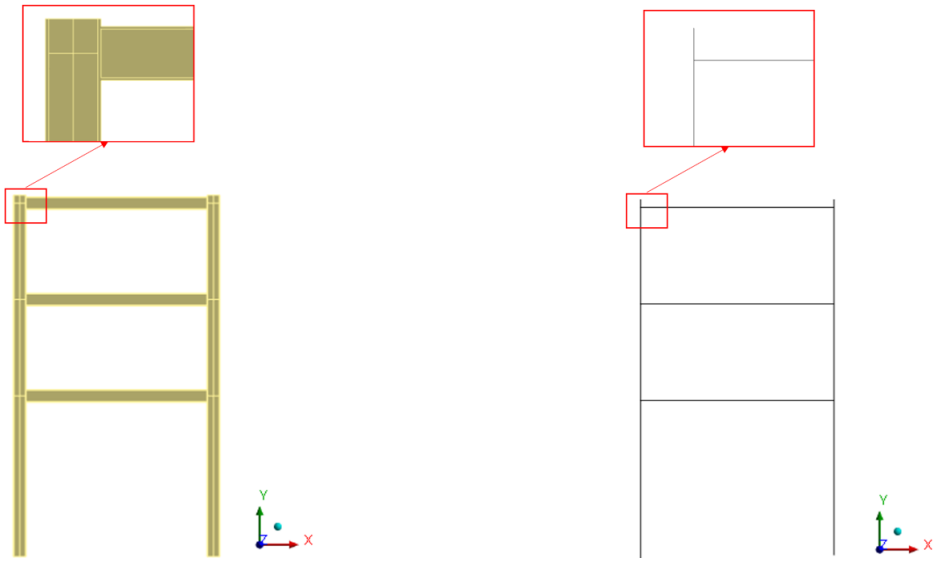

(a) Solid-Rigid **(b)** Line-Rigid

Figure 5.4: Three-story frame structure with rigid connection models

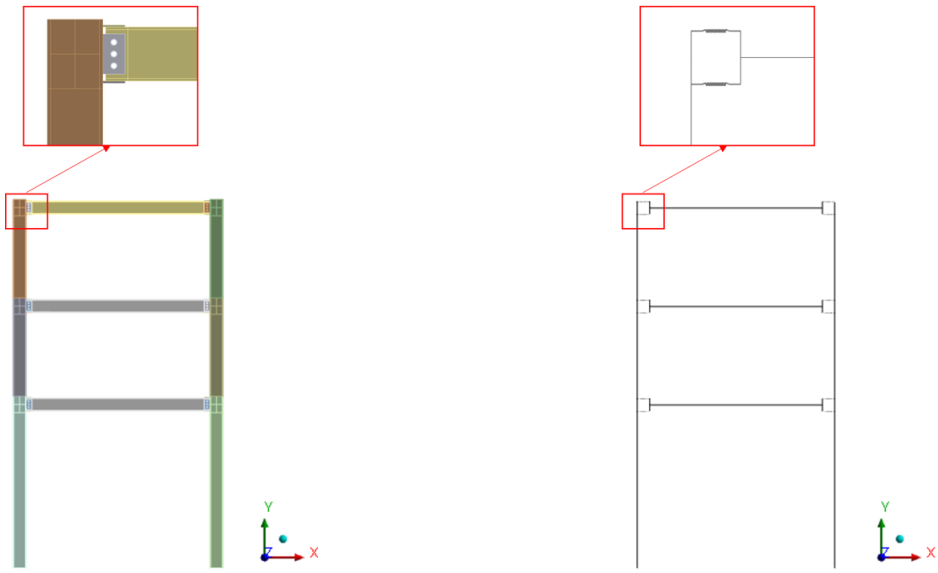

(a) Solid-SemiRigid **(b)** Line-SemiRigid

Figure 5.5: Three-story frame structure with semi-rigid connection models

Static structural analysis is performed to evaluate the frame's response under dead load, live load, and wind load using ANSYS software. The 'Large deflection' setting is enabled to account for geometric nonlinearity and P-Δ effects on the structure. The frame is subjected to both vertical and lateral loads, with particular emphasis on the influence of connection on the behaviour of the frame deflection.

5.2.2. Static Structural Analysis Results

The static structural analysis of the frame models under the given loading conditions (Dead Load: 43.2 kN/m and 21.6 kN/m; Wind Load: 18 kN/m) provides key insights into the trade-offs between computational efficiency and accuracy of the modelling approach. Deflections in both the vertical (Dy) and lateral (Dx) directions are measured at two critical locations: the column node connecting the column axis with the beam axis (Table 5.1) and the mid-point of the beam (Table 5.2) for each of the three stories (y = +5m, y = +8m, y = +11m).

Table 5.1: Three-story frame deflection results at column node

Model	Beam at y = +5m		Beam at y = +8m		Beam at y = +11m	
	Dy (mm)	Dx (mm)	Dy (mm)	Dx (mm)	Dy (mm)	Dx (mm)
Solid-Rigid	0.271	13.27	0.370	19.60	0.406	23.05
Line-Rigid	0.294	12.58	0.411	18.61	0.450	21.70
Solid-SemiRigid	0.274	16.57	0.371	26.41	0.406	32.42
Line-SemiRigid	0.261	16.00	0.361	25.10	0.391	30.29

Table 5.2: Three-story frame deflection results at beam mid-point

Model	Beam at y = +5m Dy (mm)	Beam at y = +8m Dy (mm)	Beam at y = +11m Dy (mm)
Solid-Rigid	3.71	3.31	1.96
Line-Rigid	3.55	3.42	2.16
Solid-SemiRigid	4.23	4.40	2.25
Line-SemiRigid	4.69	4.12	2.18

Table 5.3: Computational demands of FE models in ANSYS

Model	Time	Storage
Solid-Rigid	1m 30s	166Mb
Line-Rigid	16s	139Mb
Solid-SemiRigid	53m 52s	8.4Gb
Line-SemiRigid	18s	140.6Mb

The results presented in Table 5.1 and Table 5.2 reveal distinct deflection behaviours of semi-rigid and rigid connections in the analysed frame models. The Solid-SemiRigid model shows higher lateral deflection (Dx) compared to the Solid-Rigid model, with differences of -24.91% at y = +5m, -34.76% at y = +8m, and -40.63% at y = +11m. These significant differences highlight the impact of flexibility in semi-rigid connections, which allows for more rotation and deformation under load, as opposed to the more constrained movement in rigid connections. The underestimation of lateral deflections in rigid models highlights the risks associated with oversimplification, which can be mitigated by incorporating the semi-rigid behaviour of joints into the analysis process.

The vertical deflections (Dy) at the column node, as presented in Table 5.1, are minimal, indicating localized deformation at the connection points. To better understand the behaviour of vertical deflections, measurements were taken at the mid-point of the beams for each story (Table 5.2). The Line-SemiRigid model exhibits slightly higher deflections at y = +5m and slightly lower deflections at y = +8m and y = +11m compared to the Solid-SemiRigid model, with discrepancies ranging from -6.36% to +10.88%. The Line-Rigid model shows slightly lower deflections at y = +5m and higher deflections at y = +8m and y = +11m compared to the Solid-Rigid model.

Furthermore, the Line-SemiRigid model, which employs the Component-Based Spring Method (CBSM), provides deflection results that closely align with those of the Solid-SemiRigid model. The accuracy of the Line-SemiRigid model in replicating the semi-rigid behaviour is 96.55% at y = +5m, 95.03% at y = +8m, and 93.43% at y = +11m. As detailed in Table 5.3, this model achieves these results with a computation time of only 18 seconds and a storage requirement of 140.6 MB. This is a substantial reduction compared to the Solid-SemiRigid model, which required 53 minutes with 8.4 GB of storage. This demonstrates the efficiency of CBSM in accurately capturing semi-rigid connection behaviour while greatly reducing computational resources.

In comparison, the Line-Rigid model shows minimal discrepancies with the Solid-Rigid model, with differences in deflection values ranging from 1.28% to 4.21%. This minimal variation suggests that the Line-Rigid model can effectively replicate rigid connection behaviour while offering much greater computational efficiency.

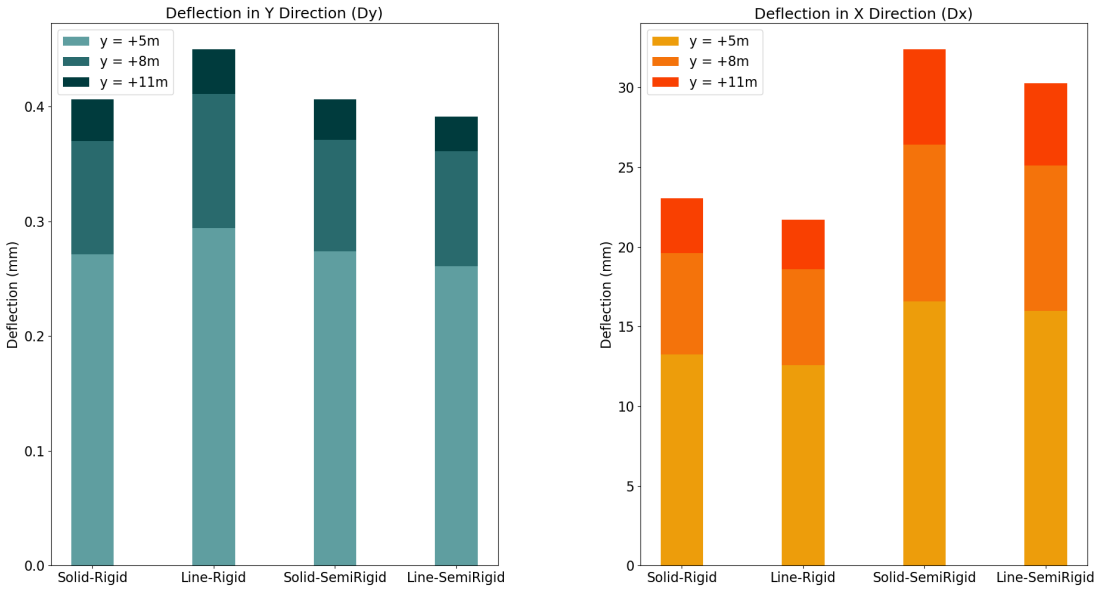

Figure 5.6: Three-storey frame deflection results at column node

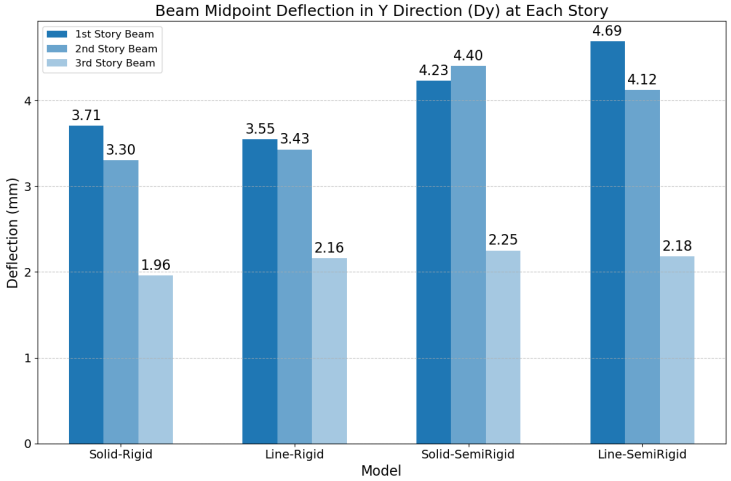

Figure 5.7: Three-storey frame deflection results at beam mid point

Figures 5.6 and 5.7 visually present these deflection results at the column node and beam mid-point, respectively. These figures reinforce the numerical findings, demonstrating that the CBSM provides accurate deflection predictions while significantly reducing computational demands. The minor discrep-

ancies in deflection values between the Solid-SemiRigid and Line-SemiRigid models are well within acceptable limits, especially when considering the substantial gains in computational efficiency.

In conclusion, these results collectively emphasize the importance of accounting for connection flexibility in structural design. The CBSM proves to be highly effective in accurately predicting deflections, all while significantly reducing computational demands. This makes CBSM an invaluable tool for efficient structural analysis and design.

5.3. Parametric Study: Effects of Loading and Joint Rigidity

This section presents two critical parametric studies aimed at evaluating the response of steel frame structures across the four models discussed in the previous section. These studies emphasize the importance of considering realistic connection behaviours in structural analysis and design under varying load conditions. The deflection results are analyzed at the column node (where the column axis intersects the beam axis) and at the mid-point of the beam for each of the three stories (y = +5m, y = +8m, y = +11m).

5.3.1. Loading Parametric Study

The loading parametric study investigates the behaviour of frame deformation under increasing load magnitudes, simulating real-world scenarios where structures experience varying loads over time—such as during different stages of occupancy or in response to environmental changes. The study evaluates four loading conditions, incrementing the load multipliers from 1.0 to 2.5, which correspond to different levels of dead loads (DL) and wind loads (WL), as presented in Table 5.4.

Table 5.4: Load multipliers and corresponding loads

Load Multiplier	Dead Load (kN/m)		Wind Load
	Story 1-2	Story 3	(kN/m)
1	43.2	21.6	18
1.5	64.8	32.4	27
2	86.4	43.2	36
2.5	108	54	45

The deflection behaviours of steel frame structures under increasing load magnitudes, as observed at the column node, are presented in Table 5.5. These results demonstrate that semi-rigid frames consistently exhibit higher lateral deflections (Dx) across all load multipliers when compared to rigid frames. The amplification factors in Table 5.6 further emphasize the differences in behaviour between rigid and semi-rigid frames as load magnitudes increase. For example, at y = +5m, the amplification factor for Solid-SemiRigid model increases from 1.25 at a load multiplier of 1 to 1.46 at a load multiplier of 2.5. Similar trends are observed at y = +8m and y = +11m, with amplification factors rising from 1.35 to 1.65 (22% increase) and from 1.41 to 1.79 (27% increase), respectively. This increased deflection highlights the inherent flexibility of semi-rigid joints, which allow more rotation and deformation under load, in contrast to the more constrained movement in rigid joints.

A similar trend is evident in the line models, where the deflections in the Line-SemiRigid model consistently exceed those of the Line-Rigid model as load multipliers increase. Specifically, at y = +5m, the amplification factor grows from 1.27 at load multiplier 1 to 1.46 at load multiplier 2.5. The amplification factors at y = +8m and y = +11m follow a similar trend, increasing from 1.35 to 1.60 and from 1.40 to 1.72, respectively. These results collectively highlight the significant impact of joint flexibility on structural performance, emphasizing the need for careful consideration in structural design.

Table 5.5: Load parametric deflection results at column node

Load Multiplier	Model	y = +5m		y = +8m		y = +11m	
		Dy (mm)	Dx (mm)	Dy (mm)	Dx (mm)	Dy (mm)	Dx (mm)
1.0	Solid-Rigid	0.27	13.27	0.37	19.60	0.41	23.05
	Line-Rigid	0.29	12.58	0.41	18.61	0.45	21.70
	Solid-SemiRigid	0.27	16.57	0.37	26.41	0.41	32.42
	Line-SemiRigid	0.26	16.00	0.36	25.10	0.39	30.29
1.5	Solid-Rigid	0.42	20.13	0.58	29.68	0.63	34.90
	Line-Rigid	0.45	18.98	0.63	28.08	0.69	32.73
	Solid-SemiRigid	0.45	26.93	0.62	43.85	0.68	54.48
	Line-SemiRigid	0.43	25.55	0.59	41.00	0.65	50.41
2.0	Solid-Rigid	0.59	27.52	0.80	40.68	0.87	47.82
	Line-Rigid	0.62	25.46	0.87	37.64	0.95	43.87
	Solid-SemiRigid	0.67	38.96	0.95	64.90	1.05	81.86
	Line-SemiRigid	0.62	35.71	0.87	58.05	0.95	72.15
2.5	Solid-Rigid	0.77	35.88	1.05	53.31	1.15	62.65
	Line-Rigid	0.80	32.75	1.12	48.57	1.23	56.54
	Solid-SemiRigid	0.99	52.38	1.43	87.96	1.64	112.28
	Line-SemiRigid	0.90	47.71	1.26	77.70	1.38	97.10

Table 5.6: Lateral deflection (Dx) amplification factors for different model comparisons

Solid-SemiRigid vs. Solid-Rigid			
Load Multiplier	Beam at y = +5m	Beam at y = +8m	Beam at y = +11m
1.0	1.25	1.35	1.41
1.5	1.34	1.48	1.56
2.0	1.42	1.60	1.71
2.5	1.46	1.65	1.79
Line-Rigid vs. Line-SemiRigid			
Load Multiplier	Beam at y = +5m	Beam at y = +8m	Beam at y = +11m
1.0	1.27	1.35	1.40
1.5	1.35	1.46	1.54
2.0	1.40	1.54	1.64
2.5	1.46	1.60	1.72
Solid-SemiRigid vs. Line-SemiRigid			
Load Multiplier	Beam at y = +5m	Beam at y = +8m	Beam at y = +11m
1.0	1.04	1.05	1.07
1.5	1.05	1.07	1.08
2.0	1.09	1.12	1.14
2.5	1.10	1.13	1.16

When comparing the performance of line and solid models, it is evident that both exhibit similar patterns in deflection results. However, solid models show slightly higher deflections due to their more detailed connection modelling as seen in Table 5.5. The comparison between Solid-SemiRigid and Line-SemiRigid models indicates that the amplification factors remain low for lower load magnitudes, with a slight increase as the loading increases. At y = +5m, the factor rises from 1.04 at load multiplier 1 to 1.10 at load multiplier 2.5. Similar modest increases are observed at y = +8m and y = +11m. This discrepancy highlights the limitations of simplified line models in fully capturing the complex nonlinear behaviours and stress redistributions that occur in more detailed solid models, especially under higher loads.

The increase in amplification factors between solid-semi-rigid and line-semi-rigid deflection results can be attributed to several factors. These include the more detailed representation of nonlinear material and connection behaviour, geometric nonlinearities, detailed load path, and stress distribution in solid models. Line models, while efficient, use simplified representations of force-displacement response in governing axial or shear direction that may not fully capture the complexities of structural behaviour under higher loads. Under higher loads, the redistribution of stresses and load paths can lead to

localized deformations that contribute to the overall deflection, which line models might not capture effectively.

Table 5.7: Load parametric deflection results at beam mid-point

Load Multiplier	Model	Beam Mid-Point (Dy)			Time	Storage
		1st Floor	2nd Floor	3rd Floor		
1.0	Solid-Rigid	3.7056	3.301	1.9585	1m 30s	388 MB
	Line-Rigid	3.549	3.4281	2.1608	16s	139 MB
	Solid-SemiRigid	4.2337	4.3986	2.2493	53m 52s	10.9 GB
	Line-SemiRigid	4.6889	4.1229	2.1791	18s	216 MB
1.5	Solid-Rigid	5.610	4.9821	2.9747	1m 40s	388 MB
	Line-Rigid	5.343	5.1626	3.2616	20s	139 MB
	Solid-SemiRigid	6.9795	7.317	3.6692	1h 1m	10.9 GB
	Line-SemiRigid	7.6319	6.9272	3.7655	21s	216 MB
2.0	Solid-Rigid	7.8454	6.7103	4.0207	1m 10s	388 MB
	Line-Rigid	7.1475	6.9112	4.3765	28s	222 MB
	Solid-SemiRigid	10.093	10.941	5.4208	1h 11m	10.92 GB
	Line-SemiRigid	10.422	9.8603	5.5402	22s	216 MB
2.5	Solid-Rigid	10.621	8.6049	5.1193	1m 50s	388 MB
	Line-Rigid	9.4577	8.7131	5.5189	29s	222 MB
	Solid-SemiRigid	12.736	14.061	7.1401	1h 49m	10.8 GB
	Line-SemiRigid	13.32	12.937	7.5376	36s	216 MB

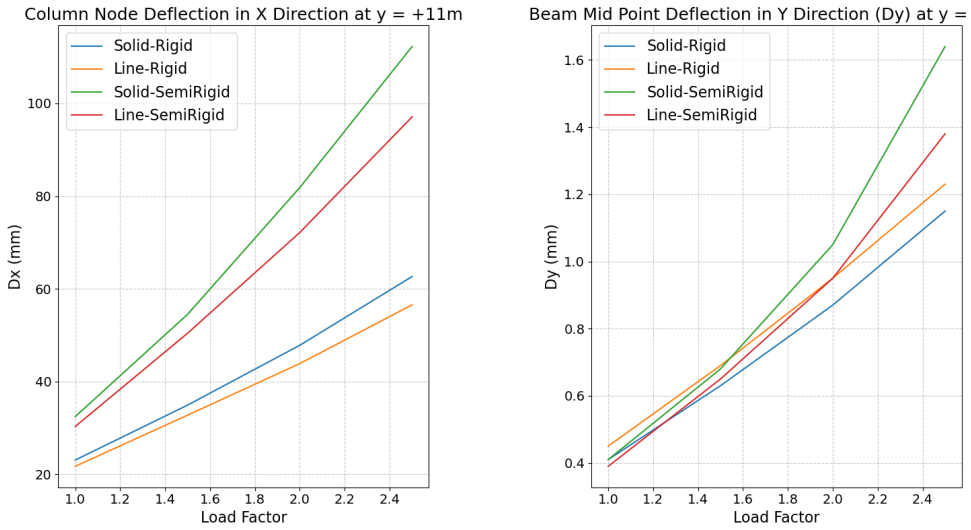

Figure 5.8: Load parametric study deflection results

The deflection behaviour of steel frames, particularly at the beam mid-point, is summarized in Table 5.7. These results reveal that the SemiRigid model consistently shows higher vertical deflections compared to the Rigid model across all floors, highlighting the impact of connection flexibility on the overall structural response. Figure 5.8 visually presents these deflection results, reinforcing the trends observed in the tabulated data.

The efficiency of the computational models is assessed by comparing the computation time and storage requirements as shown in Table 5.7. The Line-SemiRigid model consistently demonstrates superior computational efficiency compared to the Solid-SemiRigid model. For load multiplier 1, the Line-SemiRigid model requires only 18 seconds and 216 MB of storage, while the Solid-SemiRigid model demands 53 minutes and 10.9 GB. As the load multiplier increases to 2.5, the computation time for the Line-SemiRigid model rises modestly to 36 seconds with a storage requirement of 216 MB. In contrast, the Solid-SemiRigid model's computation time significantly increases to more than double with a stor-

age requirement of 10.8 GB. This substantial difference highlights the efficiency of CBSM in simulation semi-rigid connection behaviour while significantly reducing computational resources.

In conclusion, the study highlights the importance of considering connection behaviour under higher loading conditions. Semi-rigid connections result in higher deflections compared to rigid connections, necessitating careful design considerations to ensure structural integrity. CBSM proves to be an efficient and accurate method for modelling semi-rigid connections, offering substantial savings in computational resources while maintaining reasonable accuracy.

5.3.2. Connection Rigidity Parametric Study

The second parametric study evaluates the effectiveness of the Component-Based Spring Method (CBSM) in capturing the nuanced behaviours of semi-rigid connections within steel frame structures. The study varies the friction resistance between the contact interface of plates and beam elements of the semi-rigid connections, comparing six cases with different friction coefficients (0.1, 0.2, 0.3, 0.5, 0.7, and 0.9). The objective is to assess how the simplified modelling of CBSM performs when compared with complete solid modelling connections.

Table 5.8: Deflection results at column node for different friction coefficients

Friction Coefficient	Model	y = +5m		y = +8m		y = +11m	
		Dy (mm)	Dx (mm)	Dy (mm)	Dx (mm)	Dy (mm)	Dx (mm)
0.1	Solid-SemiRigid	0.28	17.27	0.38	27.93	0.41	34.72
	Line-SemiRigid	0.27	16.55	0.37	26.36	0.40	32.33
0.2	Solid-SemiRigid	0.27	16.57	0.37	26.41	0.41	32.42
	Line-SemiRigid	0.26	16.00	0.36	25.10	0.39	30.29
0.3	Solid-SemiRigid	0.27	16.04	0.36	25.26	0.40	30.77
	Line-SemiRigid	0.26	15.54	0.36	24.07	0.39	28.76
0.5	Solid-SemiRigid	0.26	15.11	0.36	23.40	0.39	28.27
	Line-SemiRigid	0.25	14.34	0.34	21.51	0.38	25.25
0.7	Solid-SemiRigid	0.26	14.88	0.35	22.92	0.39	27.64
	Line-SemiRigid	0.24	13.48	0.34	19.92	0.37	23.36
0.9	Solid-SemiRigid	0.26	14.79	0.35	22.74	0.39	27.39
	Line-SemiRigid	0.24	13.36	0.34	19.69	0.37	23.05

Table 5.9: Deflection results at beam mid-point and computational demands of structural models

Friction Coefficient	Model	Beam Mid-Point (Dy)			Time	Storage
		1st Floor	2nd Floor	3rd Floor		
0.1	Solid-SemiRigid	4.293	4.616	2.382	57m	10.9 GB
	Line-SemiRigid	4.7523	4.3292	2.4193	18s	216 MB
0.2	Solid-SemiRigid	4.234	4.399	2.249	53m 52s	10.9 GB
	Line-SemiRigid	4.689	4.123	2.179	18s	216 MB
0.3	Solid-SemiRigid	4.060	4.177	2.199	59m 38s	10.9 GB
	Line-SemiRigid	4.5391	3.8809	2.0834	20s	216 MB
0.5	Solid-SemiRigid	3.688	3.906	2.144	1h 32m	10.9 GB
	Line-SemiRigid	3.9682	3.3138	1.9709	18s	216 MB
0.7	Solid-SemiRigid	3.594	3.853	2.127	1h 13m	10.9 GB
	Line-SemiRigid	3.4875	3.1933	1.9412	17s	216 MB
0.9	Solid-SemiRigid	3.571	3.827	2.118	1h 4m	10.9 GB
	Line-SemiRigid	3.4402	3.1573	1.926	16s	216 MB

The deflection results at the column node, as presented in Table 5.8, reveal that the Line-SemiRigid model, which utilizes the Component-Based Spring Method (CBSM), closely aligns with the more de-

tailed Solid-SemiRigid model. The difference between the two models remains minimal for lower friction coefficients (0.1 to 0.3), with discrepancies around 6.5%. However, as the friction coefficient increases, the difference in deflection between the models becomes more pronounced, reaching up to 15.84% for the highest friction coefficient. This trend highlights the significance of friction in influencing structural response, with the Solid-SemiRigid model, which better captures geometric nonlinearities and material behaviour, exhibiting higher deflections due to its more detailed representation of the connection.

At the beam mid-point, the vertical deflection (Dy) results exhibit similar trends, as shown in Table 5.9. The Solid-SemiRigid model generally shows higher deflections than the Line-SemiRigid model across all friction coefficients. For lower friction coefficients (0.1-0.3), the difference is relatively small, ranging from 1.5% to 5.6%, but it increases to 9.05% for a friction coefficient of 0.9. his difference points to the limitations of line models using CBSM in fully capturing the complex load transfer and stress distribution characteristics inherent in solid modelling of semi-rigid connections. The visual representation in Figure 5.9 further illustrates these trends, showing the increasing deflection as the friction coefficient rises and highlighting the differences between the Solid-SemiRigid and Line-SemiRigid models.

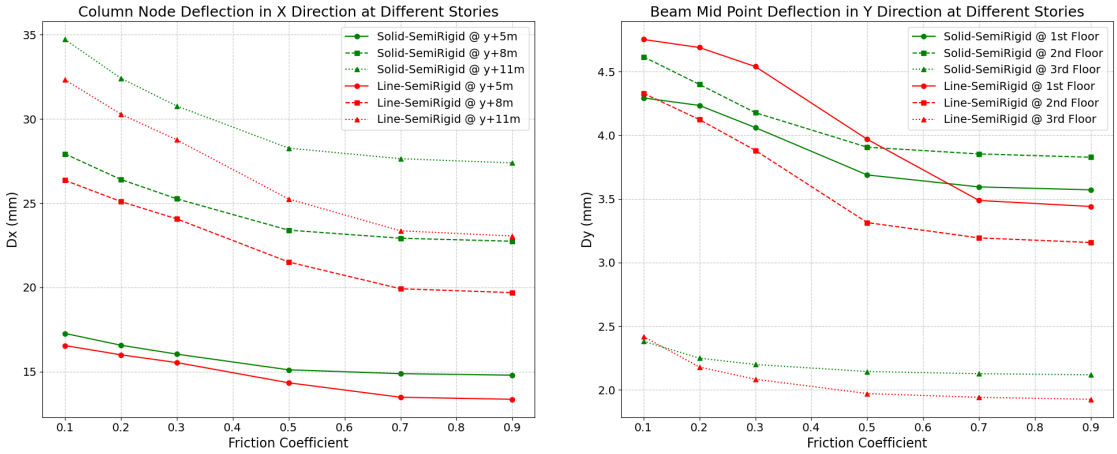

Figure 5.9: Friction parametric study deflection results

However, as demonstrated in Table 5.9, the Line-SemiRigid model consistently demonstrates superior computational efficiency compared to the Solid-SemiRigid model. The Line-SemiRigid model requires only about 20 seconds of computation time, compared to the several hours needed by the Solid-SemiRigid model. This substantial difference highlights the efficiency of the CBSM approach in providing accurate semi-rigid connection behaviour while significantly reducing computational resources.

In conclusion, the parametric study proved important to assess the deflection behaviour of semi-rigid frames with increasing connection rigidity. The comparison between CBSM and detailed solid modelling reveals that while CBSM is effective in approximating semi-rigid behaviour, it does have limitations in capturing the full complexity of connection interactions. Nonetheless, CBSM offers a highly efficient alternative for structural analysis, particularly when computational resources are a key consideration.

6

Discussions

This chapter provides an extensive discussion of the research conducted by critically evaluating methodologies, findings, and their broader implications. The chapter begins with a detailed summary of the research work, followed by an assessment of the results. It concludes by identifying the limitations of the study and discussing the implications of the findings for both academic research and industry practice.

6.1. Summary of Research Work

This research aimed to deepen the understanding of joint behaviour and its impact on the overall performance of steel frame structures. The study began with a focused investigation into the behaviour of an individual beam-column joint assembly, which included top, bottom and web plates welded to the column flange and bolted to the beam flanges and webs. Using numerical simulations in ANSYS, the study analysed the joint under both monotonic and cyclic loading conditions, focusing on the force transfer and relative deformation between the connection components.

The static analysis identified key elements within the connection, such as the Top Plate & Top Beam Flange, Web Plate & Beam Web, and Bottom Plate & Bottom Beam Flange, that govern the force transfer and deformation in the joint assembly. The force-displacement response curves provided insights into the pre-yield and post-yield behaviour of the connection. Additionally, the dynamic analysis further demonstrated the effective stiffness and energy dissipation characteristics of these components. A parametric study, varying friction, bolt pretension, and loading magnitude, further explored how these parameters influence the stiffness, energy dissipation, and overall behaviour of the connection. This analysis highlighted the need to balance different parameters based on the performance requirements when designing beam-column connections.

Building on these findings, the research expanded its focus to explore the effects of joint behaviour on the response of an entire steel frame structure. Traditionally, engineers have simplified joint behaviour by modelling beam-column connections as either rigid or pinned. While this approach eases analysis and reduces computational demands, it does not adequately reflect the complexities of real-world joint behaviour, which includes semi-rigid joint behaviour. The literature review identified a persistent gap in efficiently modelling these semi-rigid joints during the analysis of structures.

This research addressed this gap by proposing and validating a Component-Based Spring Method (CBSM) for modelling semi-rigid joints in steel frame structures. The CBSM was applied to a three-story, single-bay steel frame structure, where it was evaluated against complete solid modelling techniques. The results demonstrated that the CBSM achieved an accuracy of 93% to 96% compared to the solid model while reducing the computational time by 99.5%, from nearly an hour to mere seconds. This

significant reduction in computational expense makes the CBSM a practical and efficient alternative for incorporating semi-rigid joint behaviour into structural analysis.

The research also highlighted the risks associated with rigid joint models, particularly in their tendency to underestimate lateral deflections. Under lateral load multipliers ranging from 1.0 to 2.5, the lateral deflections in semi-rigid models were, on average, 35% higher than those in rigid models. For example, at a load multiplier of 2.5, the Solid-SemiRigid model showed a lateral deflection at the top story (y = +11m) that was 40.63% greater than the Solid-Rigid model. This significant discrepancy highlights the potential dangers of relying on oversimplified rigid joint models, particularly in structures subjected to substantial lateral loads.

For the industry, this research provides a viable method for improving the accuracy of structural analysis without significantly increasing computational demands. The CBSM approach, validated against detailed finite element models, enables engineers to better predict the behaviour of semi-rigid connections, leading to safer and more resilient structural designs. By recognizing and addressing the limitations of rigid joint models, this research offers a path forward for more efficient structural analyses and design.

6.2. Research Limitations

Despite its contributions, this research has several limitations. First, the study focused on a specific type of beam-column connection, which may limit the applicability of the findings to other connections or structural systems. Second, the parametric studies, while comprehensive, were conducted within a limited range of parameters, allowing the potential for additional investigation of more extreme or diverse conditions.

Additionally, the Component-Based Spring Method (CBSM), while accurate and cost efficient, simplifies the complex interactions within semi-rigid joints to equivalent spring system. This simplification, while beneficial for reducing computational costs, may not fully capture all the behaviour of a joint, particularly in cases involving highly nonlinear material properties or complex loading scenarios. The study's focus on a three-story frame structure also limits the applicability of the findings to taller or more complex structures, where additional validation would be required.

Another limitation of this research is related to the scope of the dynamic analysis. The study concentrated on the stiffness and energy dissipation characteristics of the connection components, offering valuable insights into the behaviour of individual joint assemblies. However, the implementation of CBSM in the dynamic analysis of frame structures was not explored, as it was beyond the scope of this study. Acknowledging these limitations highlights the potential for further research to address these areas.

6.3. Research Implications

The findings of this research carry significant implications for both academic research and industry practice. Academically, the validation of the CBSM contributes to the ongoing development of cost efficient methods for modelling semi-rigid joints in structural analysis. Future research could extend this work by applying the CBSM to other types of connections or by exploring its application in more complex structural systems.

For the industry, this research highlights the risks associated with oversimplified joint models, particularly in underestimating lateral deflections. Adopting the CBSM could lead to more efficient and reliable structural designs. The research suggests that incorporating joint flexibility into structural analysis could become a standard practice, enhancing both the safety and resilience of steel frame structures. This is particularly critical for structures subjected to significant lateral loads, where conventional rigid joint models may fail to predict critical deflections, potentially leading to structural failures.

In conclusion, this research provides a robust framework for understanding and modelling the behaviour of semi-rigid beam-column joints, delivering valuable insights and practical tools for both academic researchers and practising engineers. The Component-Based Spring Method provides a practical and efficient solution for incorporating joint flexibility into the analysis of steel structures in a computationally efficient manner, making it highly relevant for the design and assessment of steel structures.

7

Conclusions and Recommendations

This chapter provides the conclusions drawn from the research and outlines recommendations for future studies. The conclusions address the research questions posed in Chapter 1, summarizing the key findings and their implications. The recommendations suggest areas for further investigation to enhance the understanding and application of joint behaviour in multi-story steel frame structures, offering a framework for future research and design improvements.

7.1. Conclusions

Reflecting on the work done, the research questions outlined in Chapter 1 can be concluded as follows:

1. **How does the friction behaviour in bolted joints impact the overall structural performance of multi-story frame structures?**

   The friction behaviour in bolted joints has a considerable impact on the structural performance of multi-story frame structures. Friction between contact surfaces in beam-column connections plays a critical role in determining the stiffness, deflection, and energy dissipation characteristics of these joints, which in turn affect the global response of the structure.

   The study found that as the frictional resistance at the contact interfaces increases, the stiffness of the connection, both pre-yield and post-yield, also increases. This increase in stiffness is primarily due to the reduced slip between the connected surfaces, which enhances the resistance of joints to deformation under applied loads. The ability of the structure to bear loads without excessive deformation improves, resulting in a more stable and robust framework, particularly under static loading conditions. However, the parametric study on friction coefficients revealed that this increase in stiffness is accompanied by a reduction in the energy dissipation capacity of the connection. Higher friction coefficients correlate with lower energy absorption during cyclic loading, potentially diminishing the structure's ability to dissipate dynamic loads such as those encountered during earthquakes or wind events. This trade-off between stiffness and damping capacity underscores the importance of optimizing friction levels to balance structural integrity with energy dissipation needs.

   Additionally, the study highlighted that as friction resistance increases, the joints become less flexible, further limiting the deformation behaviour of the frame structure. While this reduction in flexibility contributes to a stiffer, more stable frame, it may also reduce the structure's adaptability to dynamic loads. Therefore, accurately modelling the friction behaviour in bolted joints is essential for achieving an optimal balance between stiffness and energy dissipation, ensuring that multi-story steel frame structures are both stable and resilient under various loading scenarios.

2. **What are the effects of varying friction resistance, bolt preloads, and loading conditions on the stiffness and damping characteristics of bolted beam-column connections?**

   The parametric study presented in Chapter 4 demonstrated that varying friction resistance, bolt pretension, and loading conditions have significant effects on the stiffness and damping characteristics of bolted beam-column connections. Higher friction coefficients enhanced the connection's stiffness, particularly in the top and bottom plate & beam flange components, by reducing slip and improving load transfer between the connected elements. However, this increase in stiffness was accompanied by a decrease in energy dissipation, as higher friction levels led to a reduction in the connection's ability to absorb and dissipate energy during cyclic loading.

   Similarly, increasing bolt pretension was shown to improve the connection's stiffness, with higher pretension levels enhancing both pre-yield and post-yield stiffness. However, as with friction, higher pretension resulted in a slight decrease in energy dissipation, indicating a trade-off between increased rigidity and reduced damping capacity.

   Furthermore, the study revealed that as the magnitude of cyclic loads increased, the stiffness of the connection decreased across all components. Despite this reduction in stiffness, there was a significant increase in energy dissipation, particularly in the top and bottom plate & beam flange components. This finding highlights the critical role of these components in absorbing and mitigating dynamic forces, contributing to the connection's resilience under severe loading conditions. Overall, the parametric study emphasizes the need to carefully balance these design parameters to optimize the structural performance of bolted connections in multi-story steel frames.

3. **How can Finite Element Modelling (FEM) be optimized to accurately simulate the behaviour of semi-rigid joints while minimizing computational resources for the efficient design and analysis of frame structures?**

   The research has shown that optimizing FEM to accurately simulate the behaviour of semi-rigid joints while minimizing computational resources is both feasible and essential for the efficient design and analysis of frame structures. Chapter 3 demonstrated that detailed FEM can effectively capture the complex interactions within bolted beam-column connections, providing critical insights into the force transfer and displacement mechanisms. Using advanced contact algorithms and material models in ANSYS, the study was able to accurately reflect the nonlinearities and slip behaviour inherent in bolted connections. The force-displacement curves and hysteresis loops obtained from FEM simulations under monotonic and cyclic loading conditions offered valuable data for characterizing the initial, post-yield, and effective stiffness of the connection components. This detailed analysis revealed the significant impact of friction coefficients and bolt preloads on the stiffness and damping properties of the connections.

   To further enhance efficiency, the Component-Based Spring Method (CBSM), introduced in Chapter 5, emerged as a highly effective alternative to detailed solid element models for simulating semi-rigid joint behaviour. The CBSM involves creating equivalent spring elements that replicate the load transfer and deformation behaviour of a steel beam-column connection, as derived from the detailed FEM analysis of individual components. The study showed that the CBSM successfully replicated the load transfer and deformation behaviour of semi-rigid joints with a high degree of accuracy (93-96%) compared to complete solid modelling of joints. Remarkably, this method also reduced computational time by approximately 99.5%, making it a practical tool for large-scale structural analyses where computational efficiency is paramount. The CBSM thus provides a valuable solution for incorporating semi-rigid behaviour into the design and analysis of frame structures without compromising the accuracy of the simulation.

4. **How does the flexibility of joints influence the performance of multi-story steel frame structures?**

   The flexibility of joints has a significant impact on the performance of multi-story steel frame structures, particularly in terms of stiffness, stability, energy dissipation, and load distribution. The study showed that semi-rigid joints, which possess greater flexibility than rigid joints, lead to higher lateral deflections within the structure. For example, the Solid-SemiRigid model exhibited up to 40.63% more deflection at the top story (y = +11m) compared to the Solid-Rigid model. This

increased flexibility enhances the damping capabilities of the structure, as it allows for greater energy dissipation through friction and slip mechanisms within the connections. This is crucial for improving the dynamic performance of structures under cyclic loads, such as wind and earthquakes.

The research also highlighted that joint flexibility alters the internal load distribution within the structure, leading to varied stress distributions and potentially amplifying second-order effects like the P-Delta effect. The CBSM approach proved effective in capturing these semi-rigid behaviours, providing engineers with a more efficient tool for predicting structural responses and enhancing the safety and performance of steel frame structures. Ultimately, understanding and accurately modelling joint flexibility is key to designing resilient and efficient multi-story steel frame structures.

7.2. Recommendations for future research

Based on the findings and conclusions of this study, several recommendations for future research are proposed:

1. **Application of CBSM to Complex Semi-Rigid Connections**

   The study utilized a beam-column connection with bolts between plates and beams and welds between the plates and columns. This allowed axial and shear behaviour only between the plates and beam elements, eliminating the column behaviour in the component-based method. Future research should apply the Component-Based Spring Method (CBSM) to more complex beam-column connections, considering the effects of the column on connection stiffness and damping characteristics. This includes accounting for axial and bending deformations of the column and the stiffening effects of column flanges under shear forces. Expanding the scope of CBSM to include different geometries, bolt configurations, and connection details could help identify optimal designs that maximize performance while minimizing cost and complexity.

2. **Dynamic Behaviour and Fatigue Analysis**

   The local behaviour of connections was examined for both static and dynamic cases in this study. However, the implementation of CBSM in the dynamic analysis of frame structures was not performed as it was beyond the scope of this research study. Future studies should focus on the dynamic behaviour of semi-rigid connections, including fatigue analysis under cyclic loading. Investigating the effects of repeated loading on the degradation of connection stiffness and strength over time will provide a better understanding of the durability and service life of these joints. This is particularly important for structures subjected to dynamic loads such as earthquakes or wind. Incorporating such analyses will ensure the resilience and longevity of structures designed with semi-rigid connections.

3. **Application to Different Structural Systems**

   Extending the application of CBSM to various structural systems beyond multi-story steel frames is recommended. Future research could begin by applying CBSM to 3D portal frames and other structural systems, such as trusses, bridges, and offshore structures. This extension would validate the versatility and robustness of the CBSM approach in diverse structural applications, contributing to safer and more efficient designs across various engineering fields.

4. **Improving the CBSM Approach**

   To enhance the CBSM approach, future research should explore additional component behaviours that contribute to force transfer and deformation within beam-column joints. This could include developing more efficient algorithms and incorporating machine learning techniques to predict joint behaviour, streamlining the incorporation of CBSM into practical applications. Automating the process of creating nonlinear FE models and generating datasets of force-displacement relationships for various connection details through scripts in ANSYS Workbench could significantly en-

hance efficiency and reduce the potential for human error, facilitating broader adoption of CBSM in structural design.

In conclusion, the CBSM approach offers a powerful and efficient tool for accurately modelling semi-rigid joints, providing a practical solution for engineers and researchers. Future research should focus on expanding and refining this method, ensuring its applicability to a wider range of structural systems and dynamic loading conditions.

8

References

[1] C. F. Beards, “Damping in structural joints,” *The Shock and Vibration Digest*, 1979.

[2] F. M. Mazzolani, V. Piluso, *et al.*, “Theory and design of seismic resistant steel frames,” 1996.

[3] S.-L. Chan and P.-T. Chui, *Non-linear static and cyclic analysis of steel frames with semi-rigid connections*. Elsevier, 2000.

[4] A. Elnashai, A. Elghazouli, and F. Denesh-Ashtiani, “Response of semirigid steel frames to cyclic and earthquake loads,” *Journal of structural Engineering*, vol. 124, no. 8, pp. 857–867, 1998.

[5] K. Weynand, J.-P. Jaspart, and M. Steenhuis, “Economy studies of steel building frames with semi-rigid joints,” 1998.

[6] W.-F. Chen, Y. Goto, and J. R. Liew, *Stability design of semi-rigid frames*. John Wiley & Sons, 1995.

[7] B. Guo, M. Su, and S. Lei, “Experimental behavior of rigid and semirigid steel frames under cyclic loading,” in *Earth and Space 2010: Engineering, Science, Construction, and Operations in Challenging Environments*, 2010, pp. 2785–2792.

[8] A. M. G. Coelho, F. S. Bijlaard, and L. S. da Silva, “Experimental assessment of the ductility of extended end plate connections,” *Engineering Structures*, vol. 26, no. 9, pp. 1185–1206, 2004.

[9] “Experimental assessment of the behaviour of bolted t-stub connections made up of welded plates,” *Journal of Constructional Steel Research*, vol. 60, no. 2, pp. 269–311, 2004, ISSN: 0143-974X. DOI: https://doi.org/10.1016/j.jcsr.2003.08.008.

[10] A. Rigi, B. JavidSharifi, M. A. Hadianfard, and T. Yang, “Study of the seismic behavior of rigid and semi-rigid steel moment-resisting frames,” *Journal of Constructional Steel Research*, vol. 186, p. 106 910, 2021.

[11] L. Calado, “Non-linear cyclic model of top and seat with web angle for steel beam-to-column conections,” *Engineering Structures*, vol. 25, no. 9, pp. 1189–1197, 2003.

[12] M. Latour, V. Piluso, and G. Rizzano, “Cyclic modeling of bolted beam-to-column connections: Component approach,” *Journal of Earthquake Engineering*, vol. 15, no. 4, pp. 537–563, 2011.

[13] R. M. Richard, W.-k. Hsia, and M. Chmielowiec, “Derived moment rotation curves for double framing angles,” *Computers & Structures*, vol. 30, no. 3, pp. 485–494, 1988.

[14] W. Youssef-Agha, H. Aktan, and O. Olowokere, “Seismic response of low-rise steel frames,” *Journal of Structural Engineering*, vol. 115, no. 3, pp. 594–607, 1989.

[15] N. Kishi and W.-F. Chen, “Moment-rotation relations of semirigid connections with angles,” *Journal of Structural Engineering*, vol. 116, no. 7, pp. 1813–1834, 1990.

[16] A. R. Kukreti and A. S. Abolmaali, “Moment-rotation hysteresis behavior of top and seat angle steel frame connections,” *Journal of structural Engineering*, vol. 125, no. 8, pp. 810–820, 1999.

[17] N. Krishnamurthy, “Modelling and prediction of steel bolted connection behavior,” *Computers & Structures*, vol. 11, no. 1-2, pp. 75–82, 1980.

[18] D. Li, D. Botto, R. Li, C. Xu, and W. Zhang, “Experimental and theoretical studies on friction contact of bolted joint interfaces,” *International Journal of Mechanical Sciences*, vol. 236, p. 107 773, 2022.

[19] L. Tan, W. Zhang, Z. Wang, B. Hou, and W. Sun, “Variation in the nonlinear stiffness of bolted joints due to tangential hysteresis behavior,” *International Journal of Non-Linear Mechanics*, vol. 158, p. 104 577, 2024.

[20] A. N. Sherbourne and M. R. Bahaari, “3d simulation of end-plate bolted connections,” *Journal of Structural Engineering*, vol. 120, no. 11, pp. 3122–3136, 1994.

[21] A. Azizinamini and J. B. Radziminski, “Static and cyclic performance of semirigid steel beam-to-column connections,” *Journal of Structural engineering*, vol. 115, no. 12, pp. 2979–2999, 1989.

[22] A. Citipitioglu, R. Haj-Ali, and D. White, “Refined 3d finite element modeling of partially-restrained connections including slip,” *Journal of constructional Steel research*, vol. 58, no. 5-8, pp. 995–1013, 2002.

[23] Y. I. Maggi, R. M. Gonçalves, R. T. Leon, and L. F. L. Ribeiro, “Parametric analysis of steel bolted end plate connections using finite element modeling,” *Journal of Constructional Steel Research*, vol. 61, no. 5, pp. 689–708, 2005.

[24] J. Da Silva, L. De Lima, P. d. S. Vellasco, S. De Andrade, and R. De Castro, “Nonlinear dynamic analysis of steel portal frames with semi-rigid connections,” *Engineering Structures*, vol. 30, no. 9, pp. 2566–2579, 2008.

[25] J. Shen and A. Astaneh-Asl, “Hysteresis model of bolted-angle connections,” *Journal of constructional steel research*, vol. 54, no. 3, pp. 317–343, 2000.

[26] L. S. Da Silva and A. G. Coelho, “An analytical evaluation of the response of steel joints under bending and axial force,” *Computers & Structures*, vol. 79, no. 8, pp. 873–881, 2001.

[27] S. Yan and K. J. Rasmussen, “Generalised component method-based finite element analysis of steel frames,” *Journal of Constructional Steel Research*, vol. 187, p. 106 949, 2021.

[28] R. Shi, “A simplified steel beam-to-column connection modelling approach and influence of connection ductility on frame behaviour in fire,” Ph.D. dissertation, University of Sheffield, 2017.

[29] R. Al-Sherif and M. A. Ismael, “Structural performance of semi-rigid connection steel frames,” *Diyala Journal of Engineering Sciences*, pp. 64–82, 2022.

[30] J. Abad, J. Franco, R. Celorrio, and L. Lezáun, “Design of experiments and energy dissipation analysis for a contact mechanics 3d model of frictional bolted lap joints,” *Advances in Engineering Software*, vol. 45, no. 1, pp. 42–53, 2012.

[31] H. Ouyang, M. Oldfield, and J. Mottershead, “Experimental and theoretical studies of a bolted joint excited by a torsional dynamic load,” *International Journal of Mechanical Sciences*, vol. 48, no. 12, pp. 1447–1455, 2006.

[32] Y. Li and Z. Hao, “Experimental and constitutive investigation on tangential sliding behavior of bolted joints with high preload,” *Journal of Manufacturing Processes*, vol. 64, pp. 889–897, 2021.

[33] L. Ma and P. Bocchini, “Hysteretic model of single-bolted angle connections for lattice steel towers,” *Journal of Engineering Mechanics*, vol. 145, no. 8, p. 04 019 052, 2019.

[34] E. Berger, “Friction modeling for dynamic system simulation,” *Appl. Mech. Rev.*, vol. 55, no. 6, pp. 535–577, 2002.

[35] J. Armand, L. Salles, C. W. Schwingshackl, D. Süss, and K. Willner, “On the effects of roughness on the nonlinear dynamics of a bolted joint: A multiscale analysis,” *European Journal of Mechanics-A/Solids*, vol. 70, pp. 44–57, 2018.

[36] M. Mahmoudi, M. Kosari, M. Lorestani, and M. J. S. Abad, “Effect of contact surface type on the slip resistance in bolted connections,” *Journal of Constructional Steel Research*, vol. 166, p. 105 943, 2020.

[37] M. Eriten, A. Polycarpou, and L. Bergman, “Surface roughness effects on energy dissipation in fretting contact of nominally flat surfaces,” 2011.

[38] M. Brake, C. Schwingshackl, and P. Reuß, “Observations of variability and repeatability in jointed structures,” *Mechanical Systems and Signal Processing*, vol. 129, pp. 282–307, 2019.

[39] C. Heistermann, M. Veljkovic, R. Simões, C. Rebelo, and L. S. Da Silva, “Design of slip resistant lap joints with long open slotted holes,” *Journal of Constructional Steel Research*, vol. 82, pp. 223–233, 2013.

[40] C. M. Butner, D. E. Adams, and J. R. Foley, “Experimental investigation of the effects of bolt preload on the dynamic response of a bolted interface,” *Journal of Applied Mechanics*, vol. 80, no. 1, p. 011 016, 2013.

[41] J. Bickford and H. Saunders, “An introduction to the design and behaviour of bolted joints,” 1983.

[42] V. Kaminskaya and A. Lipov, “Self-loosening of bolted joints in machine tools during service,” *Soviet Engineering Research*, vol. 10, no. 8, pp. 81–85, 1990.

[43] G. Yang, C. Che, S. Xiao, B. Yang, T. Zhu, and S. Jiang, “Experimental study and life prediction of bolt loosening life under variable amplitude vibration,” *Shock and Vibration*, vol. 2019, pp. 1–8, 2019.

[44] M. Yang, S.-M. Jeong, and J.-Y. Lim, “A phenomenological model for bolt loosening characteristics in bolted joints under cyclic loading,” *International Journal of Precision Engineering and Manufacturing*, vol. 24, no. 5, pp. 825–835, 2023.

[45] Y. Jiang, M. Zhang, and C.-H. Lee, “A study of early stage self-loosening of bolted joints,” *J. Mech. Des.*, vol. 125, no. 3, pp. 518–526, 2003.

[46] N. G. Pai and D. P. Hess, “Three-dimensional finite element analysis of threaded fastener loosening due to dynamic shear load,” *Engineering failure analysis*, vol. 9, no. 4, pp. 383–402, 2002.

[47] J. Stephen, M. Marshall, and R. Lewis, “Relaxation of contact pressure and self-loosening in dynamic bolted joints,” *Proceedings of the Institution of Mechanical Engineers, Part C: Journal of Mechanical Engineering Science*, vol. 231, no. 18, pp. 3462–3475, 2017.

[48] D. J. Borello, M. D. Denavit, and J. F. Hajjar, “Bolted steel slip-critical connections with fillers: I. performance,” *Journal of Constructional Steel Research*, vol. 67, no. 3, pp. 379–388, 2011.

[49] J. Huang, J. Wang, W. Chen, and Z. Wang, “Cyclic performance of double tee connections with short slotted holes,” *Journal of Constructional Steel Research*, vol. 145, pp. 254–265, 2018.

[50] Z. Shu, R. Ma, and M. He, “Comprehending the ductile behavior of slotted bolted connections,” *The Structural Design of Tall and Special Buildings*, vol. 26, no. 3, e1309, 2017.

[51] C. E. Grigorian, T.-S. Yang, and E. P. Popov, “Slotted bolted connection energy dissipators,” *Earthquake Spectra*, vol. 9, no. 3, pp. 491–504, 1993.

[52] X.-C. Liu, M.-L. Chen, X. Chen, Y.-M. Li, Y. Wang, and L. Xu, “Seismic behavior of bolted truss-to-column joint with oversized or slotted bolt hole,” *Engineering Structures*, vol. 247, p. 113 110, 2021.

A

Appendix A : Hand Calculation of Simple Joint with Fin Plate Connection for Validation

For validation of the nonlinear finite element modelling techniques used in ANSYS, the results from FEA are compared with manual calculations based on Eurocode 3 guidelines. This appendix presents the calculation for the resistance of various components of a fin plate beam-column connection, which consists of a single web plate welded to the column flange and bolted to the beam web, as illustrated in Figure A.1. The detailed joint geometry configuration is provided first, followed by calculations to perform various strength and resistance checks for each component of the connection.

A.1. Joint Geometry Data

A.1.1. Beam and Column Section Properties

Parameter	HEA400 Beam	HEB400 Column	Units
Yield stress, f_y	275	275	N/mm^2
Ultimate stress, f_u	430	430	N/mm^2
Height, h_b	390	400	mm
Web Height, h_{wb}	352	352	mm
Flange Width, h_b	300	300	mm
Web thickness, t_w	11	13.5	mm
Flange thickness, t_f	19	24	mm
Fillet radius, r	27	27	mm
Weight/meter, g	128	128	kg/m
Area, A	15898	19778	mm^2
Resistance modulus, W_y	872900	3232000	mm^3
Inertia moment, J_y	450700000	576800000	mm^4
Shear Area, A_v	5733	6998	mm^2

A.1.2. Fin Plate Configuration

Parameter	Value	Unit
Length, b_p	160	mm
Height, h_p	290	mm
Thickness, t_p	20	mm
Welding throat	12	mm (minimum 4.4mm)

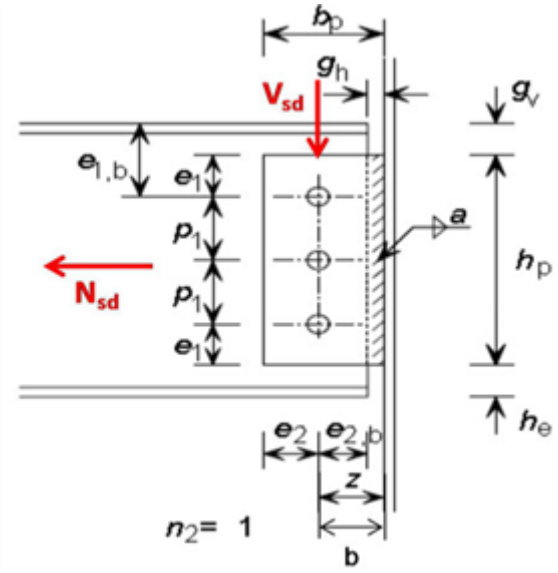

Figure A.1: Details of fin plate connection

A.1.3. Bolt and Plate position

Parameter	Value	Unit
Number of vertical columns of bolts (n_1)	1	-
Number of horizontal rows of bolts (n_2)	3	-
Total number of bolts ($n = n_1 \times n_2$)	3	-
Max hole diameter (d_0)	33	mm
Total height of the fin plate (h_p)	290	mm
Vertical distance between bolts ($p_1 > 2.2d_0$)	85	mm
Distance of 1st row from bottom plate edge (e_1)	60	mm
Distance of bolts from beam top flange ($e_{1,b}$)	110	mm
Distance from left vertical plate edge ($e_2 > 1.2d_0$)	80	mm
Distance of 1st bolt column from left vertical edge (b)	80	mm
Distance between beam and column (g_h)	20	mm
Distance of bolts from beam edge ($e_{2,b} = e_2 - g_h$)	60	mm
Eccentricity of shear from beam axis (z)	80	mm
Distance of thin plate from beam top flange (g_v)	50	mm
Distance of thin plate from beam bottom flange (h_e)	50	mm

A.1.4. Bolt Data

Parameter	Value	Unit
Bolt diameter (d_b)	30	mm
Bolt hole diameter (d_0)	33	mm
Area (A_s)	706.86	mm^2
Yield stress (f_y)	640	N/mm^2
Ultimate stress (f_u)	800	N/mm^2

A.1.5. Bolt Preload Parameter

Parameter	Value	Unit
Used Preload	400	kN
Preload as per EC3, $F_{p,C}$	395.84	kN
Hole coefficient, k_s (Non-oversized bolt holes)	1	-
k_s (Oversized bolt holes)	0.85	-
Friction coefficient, μ	0.2	-

A.2 Design of Fin Plate Connection

A.2.1 Requirement to ensure sufficient rotation capacity

2.1.a The height of the fin plate should be smaller than the depth of the beam:

$$h_{\text{plate}} = 290\,\text{mm}$$
$$h_{\text{beam}} = 390\,\text{mm}$$

2.1.b Φ available should be bigger than Φ required:

$$z = 80\,\text{mm}$$
$$\phi = \sqrt{(z-g_h)^2 + \left(\frac{h_p}{2} + h_e\right)^2}$$
$$= 204.02\,\text{mm}$$
$$\phi_{\text{available}} = \arcsin\left[\frac{z}{\sqrt{(z-g_h)^2 + \left(\frac{h_p}{2} + h_e\right)^2}}\right] - \arctan\left[\frac{z-g_h}{\frac{h_p}{2} + h_e}\right]$$
$$= 0.104$$

$Q_{\text{load}} = 80\,\text{kN/m}$

$\phi_{\text{required}} = \frac{Q_{\text{load}} \cdot (6\,\text{m})^3}{24 \cdot 210000\,\text{MPa} \cdot I_{\text{beam}}} = 0.007607$

A.2.2 Requirement to avoid premature weld failure

$\beta_{\text{weld}} = 0.9$

$a_{\text{minimum}} = \frac{\beta_{\text{weld}} \cdot f_y \cdot 1.25 \cdot t_{\text{plate}}}{\sqrt{2} \cdot f_u} = 10.175\,\text{mm}$

The selected weld thickness was assumed to be 12 mm. The criterion is thus fulfilled.

A.2.3 Supported beam – Bolt group

A.2.3.1 Bolts in shear

Basic requirements: $V_{\text{Ed}} \leq V_{\text{Rd}}$

$$V_{\text{Rd}} = \frac{n \cdot F_{v,b,Rd}}{\sqrt{(1+\alpha n_b)^2 + (\beta n_b)^2}}$$

For M30 8.8 bolts:

$$F_{v,b,Rd} = \frac{(0.6 \times 800 \times 706.86)}{1.25} \times 10^{-3} = 271.43\,\text{kN}$$

For a single vertical line of bolts ($n_2 = 1$ and $n = n_1$):

$$\alpha = 0$$

$$\beta = \frac{6z}{n_1(n_1+1)p_1} = 0.627451$$

Therefore,

$$V_{\text{Rd}} = \frac{3 \times 271.43}{\sqrt{(1+0)^2 + (0.627 \times 3)^2}} = 382.03\,\text{kN}$$

A.2.3.2 Fin Plate in bearing

Basic requirements: $V_{\text{Ed}} \leq V_{\text{Rd}}$

$$V_{\text{Rd}} = \frac{n_b}{\sqrt{\left(\frac{1+\alpha n_b}{F_{b,ver,Rd}}\right)^2 + (\frac{\beta n_b}{F_{b,hor,Rd}})^2}}$$

Where,

$$F_{b,ver,Rd} = k_{1,v} k_s \alpha_{b,v} d t_p \frac{f_{ub}}{\gamma M2}$$

$$F_{b,hor,Rd} = k_{1,h} k_s \alpha_{b,h} d t_p \frac{f_{up}}{\gamma M2}$$

Given:

$$k1, v = 2.5$$
$$\alpha_{b,v} = 0.606$$
$$k1, h = 2.5$$
$$\alpha_{b,h} = 0.808$$

Calculating $F_{b,ver,Rd}$:

$$F_{b,ver,Rd} = 2.5 \times 0.606 \times 30 \times 20 \times \frac{430}{1.25} = 312.72\,\text{kN}$$

Calculating $F_{b,hor,Rd}$:

$$F_{b,hor,Rd} = 2.5 \times 0.808 \times 30 \times 20 \times \frac{430}{1.25} = 416.9\,\text{kN}$$

Thus,

$$V_{\text{Rd}} = \frac{3}{\sqrt{\left(\frac{1+0.606\times3}{312.72}\right)^2 + (\frac{0.627\times3}{416.9})^2}} = 542.28\,\text{kN}$$

A.2.3.3 Beam web in bearing

Basic requirements: $V_{Ed} \leq V_{Rd}$

$$V_{Rd} = \frac{n_b}{\sqrt{\left(\frac{1+\alpha n_b}{F_{b,ver,Rd}}\right)^2 + (\frac{\beta n_b}{F_{b,hor,Rd}})^2}}$$

Where $\alpha = 0$ and $\beta = 0.627$, as above.

The vertical bearing resistance of a single bolt:

$$F_{b,ver,Rd} = k_{1,v} k_s \alpha_{b,v} d t_w \frac{f_{ub}}{\gamma M2}$$

Given:

$$k_{1,v} = \text{min}(2.8\frac{e2}{d0} - 1.7, 2.5) = 2.5$$

$$\alpha_{b,v} = \text{min}\left(\frac{e1}{3d0}, \frac{p}{3d0} - \frac{1}{4}, \frac{f_{ub}}{fu}, 1\right) = 0.608$$

Thus,

$$F_{b,ver,Rd} = 2.5 \times 0.608 \times 30 \times 11 \times \frac{430}{1.25} = 172.72\,\text{kN}$$

The horizontal bearing resistance of a single bolt:

$$F_{b,hor,Rd} = k_{1,h} k_s \alpha_{b,h} d t_w \frac{f_{up}}{\gamma M2}$$

Given:

$$k_{1,h} = \text{min}(2.8\frac{e1}{d0} - 1.7, 1.4\frac{p1}{d0} - 1.7, 2.5) = 2.5$$

$$\alpha_{b,h} = \text{min}\left(\frac{e2,b}{3d0}, \frac{p2}{3d0} - \frac{1}{4}, \frac{f_{ub}}{fu}, 1\right) = 0.606$$

Thus,

$$F_{b,hor,Rd} = 2.5 \times 0.606 \times 30 \times 11 \times \frac{430}{1.25} = 172\,\text{kN}$$

Therefore,

$$V_{Rd} = \frac{n_b}{\sqrt{\left(\frac{1+\alpha n_b}{F_{b,ver,Rd}}\right)^2 + (\frac{\beta n_b}{F_{b,hor,Rd}})^2}} = 242.305\,\text{kN}$$

A.2.4 Supported beam – Fin Plate

A.2.4.1 Fin Plate in Shear

Basic requirements: $V_{Ed} \leq V_{Rd,min}$

$$V_{Rd,min} = \text{min}(V_{Rd,g}, V_{Rd,n}, V_{Rd,b})$$

Gross section:

$$V_{Rd,g} = \frac{h_p t_p}{1.27} \cdot \frac{f_{y,p}}{\sqrt{3} \times \gamma_{M0}} = 725kN$$

Net section:

$$A_{v,net} = t_p \times (h_p - n_1 d_0) = 20 \times (290 - 3 \times 33) = 3820\,\text{mm}^2$$

$$V_{Rd,n} = A_{v,net} \cdot \frac{f_{u,p}}{\sqrt{3} \times \gamma_{M2}} = 758.68kN$$

Block tearing:

$$V_{Rd,b} = \frac{0.5 A_{nt} f_{u,p}}{\gamma_{M2}} + \frac{A_{nv} f_{y,p}}{\sqrt{3} \times \gamma_{M0}}$$

Net area subject to tension:

$$A_{nt} = (e2 - 0.5d0) \times t_p = 1270\,\text{mm}^2$$

Net area subject to shear:

$$A_{nv} = t_p \times (h_p - e1 - (n_{b,v} - 0.5)d0) = 2950\,\text{mm}^2$$

$$V_{Rd,b} = \frac{0.5 A_{nt} f_{u,p}}{\gamma_{M2}} + \frac{A_{nv} f_{y,p}}{\sqrt{3} \times \gamma_{M0}} = 686.81kN$$

Thus,

$$V_{Rd,min} = \text{min}(725\,\text{kN}, 758.68\,\text{kN}, 686.81\,\text{kN}) = 686.81\,\text{kN}$$

A.2.4.2 Fin Plate in Bending

Basic requirements: $V_{Ed} \leq V_{Rd}$

$$V_{Rd} = \frac{W_{el,p} \cdot f_{yp}}{z \cdot \gamma_{M0}}$$

$$V_{Rd} = \frac{W_{el,p} \cdot f_{yp}}{z \cdot \gamma_{M0}} = \frac{290 \cdot 20^2 \cdot 275}{6 \cdot 80 \cdot 1 \cdot 1000} = 963.6\ \text{kN}$$

Therefore, $V_{Ed} = 120\,\text{kN} < 963.65\,\text{kN}$

A.2.5 Supported beam – Web in shear

A.2.5.1 Beam Web in Shear

Basic requirements: $V_{Ed} \leq V_{Rd,min}$

$$V_{Rd,min} = \text{min}(V_{Rd,g}, V_{Rd,n}, V_{Rd,b})$$

Gross section:

$$V_{Rd,g} = \frac{A_{v,wb} f_y}{\sqrt{3}\gamma M0}$$

Without notch:

$$A_v = [(A - 2b \times t_f) + (t_w + 2r) \times t_f] = [(15898 - 2 \times 352 \times 19) + (11 + 2 \times 27) \times 19] = 3757\,\text{mm}^2$$

$$V_{Rd,g} = \frac{3757 \times 275}{\sqrt{3} \times 1 \times 10^{-3}} = 1388.23\,\text{kN}$$

Net section: Net area:

$$A_{v,net} = (A_v - n_1 d_0 t_w) = (3757 - 3 \times 33 \times 11) = 2503\,\text{mm}^2$$

$$V_{Rd,n} = \frac{A_{v,net} f_{u,p}}{\sqrt{3}\gamma M2} = \frac{2503 \times 430}{\sqrt{3} \times 1.25} = 474\,\text{kN}$$

Block tearing:

$$V_{Rd,b} = \frac{0.5 A_{nt,b} f_{u,p}}{\gamma M2} + \frac{A_{nv,b} f_{y,p}}{\sqrt{3}\gamma M0}$$

Net area subject to tension:

$$A_{nt,b} = (e2, b - 0.5d0) \times t_w = 478.5\,\text{mm}^2$$

Net area subject to shear:

$$A_{nv,b} = t_w(e1, b + (n_{b,h} - 1)p1 - (n_{b,h} - 0.5)d0) = 1028.5\,\text{mm}^2$$

$$V_{Rd,b} = \frac{0.5 \times 478.5 \times 430}{1.25} + \frac{1028.5 \times 430}{\sqrt{3} \times 1} = 245.59\,\text{kN}$$

Therefore,

$$V_{Rd,min} = \text{min}(V_{Rd,g}, V_{Rd,n}, V_{Rd,b}) = 245.59\,\text{kN}$$

Thus, $V_{Ed} = 120\,\text{kN} < 245.59\,\text{kN}$

B

Appendix B : APDL Code for Spring Modelling

In this appendix, the ANSYS Parametric Design Language (APDL) commands used to model the nonlinear springs representing the force-displacement behavior of beam-column connection components are provided. The nonlinear spring elements are modeled using the COMBIN39 element type, which is particularly suitable for capturing the complex, nonlinear force-displacement responses observed in semi-rigid connections.

COMBIN39 is a unidirectional element with nonlinear generalized force-deflection capabilities. The springs are defined between two node points, and the user can input the specific force-deflection curve that governs the element's behavior. The following are the key APDL commands used in modeling the spring elements:

- `et,_sid,39`: This command defines the element type for the spring as `COMBIN39`. The `_sid` variable represents the element ID in the ANSYS Workbench model.
- `keyopt,_sid,4,1`: This command sets the key option for nonlinear behavior in the X direction, enabling the element to respond to displacements along the X-axis with the defined force-displacement curve.
- `keyopt,_sid,3,1`: Similarly, this command sets the key option for nonlinear behavior in the Y direction, allowing the element to respond to displacements along the Y-axis if required.
- `R,_sid,.`: The `R` command is used to define the real constants for the element, which include the specific force-displacement data points that dictate the element's behavior under loading. Multiple `RMORE` commands can be used to extend this definition across the entire range of expected displacements.

B.1. Spring 1: Top Plate and Top Beam Flange Spring

This section outlines the APDL code that models the axial spring interaction between the top plate and the top beam flange in X direction.

Listing B.1: APDL Code for Modelling Top Plate and Top Beam Flange Spring

```
! Define the element type for the joint
et,_sid,39
! Set key options for the element (nonlinear behavior in X direction)
keyopt,_sid,4,1

```

```
! Define the real constants for the nonlinear spring using the provided force-displacement
    data in X direction
R,_sid,0,0,0.001241,12477,0.005244,20801,0.009247,29141,0.01331,37424
RMORE,0.01738,45729,0.02157,54003,0.02584,62293,0.03017,70577
RMORE,0.03454,78854,0.03897,87109,0.04347,95352,0.04804,103590
RMORE,0.05269,111820,0.05744,120020,0.06225,128210,0.06716,136390
RMORE,0.07214,144550,0.07722,152680,0.0825,160750,0.08809,168670
RMORE,0.09411,176420,0.10078,183960,0.10907,191070,0.1195,197610
RMORE,0.13149,203710,0.14449,209540,0.15801,215230,0.17211,220780
RMORE,0.18728,226030,0.20299,231220,0.21939,236440,0.23623,241650
RMORE,0.25314,246970,0.27055,252300,0.28828,257650,0.3063,262980
RMORE,0.32452,268300,0.3431,273610,0.3621,278900,0.3812,284160
RMORE,0.4007,289370,0.4204,294520,0.4403,299580,0.4604,304600
RMORE,0.4811,309480,0.5017,314360,0.5228,319070,0.5442,323680
RMORE,0.5658,328160,0.5877,332500,0.5878,332500
```

B.2. Spring 2: Web Plate and Beam Web Spring

The following APDL code models the shear spring interaction between the web plate and beam web in the Y direction.

Listing B.2: APDL Code for Modelling Web Plate and Beam Web Spring

```
! Define the element type for the joint
et,_sid,39
! Set key options for the element (nonlinear behavior in Y direction)
keyopt,_sid,3,1

! Define the real constants for the nonlinear spring using the provided force-displacement
    data in Y direction
R,_sid,-0.012924,-11229,-0.01777,-17645,-0.02261,-24063,-0.02747,-30480
RMORE,-0.03236,-36729,-0.03726,-42715,-0.04217,-48586,-0.04712,-54422
RMORE,-0.05209,-60250,-0.05709,-66059,-0.06212,-71846,-0.06719,-77634
RMORE,-0.07229,-83418,-0.07743,-89198,-0.08261,-94976,-0.08784,-100750
RMORE,-0.09311,-106540,-0.09849,-112340,-0.10384,-118160,-0.1095,-124080
RMORE,-0.1156,-130220,-0.1225,-136680,-0.1301,-143440,-0.1381,-150370
RMORE,-0.1463,-157350,-0.1546,-164320,-0.163,-171310,-0.1718,-178340
RMORE,-0.1809,-185410,-0.1909,-192380,-0.2014,-199300,-0.2128,-206090
RMORE,-0.2247,-212830,-0.2374,-219510,-0.2506,-226150,-0.2647,-232710
RMORE,-0.2792,-239210,-0.2944,-245630,-0.3102,-251980,-0.3264,-258330
RMORE,-0.343,-264690,-0.3599,-271040,-0.3772,-277370,-0.3954,-283730
RMORE,-0.4137,-290000,-0.4327,-296320,-0.4525,-302640,-0.4728,-308980
RMORE,-0.4939,-315420,-0.4940,-315420
```

B.3. Spring 3: Bottom Plate and Bottom Beam Flange Spring

This section provides the APDL code to model the axial spring interaction between the bottom plate and bottom beam flange in X direction.

Listing B.3: APDL Code for Modelling Bottom Plate and Bottom Beam Flange Spring

```
! Define the element type for the joint
et,_sid,39
! Set key options for the element (nonlinear behavior in X direction)
keyopt,_sid,4,1

! Define the real constants for the nonlinear spring using the provided force-displacement
    data in X direction
R,_sid,0.008605,7150,0.013501,17511,0.018403,27858,0.023346,38211,0.0283,48544
RMORE,0.03325,58954,0.03824,69444,0.04326,79958,0.0484,90431
RMORE,0.05358,100900,0.05874,111390,0.06395,121890,0.06924,132370
RMORE,0.07461,142830,0.08005,153260,0.08558,163680,0.09118,174090
RMORE,0.09692,184440,0.10272,194780,0.10884,205020,0.11589,214860
RMORE,0.12577,223600,0.13948,230870,0.15617,236980,0.174,242640
RMORE,0.19165,248380,0.20873,254360,0.22561,260440,0.24228,266670
```

```
RMORE,0.25929,272790,0.27698,278990,0.29535,285100,0.3143,291310
RMORE,0.33374,297490,0.35343,303720,0.37332,310010,0.39337,316370
RMORE,0.41395,322650,0.43485,328940,0.45628,335150,0.47802,341310
RMORE,0.49993,347420,0.52211,353490,0.54455,359500,0.56848,365090
RMORE,0.59192,370900,0.61596,376500,0.64125,381790,0.66671,387070
RMORE,0.69294,392110,0.69295,392110
```

C

Appendix C : Load Calculation of Single Bay Multi Story Steel Structure

C.1. Building and Structural Data

The structural model of the frame is given in Figure C.1. The geometry of the structure and the position of the steel members were decided considering a single-bay steel structure that experiences second-order effects. The described calculations are based on preliminary load data of the structure.

The frame structure spans 6 meters in length, with a height of 11 meters and a width of 6 meters, measured from centre to centre between frames. It consists of three storeys. The material used for profiles, plates, and welds is steel grade S275, and the bolts are of grade 8.8.

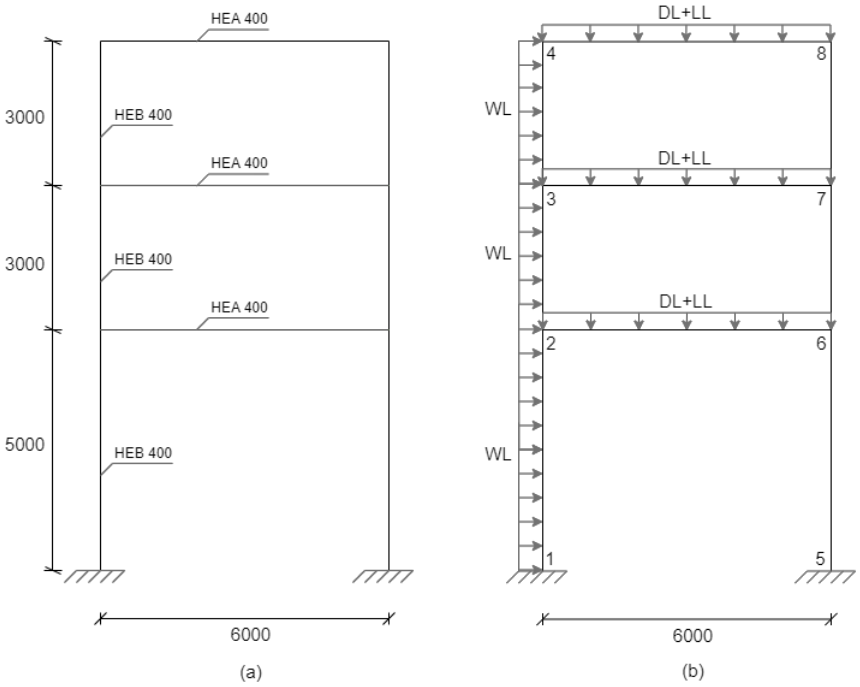

Figure C.1: (a)Elevation and (b)Load application of frame structure

C.2. Loads Applied

The following loads have been considered:

- **Self-weight loads (SWL)**: These include the weight of the steel frame members only. To take into account the weight of the joint elements (i.e., fin plate, angles, welds, bolts), these elementary self-weight loads have been increased by 10% in the analysis, and thus, a $\lambda = 1.1$ load factor is always adopted.
- **Dead loads (DL)**:
  - Level I-II: Uniform load 18 kN/m
  - Level III: Uniform load 9 kN/m
- **Imposed loads (IL)**:
  - Level I-II: Uniform load 18 kN/m
  - Level III: Uniform load 9 kN/m
- **Wind loads (WL)**:
  - Level I-III: Uniform load 12 kN/m

C.3. Load Combinations According to Eurocode (EN 1990)

Ensuring safety and serviceability, the main load combinations according to Eurocode (EN 1990) are:

1. Fundamental Combinations (for ultimate limit state, ULS)
2. Serviceability Combinations (for serviceability limit state, SLS)

C.3.1. Fundamental Combinations (for Ultimate Limit State, ULS)

According to Eurocode, the general format for ULS load combinations is:

$$\text{Design load} = \gamma_G \cdot G + \gamma_Q \cdot Q + \psi_0 \cdot \gamma_W \cdot W$$

Where:

- γ_G is the partial safety factor for dead loads (typically 1.35).
- γ_Q is the partial safety factor for live loads (typically 1.5).
- γ_W is the partial safety factor for wind loads (typically 1.5).
- ψ_0 is the combination factor for variable actions (typically 0.7 for live load).

Load Combinations for ULS:

1. $1.35G + 1.5Q$
2. $1.35G + 1.5W$
3. $1.35G + 1.5Q + 1.05W$
4. $1.35G + 1.05Q + 1.5W$

C.3.2. Serviceability Combinations (for Serviceability Limit State, SLS)

The general format for SLS load combinations is:

$$\text{Serviceability load} = G + \psi_2 \cdot Q + \psi_2 \cdot W$$

Where ψ_2 is another combination factor for variable actions (typically 0.3 for live load).

Load Combinations for SLS:

1. $G + Q$
2. $G + W$
3. $G + \psi_2 Q + \psi_2 W$

C.3.3. Applied Load Combination

The governing load combination $1.35G + 1.05Q + 1.5W$ is applied in ANSYS, and static analysis is performed to assess the vertical and lateral deformation of the structure.

- Vertical Load on 1st Floor: $1.35 \times 18 + 1.05 \times 18 = 43.2$ kN/m
- Vertical Load on 2nd Floor: $1.35 \times 18 + 1.05 \times 18 = 43.2$ kN/m
- Vertical Load on 3rd Floor: $1.35 \times 9 + 1.05 \times 9 = 21.6$ kN/m
- Lateral Wind Load (WL): $1.5 \times 12 = 18$ kN/m